



Supplementary Materials for

Cell-free chemoenzymatic starch synthesis from carbon dioxide

Tao Cai *et al.*

Corresponding author: Yanhe Ma, ma_yh@tib.cas.cn

Science **373**, 1523 (2021)
DOI: 10.1126/science.abh4049

The PDF file includes:

Materials and Methods
Supplementary Text
Figs. S1 to S13
Tables S1 to S7
References

Other Supplementary Material for this manuscript includes the following:

MDAR Reproducibility Checklist

Materials and Methods

Chemicals and agents

Common chemicals were bought from Sigma-Aldrich (Shanghai, China), SolarBio (Beijing, China) and Sangon Biotech (Shanghai, China). Standard amylose (160501) was purchased from Megazyme (Wicklow, Ireland). Standard amylopectin (ZC-57222) was purchased from ShangHai ZZBIO (China). Restriction enzymes, T4 DNA ligase and DNA polymerase were purchased from Thermo Fisher Scientific (Shanghai, China), New England Biolabs and TransGen Biotech (Beijing, China). Kits for DNA manipulation were purchased from Axygen (Shanghai, China) and TransGen Biotech (Beijing, China). Alcohol dehydrogenase (A7011), alcohol oxidase (A2404) and formaldehyde dehydrogenase (F1879) were purchased from Sigma-Aldrich (Shanghai, China). Total Starch (AA/AMG) Assay kit and glucose assay kit was purchased from Megazyme (Wicklow, Ireland) and Applygen (Beijing, China), respectively. Primers and synthesized genes were obtained from BGI (Beijing, China), GENEWIZ (Suzhou, China) or Qinglan Biotech (Wuxi, China). Materials and equipment for protein purification were obtained from GE Healthcare (Beijing, China) and BioRad (Beijing, China).

Bacterial strains and growth condition

Escherichia coli Trans T1 strain (TransGenTM) was grown at 37 °C in LB medium for gene cloning, site directed mutagenesis and other DNA manipulations. *E. coli* BL21 (DE3) (TransGenTM) was grown at 37 °C or 16 °C in LB medium for protein expression. Antibiotics for selection purposes were used accordingly at 100 µg ml⁻¹ ampicillin or 50 µg ml⁻¹ kanamycin.

Genetic manipulations

Genes from different organisms were first obtained either by PCR with primers as summarized in Table S6 or gene synthesis as shown in Table S7, and then cloned to the corresponding vectors to provide the final plasmids (Table S6). Site directed mutagenesis experiments were performed with pEASY[®]-Uni Seamless Cloning and assembly kit (TransGen Biotech, Beijing, China).

Construction of formolase error-prone (epPCR) library and screening

epPCR libraries were generated by the standard epPCR method using variant formolase (fls) gene as template (21). For the mutagenic PCR (95 °C for 2 min, 1 cycle; 95 °C, 20 s/60 °C, 20 s/72 °C, 3 min, 25 cycles; 72 °C for 5 min, 1 cycle). EasyTaq DNA polymerase (2.5 U), dNTP mix (0.20 mM), template (25 ng, pET21a harboring the fls gene), MnCl₂ (0.1 mM), and 10 pmol each primers) were used. The PCR products were purified by using a PCR purification kit. The purified epPCR products were cloned into expression plasmid pET21a and transformed into *E. coli* BL21 (DE3) cells for further expression and screening.

Clones grown on LB agar plates with ampicillin were transferred into 96-well microtiter plates, containing 150 µl LB liquid medium with ampicillin. After overnight cultivation in a microtiter plate shaker (37 °C, 800 rpm), each well was replicated into a second series of 96-well microtiter plates containing 200 µl LB liquid medium with ampicillin and 0.1 mM isopropyl β-D-thiogalactoside (IPTG). All the 96-well microtiter plates were cultivated in the microtiter plate shaker at 800 rpm at 37 °C for 4 h and then shaken at 20 °C for the subsequent 24 h. After expressions, the pellets were harvested in 96-well microtiter plates with a centrifuge (4 °C, 3400 rpm, 15 min) and then resuspended in 200 µl phosphate buffer. After centrifugation, the 96-well microtiter plates were stored at -20 °C for the following screening.

The cell pellets in 96-well microtiter plates were resuspended in 50 μ l buffer (100 mM HEPES-NaCl, pH 7.4), then 50 μ l formaldehyde solution containing 1mM thiamine diphosphate (TPP) was added in the above plates for reactions. 90 μ l reaction solutions were transferred into 96-well microtiter plates (flat-bottomed, polystyrene plates). Then 60 μ l assay solution A (0.3 mg ml⁻¹ galactose oxidase, 36 U ml⁻¹ horseradish peroxidase) and 50 μ l assay solution B (8 mM ABTS) were added in the plate successively. The plates were subjected to UV/Vis measurements at 410 nm using a microtiter plate reader (VersaMax; Molecular Devices, Sunnyvale, USA).

General protein expression and purification

E. coli BL21 (DE3) with expression plasmids (Table S6) were grown in LB medium at 37 °C by shaking up to an OD₆₀₀ of 1.0 and induced with 0.5 mM IPTG at 16 °C overnight. The cells were harvested by centrifugation at 10,000 rpm for 15 min and resuspended in lysis buffer (20 mM Tirs-HCl pH 8.5, 500 mM NaCl), and then cells were lysed by ultra-sonification and cleared by centrifugation at 17,000 rpm for 45 min. The cleared supernatants were loaded onto Ni sepharose™ resin and unbound protein was washed out by 50 mM Tris-HCl pH 7.5, 500 mM NaCl, 20 mM imidazole. The target protein was eluted in 50 mM Tris-HCl pH 7.5, 500 mM NaCl, 250 mM imidazole and dialyzed against 50 mM Tris-HCl pH 7.5, 500 mM NaCl, 1 mM DTT. The parent fls and its variants were manipulated in 100 mM HEPES and 100 mM NaCl. Protein concentrations were determined by Bradford method with bovine serum albumin as a standard (41). Purified proteins were stored at -80 °C for further applications.

Activity assay of enzymes

The kinetic constants (K_m and k_{cat}) were obtained through Michaelis-Menten plots and the specific activities were acquired at the denoted substrates.

Acetyl-CoA synthase (acs, EC 6.2.1.1)

The activity of acs was determined by monitoring the production of free phosphate in the presence of pyrophosphatase (ppa), using Malachite green and molybdate (42), which formed a green complex with phosphate that was detected by UV/Vis at 617 nm. The standard reactions contained 100 mM HEPES (pH 7.5), 100 mM NaCl, 5 mM Mg²⁺, 10 μ M Zn²⁺, 1 mM CoA, 1 mM ATP, 0.8 g L⁻¹ ppa and acs from different organisms. The reactions were started at 30 °C by addition of 50 mM sodium formate. At defined time points, 50 μ l properly diluted sample was added to 100 μ l freshly made working reagent (MG/AM/ST) (42). After incubating 20 min at 30 °C, 15 μ l 1 M sodium citrate was added to stabilize the color and the sample was measured by UV/Vis at 617 nm. The specific activity of acs was calculated as the number of μ mol formyl-CoA formed per min per milligram of acs protein.

Acetaldehyde dehydrogenase (acdh, EC 1.2.1.10)

The activity of acdh was determined by spectrophotometrically monitoring the depletion of NADH at 340 nm (21). The standard reactions contained 100 mM HEPES (pH 7.5), 100 mM NaCl, 5 mM Mg²⁺, 10 μ M Zn²⁺, 1 mM NADH, and acdh from different organisms. The reactions were started at 30 °C by addition of acetyl-CoA. Michaelis-Menten kinetic parameters were determined by varying the concentration of acetyl-CoA from 0.1 to 2 mM.

Acetate kinase (acka, EC 2.7.2.1)

The activity of acka was determined by monitoring the production of ADP through a coupled assay with pyruvate kinase, which converts ADP and phosphoenolpyruvate to pyruvate and ATP,

and lactate dehydrogenase, which converts pyruvate to lactate with the oxidation of NADH to NAD⁺ (43). Consumption of NADH was detected spectrophotometrically at 340 nm. The standard reaction contained 100 mM HEPES (pH 7.5), 100 mM NaCl, 5 mM Mg²⁺, 10 µM Zn²⁺, 1 mM NADH, 1 mM ATP, 3 mM PEP, 5 U ml⁻¹ pyruvate kinase, 15 U ml⁻¹ lactate dehydrogenase, and acka from different organisms. A typical reaction was detected at 30 °C by addition of sodium formate. Michaelis-Menten kinetic parameters were determined by varying the concentration of sodium formate from 5 to 200 mM.

Phosphotransacetylase (pta, EC 2.3.1.8)

The activity of pta was determined by monitoring the depletion of CoA via HPLC (Shimadzu, Japan) equipped with ZORBAX SB-C18 column (Agilent, USA) and a UV-detector at 254 nm for analysis of acetyl-CoA (44). The standard reactions contained 100 mM HEPES (pH 7.5), 100 mM NaCl, 5 mM Mg²⁺, 2 mM CoA, 10 µM Zn⁺ and pta from different organisms. A typical reaction was started at 30 °C by addition of 1 mM sodium acetyl phosphate. The specific activity of pta was calculated as the number of µmol CoA consumed per min per milligram of pta protein.

Formolase (fls, EC 4.1.2.-)

The activity of fls was determined by monitoring production of DHA using galactose oxidase, which converts DHA and oxygen to hydrogen peroxide, and horseradish peroxidase, which converts hydrogen peroxide to water with oxidation of ABTS (2,2'-azino-bis[3-ethylbenzothiazoline-6-sulfonic acid]) to its colored cation radical. It was detected at 410 nm. The standard reactions contained 50 mM phosphate (pH 7.5), 0.5 mM TPP and formaldehyde. The reactions were initiated at 30 °C by the addition of purified fls variants. Samples were taken at different time points and the produced DHA was determined as following: 90 µl reaction solutions containing DHA were transferred to a 96-well microtiter plate, 60 µl assay solution A (0.3 g L⁻¹ galactose oxidase, 36 U ml⁻¹ horseradish peroxidase, 100 mM HEPES pH7.5, 100 mM NaCl) were added to the wells of the microtiter plate, and then 50 µl solution B (8 mM ABTS, 100 mM HEPES (pH7.5), 100 mM NaCl) were added. Michaelis-Menten kinetic parameters were determined by varying the concentration of formaldehyde from 2 to 150 mM.

Dihydroxyacetone kinase (dak, EC 2.7.1.29)

The activity of dak was determined by monitoring the production of dihydroxyacetone phosphate (DHAP) through a coupled assay with Triose-phosphate isomerase (tpi), which converts DHAP to D-glyceraldehyde 3-phosphate (GAP), and glyceraldehyde-3-phosphate dehydrogenase (GAPDH), which converts GAP and phosphate to 1,3-bisphosphoglycerate with the reduction of NAD⁺ to NADH (45). Production of NADH was detected spectrophotometrically at 340 nm. The standard reactions contained 100 mM HEPES (pH 7.4), 100 mM NaCl, 5 mM Mg²⁺, 0.1 mM EDTA, 2.5 mM NADH, 20 U ml⁻¹ tpi and 20 U ml⁻¹ GAPDH, 4 mM ATP, and dak from different organisms. A typical reaction was started at 30 °C by addition of DHA. Michaelis-Menten kinetic parameters were determined by varying the concentration of DHA from 0.1 to 2 mM.

Triose-phosphate isomerase (tpi, EC 5.3.1.1)

The activity of tpi was determined by monitoring the production of GAP through a coupled assay with GAPDH (46). Production of NADH was detected spectrophotometrically at 340 nm. The standard reactions contained 100 mM HEPES (pH 7.5), 100 mM NaCl, 5 mM Mg²⁺, 1 mM NAD⁺, 10 µM Zn²⁺, 4 mM potassium arsenite, 20 U ml⁻¹ GAPDH, and tpi from different

organisms. A typical reaction was started at 30 °C by addition of DHAP. Michaelis-Menten kinetic parameters were determined by varying the concentration of DHAP from 0.5 to 10 mM.

Fructose-bisphosphate aldolase (fba, EC 4.1.2.13)

The activity of fba was determined by monitoring the production of F-1,6-BP through a coupled assay with fructose-bisphosphatase (FBP), which converts F-1,6-BP to F-6-P and phosphate, and phosphoglucose isomerase (pgi), which converts F-6-P into G-6-P, and glucose-6-phosphate dehydrogenase (G6PDH), which converts G-6-P to 6-phosphogluconolactone with the reduction of NAD⁺ to NADH (47). Production of NADH was detected spectrophotometrically at 340 nm. The standard reactions contained 100 mM HEPES (pH 7.5), 100 mM NaCl, 5 mM Mg²⁺, 0.1 mM EDTA, 2 mM NAD⁺, 10 µM Zn²⁺, 20 U ml⁻¹ pgi, 20 U ml⁻¹ G6PDH, 20 U ml⁻¹ FBP, 2 mM GAP, and fba from different organisms. The reactions were started at 30 °C by addition of DHAP. Michaelis-Menten kinetic parameters were determined by varying the concentration of DHAP from 0.2 to 2 mM.

Fructose-bisphosphatase (FBP, EC 3.1.3.11)

The activity of FBP was determined by monitoring the production of F-6-P through a coupled assay with pgi and G6PDH (48). Production of NADH was detected spectrophotometrically at 340 nm. The standard reactions contained 100 mM HEPES (pH 7.5), 100 mM NaCl, 5 mM Mg²⁺, 0.1 mM EDTA, 2 mM NAD⁺, 10 µM Zn²⁺, 20 U ml⁻¹ pgi, 20 U ml⁻¹ G6PDH, and FBP from different organisms. A typical reaction was started at 30 °C by addition of 1 mM F-1,6-BP. The specific activity of FBP was calculated as the number of µmol F-6-P formed per min per milligram of FBP protein.

Fructose-6-phosphate aldolase (fsa, EC 4.1.2.-)

The activity of fsa was determined by monitoring the production of F-6-P through a coupled assay with pgi and G6PDH (49). Production of NADH was detected spectrophotometrically at 340 nm. The standard reactions contained 100 mM HEPES (pH 7.5), 100 mM NaCl, 5 mM Mg²⁺, 2 mM NAD⁺, 10 µM Zn²⁺, 3 mM DHA, 20 U ml⁻¹ pgi, 20 U ml⁻¹ G6PDH, and fsa from different organisms. A typical reaction was started at 30 °C by addition of GAP. Michaelis-Menten kinetic parameters were determined by varying the concentration of GAP from 0.3 to 2.1 mM.

Phosphoglucose isomerase (pgi, EC 5.3.1.9)

The activity of pgi was determined by monitoring the production of G-6-P through a coupled assay with G6PDH (50). Production of NADH was detected spectrophotometrically at 340 nm. The standard reactions contained 100 mM HEPES (pH 7.5), 100 mM NaCl, 5 mM Mg²⁺, 10 µM Zn²⁺, 2 mM NAD⁺, 20 U ml⁻¹ G6PDH and F-6-P. A typical reaction was started at 30°C by addition of pgi from different organisms. Michaelis-Menten kinetic parameters were determined by varying the concentration of F-6-P from 0.02 to 2 mM.

phosphoglucomutase (pgm, EC 2.7.5.1)

The activity of pgm was determined by monitoring the production of G-1-P through a coupled assay with ADP-Glc pyrophosphorylase (agg), which converts G-1-P to ADPG and release pyrophosphate (PPi), and ppa, which converts PPi to phosphate. Production of phosphate was measured as the same as acs. The standard reactions contained 100 mM HEPES (pH 7.5), 100 mM NaCl, 5 mM Mg²⁺, 10 µM Zn²⁺, 50 µM G-1,6-2P, 20 U ml⁻¹ agg, 0.8 g L⁻¹ ppa and pgm from different organisms. A typical reaction was started at 30 °C by addition of 5 mM G-6-P. The

specific activity of pgm was calculated as the number of μmol G-1-P formed per min per milligram of pgm protein.

α -glucan phosphorylase (α GP, EC 2.4.1.1)

The activity of α GP was determined by monitoring the production of free phosphate, which was measured the same as acs. The standard reactions contained 100 mM HEPES (pH 7.5), 100 mM NaCl, 5 mM Mg²⁺, 10 μM Zn²⁺, 0.01 g L⁻¹ dextrin and α GP from different organisms. A typical reaction was started at 30 °C by addition of 1 mM G-1-P. The specific activity of α GP was calculated as the number of μmol phosphate formed per min per milligram of α GP protein.

ADP-Glc pyrophosphorylase (agp, EC 2.7.7.27)

The activity of agp was determined by monitoring the production of free phosphate in the presence ppa the same as acs. The standard reactions contained 100 mM HEPES (pH 7.5), 100 mM NaCl, 5 mM Mg²⁺, 10 μM Zn²⁺, 1 mM ATP, 0.8 g L⁻¹ ppa and agp from different organisms. A typical reaction was started at 30 °C by addition of 1 mM G-1-P. The specific activity of agp was calculated as the number of μmol ADPG formed per min per milligram of agp protein.

Starch synthase (ss, EC 2.4.1.21)

The activity of ss was determined by monitoring the production of ADP through a coupled assay with pyruvate kinase and lactate dehydrogenase. Consumption of NADH was detected spectrophotometrically at 340 nm. The standard reactions contained 100 mM HEPES (pH 7.5), 100 mM NaCl, 5 mM Mg²⁺, 10 μM Zn²⁺, 1.5 mM NADH, 3 mM PEP, 5 U ml⁻¹ PK, 15 U ml⁻¹ LDH, 0.01 g L⁻¹ dextrin, 1 mM ADPG and ss from different organisms. A typical reaction was started at 30 °C by addition of ADPG. The specific activity of ss was calculated as the number of μmol ADP formed per min per milligram of ss protein.

Preparation of ZnO-ZrO₂ catalyst and methanol production

ZnO-ZrO₂ catalyst was synthesized by the same method according to a previous literature (34). Typically, 5.8 g of Zr(NO₃)₄ · 5H₂O and 0.6 g of Zn(NO₃)₂ · 6H₂O were stirred in order to dissolve in 100 ml water. (NH₄)₂CO₃ aqueous solution (3.06 g in 100 ml water) as the precipitant was added at a flow rate of 3 ml min⁻¹ to the aforementioned solution under vigorous stirring at the temperature of 70 °C and stirring of the mixture was continued for 2 hours to form a precipitate. The slurry was collected by filtration and washed with water three times after cooling down to room temperature. The filtered powder was dried at 110 °C for 4 hours and calcined at 500 °C in static air for 3 hours.

For CO₂ hydrogenation to methanol tests of ZnO-ZrO₂ catalyst, the reaction was carried out in a tubular fixed-bed continuous-flow reactor equipped with gas chromatography (GC) detection. Before the reaction, the ZnO-ZrO₂ catalyst (0.12 g, diluted with 0.48 g quartz sand) needs to be pretreated in a H₂ or N₂ stream (0.1 MPa and 20 ml min⁻¹) at given temperatures. The reaction was conducted under reaction conditions of 5.0 MPa, 24000 ml g⁻¹ h⁻¹, 320 to 315 °C, V(H₂)/V(CO₂)/V(Ar)=72:24:4. The exit gas from the reactor was maintained at 150 °C and immediately transported to the sample valve of the GC (Agilent 7890B), which was equipped with thermal conductivity (TCD) and flame ionization detectors (FIDs). Porapak N and 5A molecular sieve packed columns (2 m × 3.175 mm; Agilent) were connected to TCD, whereas TG-BOND Q capillary columns were connected to FID.

Reaction systems for different assemblies

The reaction of almost all modules were evaluated in 100 mM HEPES (pH 7.5) containing 100 mM NaCl, 5 mM MgCl₂, 10 μM ZnSO₄, and other ingredients as mentioned below. Except for C1b and C1b-C3a, 100 mM Tris-HCl (pH 8.5) was used to replace 100 mM HEPES (pH 7.5).

C1a: 250 mM sodium formate, 100 mM NADH and 4 mg ml⁻¹ fadh;

C1b: 1 M methanol, 100 mM NAD⁺ and 3 KU ml⁻¹ adh;

C1c: 50 mM sodium formate, 1.5 mM NADH, 10 mM ATP, 0.1 mM CoA, 3.7 mg ml⁻¹ acs, 0.2 mg ml⁻¹ acdh, 0.024 mg ml⁻¹ fdh and 0.1 mg ml⁻¹ ppa;

C1d: 50 mM sodium formate, 0.5 mM NADH, 10 mM ATP, 0.1 mM CoA, 2 mM 2-Mercaptoethanol, 0.24 mg ml⁻¹ acka, 1.2 mg ml⁻¹ pta, 0.2 mg ml⁻¹ acdh and 0.024 mg ml⁻¹ fdh;

C1e: 20 mM methanol, 1 U ml⁻¹ aox and 300 U ml⁻¹ cat;

C3a: 10 mM ATP, 0.5 mM TPP, 5 mg ml⁻¹ fls, 0.1 mg ml⁻¹ dak and 0.14 g L⁻¹ tpi and varied concentrations of formaldehyde;

C6a: 3 mM GAP, 3 mM DHA, 0.3 mg ml⁻¹ fsa, 0.17 mg ml⁻¹ pgi;

C6b: 3 mM GAP, 3 mM DHAP, 0.1 mg ml⁻¹ fba, 0.2 mg ml⁻¹ FBP and 0.17 mg ml⁻¹ pgi, 100 μM EDTA;

C6c: 3 mM GAP, 3 mM DHAP, 0.3 mg ml⁻¹ fbap and 0.17 mg ml⁻¹ pgi;

Cna: 5 mM G-6-P, 10 mg L⁻¹ dextrin, 0.275 mg ml⁻¹ pgm and 0.13 mg ml⁻¹ αGP;

Cnb: 5 mM G-6-P, 10 mM ATP, 10 mg L⁻¹ dextrin, 0.1 mg ml⁻¹ ppa, 0.275 mg ml⁻¹ pgm, 0.46 mg ml⁻¹ agp and 0.235 mg ml⁻¹ ss;

C1a+C3a: 250 mM sodium formate, 100 mM NADH and 4 mg ml⁻¹ fadh, 0.5 mM TPP, 10 mg ml⁻¹ fls, 0.14 mg ml⁻¹ tpi, 0.1 mg ml⁻¹ dak, 10 mM ATP;

C1b+C3a: 1 M methanol, 100 mM NAD⁺ and 3 KU ml⁻¹ adh, 0.5 mM TPP, 10 mg ml⁻¹ fls, 0.14 mg ml⁻¹ tpi, 0.1 mg ml⁻¹ dak;

C1c+C3a: 250 mM sodium formate, 0.5 mM TPP, 10 mg ml⁻¹ fls, 0.14 mg ml⁻¹ tpi, 0.1 mg ml⁻¹ dak, 10 mM ATP, 3.7 mg ml⁻¹ acs, 0.2 mg ml⁻¹ acdh, 1.5 mM NADH, 0.1 mM CoA, 0.1 mg ml⁻¹ ppa, 0.024 mg ml⁻¹ fdh;

C1d+C3a: 250 mM sodium formate, 0.5 mM TPP, 10 mg ml⁻¹ fls, 0.14 mg ml⁻¹ tpi, 0.1 mg ml⁻¹ dak, 10 mM ATP, 0.5 mM NADH, 0.1 mM CoA, 2 mM β-mercaptopethanol, 0.24 mg ml⁻¹ acka, 1.2 mg ml⁻¹ pta, 0.2 mg ml⁻¹ acdh, 0.024 mg ml⁻¹ fdh;

C1e+C3a: 0.5 mM TPP, 10 g L⁻¹ fls, 0.14 g L⁻¹ tpi, 0.1 g L⁻¹ dak, 5 mM ATP, 20 mM methanol, 1 U ml⁻¹ aox and 300 U ml⁻¹ cat;

(C1e+C3a) + C6a: 0.5 mM TPP, 10 g L⁻¹ fls, 20 mM methanol, 1 U ml⁻¹ aox, 300 U ml⁻¹ cat, 0.035 mg ml⁻¹ dak, 0.33 mg ml⁻¹ tpi, 0.3 mg ml⁻¹ fsa, 0.023 mg ml⁻¹ pgi, 10 mM ATP;

(C1e+C3a) + C6b: 0.5 mM TPP, 10 mg ml⁻¹ fls, 20 mM methanol, 1 U ml⁻¹ aox, 300 U ml⁻¹ cat, 0.035 mg ml⁻¹ dak, 0.33 mg ml⁻¹ tpi, 0.05 mg ml⁻¹ fba, 0.2 mg ml⁻¹ fbp, 0.023 mg ml⁻¹ pgi, 10 mM ATP, 100 μM EDTA;

(C1e+C3a) + C6b*: 0.5 mM TPP, 10 mg ml⁻¹ fls, 20 mM methanol, 1 U ml⁻¹ aox, 300 U ml⁻¹ cat, 0.035 mg ml⁻¹ dak, 0.33 mg ml⁻¹ tpi, 0.05 mg ml⁻¹ fba, 0.2 mg ml⁻¹ fbp, 0.023 mg ml⁻¹ pgi, 1 mM ADP, 0.2 mM polyphosphate, 0.22 mg ml⁻¹ ppk, 100 μM EDTA;

(C1e+C3a+C6b*) + Cna: 20 mM methanol, 1 U ml⁻¹ aox, 300 U ml⁻¹ cat, 0.5 mM TPP, 10 g L⁻¹ fls, 0.03525 g L⁻¹ dak, 0.3315 g L⁻¹ tpi, 0.05 g L⁻¹ fba, 0.2 g L⁻¹ fbp, 0.023 g L⁻¹ pgi, 1 g L⁻¹ αGP, 0.113 g L⁻¹ pgm, 10 mg L⁻¹ dextrin, 1 mM ADP, 0.2 mM polyphosphate, 0.22 g L⁻¹ ppk, 100 μM EDTA;

(C1e+C3a+C6b*) + Cnb: Table S3 for ASAP 1.0;

Partial C3a+C6b (for Fig. 2D): 100 μM EDTA, 25 mM DHA, 1 mM ADP, 0.4 mM polyphosphate, 0.77 mg ml⁻¹ dak, 0.33 mg ml⁻¹ tpi, 0.15 mg ml⁻¹ fba, 0.069 mg ml⁻¹ pgi, 0.44 mg ml⁻¹ ppk, 0.3 mg ml⁻¹ fbp or its variants and additional 0.2 mM polyphosphate was added into the system every hour;

Partial C3a+C6b+Cnb (for Fig. 2G and Fig. S10D): 100 μM mM EDTA, 3 mM DHA, 100 μM mM EDTA, 1 mM ADP, 0.077 mg ml⁻¹ dak, 0.2 mM polyphosphate, 0.22 mg ml⁻¹ppk, 10 mg L⁻¹ dextrin, 0.33 mg ml⁻¹ tpi, 0.15 mg ml⁻¹ fba, 0.43 mg ml⁻¹ fbp-AG^R, 0.069 mg ml⁻¹ pgi, 0.113 mg ml⁻¹ pgm, 0.2 mg ml⁻¹ ppa, 1 mg ml⁻¹ agp or its variants, 0.5 mg ml⁻¹ ss.

When 25 mM DHA as substrate, 0.2 mg ml⁻¹ dak, 0.4 mM polyphosphate, 0.44 mg ml⁻¹ ppk, 100 mg L⁻¹ dextrin were used instead, and additional 0.2 mM polyphosphate was added every hour;

Competition system (for Fig. 2F): 0.113 mg ml⁻¹ pgm, 1 mg ml⁻¹ agp or its variants, 0.5 mg ml⁻¹ ss, 0.2 mg ml⁻¹ ppa, 0.44 mg ml⁻¹ ppk, 100 mg L⁻¹ dextrin, 0.4 mM polyphosphate, 1 mM ADP, 10 mM G-6-P, 0.2 mg ml⁻¹ dak, 25 mM DHA.

Quantification of intermediates in ASAP

If necessary, the reactions were terminated by a 5-min water boiling, or by perchloric acid and KOH (51), unless otherwise stated. Corresponding standard curves were established for quantification of each analyte.

Methanol: Methanol was quantified by gas chromatography as reported previously (52), and the samples were treated with fadh and NAD⁺ to eliminate the residual formaldehyde before gas chromatography.

Formaldehyde: Formaldehyde was quantified by the acetylacetone method (53). A 250 μl sample (diluted, if necessary) was reacted with 25 μl acetylacetone solution (0.02 M acetylacetone, 0.05 M acetic acid, 2 M ammonium acetate). After incubation at 60 °C for 15 min, the mixture was cooled down, centrifuged and analyzed at 414 nm.

DHAP and GAP: DHAP and GAP were quantified by a glyceraldehyde-3-phosphate dehydrogenase (GAPDH)-based method (54). Properly diluted samples were terminated and coupled with 100 mM HEPES buffer (pH 7.5), 20 U ml⁻¹ GAPDH, 20 U ml⁻¹ tpi (if necessary), 10 mM NAD⁺, and 4 mM arsenate. The amount of DHAP or/and GAP was calculated by equilibrium absorption at 340 nm according to a GAP standard curve.

G-6-P: G-6-P was quantified by a glucose-6-phosphate dehydrogenase (G6PDH)-based method. Properly diluted samples were coupled with 100 mM HEPES buffer (pH 7.5), 20 U ml⁻¹

G6PDH and 10 mM NAD⁺. The amount of G-6-P was calculated by equilibrium absorption at 340 nm according to a G-6-P standard curve.

Starch: Synthetic amylose or amylopectin was degraded into glucose by Total Starch Assay Kit and then the glucose was determined by Glucose Assay kit. All the procedures followed the instructions. Quantity of amylose or amylopectin was given as glucose equivalent in either mass concentration or molar concentration.

GC-MS analysis

GC-MS was specifically used for determining the ratio between DHA and GA of different fls variants and for detection of ¹³C-labeled DHA. Samples were quenched by heating at 100 °C for 5 min and prepared by derivatization as previously reported (29). Electron ionization (EI) GC-MS analyses were performed with a model 7890A GC (Agilent) with a DB-5 fused silica capillary column (30 m length, 0.25 mm inner diameter, 0.25 μm film thickness) coupled to an Agilent 7200 Q-TOF mass selective detector; Injections were performed by a model 7683B autosampler. The GC oven was programmed from 60 °C (held for 1 min) to 100 °C at 5 °C min⁻¹, to 300 °C at 25 °C min⁻¹ and then held for 5 min; the injection port temperature was 250 °C, and the transfer line temperature was 280 °C. The carrier gas, ultra-high purity helium, flowed at a constant rate of 1.2 ml min⁻¹. For full-scan data acquisition, the MS scanned from 35 to 550 atomic mass units. For DHA and GALD quantification, authentic standards (Sigma) were used to generate calibration curves by use of the ion resulting from loss of a methyl group from the trimethylsilyl group during electron impact ionization ([M-CH₃]⁺: m/z 312 for GALD and 414 for DHA). Data analysis for GC-MS was performed with Mass Hunter software (Agilent, USA) and NIST Database.

LC-MS analysis

LC-MS was specifically used for detection of ¹³C-labeled DHAP&GAP, F-1,6-BP, F-6-P&G-6-P&G-1-P, ADPG and glucose degraded from synthesized starch. A UHPLC LC-30A system (Shimadzu, Japan) equipped with a Triple TOF 6600 mass spectrometer (Sciex, USA) was used for LC-MS/MS analysis. The samples were separated using an Xbridge BEH amide column (100 mm × 2.1 mm, 1.7 μm) (Waters, USA). Solvents were composed of water/acetonitrile/ammonium acetate/ammonium hydroxide (A: 100%/0%/25 mM/10 mM, B: 0%/100%/0 mM/0 mM). The LC method was: 0–2 min, 95% B; 2–18 min, 95–65% B; 18–20 min, 65–40% B; 20–22 min, 40% B; 20–20.1 min, 40–95% B; and 22.1–30 min, 95% B. A flow rate of 0.3 ml/min was employed. The MS parameters were as follows: ESI source; negative mode; ion voltage 4500 V; declustering potential 80 V; source temperature 550 °C; curtain gas, 35 psi; nebulizer gas, 55 psi; and heater gas, 55 psi. Each scan cycle contained one TOF MS survey scan and 15 MS/MS scans. The mass ranges were m/z 63–1000 for TOF MS, and m/z 30–1000 for MS/MS. Acquisition of MS/MS spectra was controlled by the information-dependent acquisition (IDA) function of the Analyst TF 1.7 software (Sciex, USA) with dynamic background subtraction on. Mass accuracy was calibrated by automated calibrant delivery system (Sciex, USA) interfaced to the second inlet of the DuoSpray source. Calibration was performed for every five samples. Data analysis for LC-MS/MS was performed with PeakView 2.0 software (Sciex, USA).

Calculations of starch synthesis rate of ASAP

About 12 g catalyst is needed to support 1-liter biological system. However, considering that spatially and temporally separation of CO₂ hydrogenation with biological system and the extremely high stability of ZnO-ZrO₂ catalyst (more than 500 hours) (34), we suggested that 12 g

catalysts could successively produce 1500 g methanol to support about 500 batches of 1-liters biological reaction. For each batch, only about 0.024 mg ZnO-ZrO₂ catalyst is needed. Therefore, the starch synthesis rate of ASAP 3.0 is calculated on 0.024 g L⁻¹ chemical catalyst and 10.34 g L⁻¹ biological enzymes.

The computational analysis for parent fls and variants

The backrub module in Rosetta suite (55) was used to predict the structures of the fls variants with cofactor thiamine diphosphate (TPP). Then the POVME2 (56) package was used to calculate the volume changes of the binding pockets. The RosettaLigand application (57) from Rosetta program suite version 3.5 was used to dock substrate DHA into the structures of wild-type and mutant fls. The DHA structure was obtained from the PubChem (58) and a total of 144 different DHA conformers were generated using OpenBabel version 2.4 (59). After three docking stages (see XML scripts), a total of 10,000 docking models were generated in the whole simulation process. The docking models were ranked by the substrate binding energy and total energy. The top 100 models were clustered by calibur (60) and the representative model of the largest cluster was identified as the candidate. All molecular graphics were generated using PyMOL educational version (61).

¹H NMR Spectroscopy analysis of synthetic starch

The synthetic starch was precipitated by ethanol as described previously (62) and dissolved in *d*₆-DMSO at 80 °C for ¹H NMR spectroscopic analysis. TFA was added to the sample right before the NMR measurement, and about 600 µl sample was transferred into 5 mm NMR tubes. ¹H NMR spectra were recorded at 298.2 K on a Bruker AVANCE III 600 MHz NMR spectrometer (Bruker Biospin, Germany), operating at 600.18 MHz for proton frequency, using a QCI CryoProbe with z-gradient. (7.47 µs 90 pulse, and a relaxation delay of 1.00 s, 16 scans, *d*₆-DMSO).

Supplementary Text

Computational design for potential starch synthesis pathway from C1 compounds

The possible pathways from one-carbon (C1) compounds of formic acid and methanol to starch were calculated by using the combination of combinatorial algorithm and flux balance analysis (comb-FBA) algorithm and reaction set provided by previous work (24). Simulations were performed using the COBRAPy toolbox in Python (25). Two starch synthetic reactions (ADP-α-D-glucose + Glucopyranose_n_1 => starch + ADP, α-D-glucopyranose-1-phosphate + Glucopyranose_n_1 => starch + Pi), one exchange reaction (Glucopyranose_n_1 <=>), five experimentally verified ATLAS aldolase reactions and one artificially designed formolase (fls)-catalyzed reaction from FALD to dihydroxyacetone (DHA) (21) were added to form the main reaction set, which contained 6568 reactions. Each of two reaction sets (set¹⁵ containing 15 formate utilization reactions and set⁸ containing 8 methanol utilization reactions) were used as the combinatorial reaction sets for pathway calculation (Table S2). All combinations with no more than three reactions from the combinatorial reaction set were generated and were introduced into main reaction set one by one to calculate the optimal starch synthesis pathway with less reaction steps and less ATP consumption using pFBA. A total of 667 ($C_{15}^1 + C_{15}^2 + C_{15}^3 + C_8^1 + C_8^2 + C_8^3 = 667$) times of pFBA were performed. A total of 4 pathways with no more than 20 steps were

calculated (Fig. S1). Two most concise starch synthesis pathways from formic acid or methanol involving only 8 reactions were successfully drafted (Fig. S1A). These pathways have the advantages of short steps, carbon-conserving (without carbon loss), low energy consumption (only one molecule energy consumption per molecule starch monomer production), and is more valuable for *in vitro* and *in vivo* applications because this is a linear pathway which is not dependent on the availability of circulating substrates compared to the natural RuMP, serine cycle, and loop pathways predicted in this work (Fig. S1B&C) and the author's previous paper (24). The predicted results also indicate that FLS is essential for the linear conversion of one-carbon to three-carbon building block GAP, which in turn enables the conversion pathway from one-carbon to six-carbon polymeric starch in this study to be only 8 steps and linearity.

Construction of functional modules for synthetic starch pathway

To realize the computationally designed pathways *in vitro*, we divided the two pathways into four kinds of modules, which are more manageable (Fig. S1). C1 module, including chemical or electrochemical reaction, converts CO₂ into formaldehyde, C3 module then condenses formaldehyde to D-glyceraldehyde 3-phosphate (GAP), C6 module subsequently transforms GAP to D-glucose-6-phosphate (G-6-P) and Cn module finally polymerizes G-6-P into starch.

C1 modules: Since chemically or electrochemically reducing CO₂ into C1 compounds was well established (63, 34), C1 modules were constructed only from formic acid and methanol, respectively. We first constructed module C1a with formic acid as substrate using formaldehyde dehydrogenase (fadH) from *Burkholderia multivorans* (Fig. S2A) (64) and module C1b using alcohol dehydrogenase (adh) from *Saccharomyces cerevisiae*, with extra energy conserved in NADH (Fig. S2B). Modules C1a and C1b are most energy efficient, however, they produced marginal formaldehyde at the cost of high concentration of substrates and cofactors to overcome the extremely unfavorable equilibrium (Fig. S2F&G).

Two substitutive C1 modules coupled with ATP consumption were drafted by exploring the substrate promiscuity of enzymes. Module C1c (Fig. S2C) was *in vitro* constructed based on previous report (21). We also constructed C1d (Fig. S2D), where formic acid was first phosphorylated by acetate kinase (ackA) from *E. coli* into formyl phosphate, and then converted to formyl-CoA by phosphotransacetylase (pta) from *E. coli* for subsequent reduction by the reported acetaldehyde dehydrogenase (acdH) (21, 27). Note that thought the pta from *M. thermophila* displayed the highest activity towards acetyl-phosphate (Table S1), the pta from *E. coli* gave the best performance in C1d construction. In coupling with ATP consumption step, both C1c and C1d are thermodynamically more favorable than C1a and produced more formaldehyde at much lower level of substrate and cofactor (Fig. S2G). Finally, we constructed thermodynamically favorable module C1e (Fig. S2E), in which methanol was directly oxidized to formaldehyde by alcohol oxidase (aox) from *Pichia pastoris* in consuming oxygen. C1e efficiently produced 11 mM formaldehyde in 0.5 hour (Fig. S2G). To fully functionalize each module, we also introduced auxiliary pyrophosphatase (ppa) into C1c module for driving the reaction toward desired direction by hydrolyzing the byproduct pyrophosphate, formate dehydrogenases (fdh) into C1c and C1d modules for regeneration of reducing equivalents, and catalase (cat) into C1e module for detoxifying hydrogen peroxide (Table S1).

C3 modules: The C3a module (Fig. S3A) was constructed *in vitro* based on computationally designed formolase (fls) for the carboligation reaction (21), dihydroxyacetone kinase (dak) for

phosphorylation and triose-phosphate isomerase (tpi) for isomerization. After optimizing the dosage of enzymes and cofactor, C3a successfully produced desired C3 compounds at different concentrations of formaldehyde (Fig. S3C).

C6 modules: To convert C3 compounds to the desired C6 products, we initially constructed the C6a module (Fig. S4A), in which DHA and GAP were condensed into D-fructose-6-phosphate (F-6-P) by fructose-six phosphate aldolase (fsa) from *E. coli* and then isomerized to target D-glucose-6-phosphate (G-6-P) by pgi from *E. coli*. We also constructed C6b (Fig. S4B), where DHAP and GAP are reversibly converted to D-fructose-1,6-bisphosphate (F-1,6-BP) by fructose-bisphosphate aldolase (fba) from *E. coli*, then dephosphorylated by fructose-bisphosphatase (fbp) from *E. coli* and isomerized to G-6-P by pgi. Although fbp from *Synechococcus* PCC 7942 is twice as active as *E. coli* originated fbp, it is inhibited by phosphate, which will be accumulated in our system. Therefore, we chose *E. coli* fbp for C6b construction. Both C6a and C6b could efficiently produce G-6-P from the corresponding C3 substrate supplied by C3 module (Fig. S4E).

We also constructed C6c (Fig. S4C), where DHAP and GAP were irreversible condensed and dephosphorylated into F-6-P and organic phosphate (Pi) by the bifunctional fructose-1,6-bisphosphate aldolase/phosphatase (fbap) from *Cenarchaeum symbiosum*, then F-6-P was isomerized to G-6-P by pgi. C6c module is featured with irreversibility for aldol addition reaction, which may provide advantages when competitive glycolysis pathway is presented. However, bifunctional fbap, mostly found in thermophilic archaea (65, 66), displayed an extremely low activity at ambient temperature (Table S1), resulting in the poor performance of C6c (Fig. S4E).

Cn modules: For starch synthesis from G-6-P, we initially constructed the Cna module (Fig. S5A) according the drafted starch synthesis pathway. In Cna, G-6-P is isomerized to α -D-glucose-1-phosphate (G-1-P) by phosphoglucomutase (pgm) from *Lactococcus Lactis* and then polymerized into amylose starch by α -glucan phosphorylase (α GP). α GP, which plays an essential role in starch degradation and utilization (67), was extensively applied to catalyze the reverse reaction for amylose synthesis either directly with G-1-P as substrate, or by providing G-1-P from sucrose or cellulose (62, 68, 69).

We also constructed the Cnb module (Fig. S5B), in which G-6-P is isomerized to G-1-P by pgm, then converted to adenosine diphosphate glucose (ADPG) by ADP-Glc pyrophosphorylase (agp) from *E. coli* and polymerized into amylose by starch synthesis (ss) from *E. coli*. Both Cn modules were found to produce amylose starch from G-6-P (Fig. S5D). If desired, the starch branching enzyme (sbe) from *Vibrio vulnificus* was included to produce amylopectin starch (35).

It is worthwhile to note that the evaluation of different C1, C3, C6 and Cn modules was performed in very specific conditions and the productivity may not reflect the potentials of each module, since these results are highly dependent not only on the module enzymes (varied in species, concentrations and activities) but also on the activity of auxiliary enzymes and concentrations of cofactors (ATP, CoA, NADH, etc.).

Incompatibility between C1a-d modules and C3a module

Both *in vivo* and *in vitro*, the unfavorable equilibrium of a reaction can in principle be pushed by the following reaction which is thermodynamically favorable (70, 71). In our work, thermodynamically unfavorable module of C1a to C1d can be driven by favored C3a, at least

theoretically (Fig. S2F&S3B). However, the assembling these four C1 modules and C3a did not function as expected. We speculated that marginal formaldehyde production due to C1 module's unfavorable equilibrium and the extremely low formaldehyde affinity of fls from the C3a module (Table S4), making the assemblies kinetically unfeasible. In fact, formaldehyde affinity of fls is about 20-200 folds lower than that of 3-hexulose-6-phosphate synthase (hps), which condenses formaldehyde and ribulose 5-phosphate (Ru5P) in the RuMP cycle (72). To confirm our speculation, we accommodated hps and hpi (3-hexulose-6-phosphate isomerase) into C1d module by supplying with Ru5P. This produced about 3 mM G-6-P from 50 mM formic acid in 3 hours, which is much more efficient than the assembly of C1d-C3a (Fig. S7). To address this incompatibility of thermodynamics and kinetics between C1 and C3 modules, we constructed the thermodynamically favored C1e module to supply enough formaldehyde for C3a module. Our work in adapting C1 modules to the C3 module suggests that, besides the kinetic problems, incompatibility of thermodynamics and kinetics could be an obstacle when thermodynamically unfavorable reactions are followed by enzymes with low substrate affinity.

Incompatibility between C3a module and C6a module

To find the reasons behind the failure of C1e-C3a-C6a, we quantified the key intermediates in this ensemble and found that triose phosphates were significantly accumulated throughout the course of reaction, while DHA and F-6-P were barely detected (Fig. S8A). We speculated that the unbalanced enzyme activities between dak and fsa may cause DHA to be preferentially consumed by dak and thus the accumulation of triose phosphates (Fig. S8D). Kinetic-analysis in a constrained system with DHA as substrate confirmed that a lower level of dak resulted in a higher yield of F-6-P, but a lower conversion rate from DHA and that the increased dak level improved the conversion rate, but significantly decreased the yield (Fig. S8B). This trade-off between yield and conversion rate constitutes as an example of kinetic trap caused by the unbalanced activities of enzymes.

Besides the kinetic problem, we also analyzed the interplays between C1e-C3a and C6a module and found that glycolaldehyde (GA), the byproduct of fls (29), which will be accumulated in the assembly (Fig. S8A), inhibited the aldol addition of DHA to GAP by fsa (Fig. S8C). It was reported that GA can act as both donor and acceptor substrate for fsa and that GA shows a better affinity to the donor binding site of fsa relative to DHA (73). When DHA and GA co-present in the assembly of C1e-C3a-C6a (Fig. S8D), GA will inhibit the aldol addition of DHA by competing donor site of fsa. It is worthwhile to note that inhibition of GA can be more significant in C1e-C3a-C6a, where DHA was maintained less through successive consumption by dak, than in the test system. In fact, fsa, the key enzyme of C6a module, is so promiscuous that it catalyzes the aldol addition of different aldehydes and ketones (74, 75).

Inhibition of ADP and ATP on *E. coli* fbp of C6b module

Quantification of the key intermediates in the assembly of C1e-C3a-C6b suggested that the carbon flux ceased with D-fructose-1,6-bisphosphate (F-1,6-BP), the substrate of fructose-bisphosphatase (FBP) (Fig. S9A). Further analysis of the interplays between C1e-C3a and C6b suggested that ADP and ATP, the cofactors of dak of C3a module, may also inhibit the function of *E. coli* fbp of C6b module (Fig. S9B). The inhibition of AMP on *E. coli* fbp has been well studied both biochemically and crystallographically (30). Given that AMP functions at extremely low level and that mutations in fbp-A^R also alleviate AMP inhibition (31), it could be argued that the inhibition of ATP and ADP on *E. coli* fbp was caused by the marginal contamination of AMP

in reagents. There are three possible ways that ATP/ADP could be contaminated by AMP, 1) hydrolysis of ATP/ADP during reaction; 2) the AMP impurity in ATP/ADP agents; 3) hydrolysis of ATP/ADP during long-term storing.

The inhibitory effect of ATP/ADP on fbp was determined in a short time range of several minutes, such as in Figure 2B&C and Table S5. If 1) the hydrolysis of ATP/ADP is essential during this short time range, the rate of fbp would be declined along the time course to give a down-bent velocity curve due to the accumulated AMP, especially at the high concentration of ATP/ADP showing the inhibition. However, the velocity curve of fbp is a linear at all tested concentrations of ATP/ADP in the test time range, indicating at least that AMP from hydrolysis of ATP/ADP in the test time range is not determinant for ATP/ADP inhibition.

For the situations 2) and 3), where the contaminated AMP is a static concentration/ratio relative ATP/ADP during the short test time range, we calculated the IC₅₀ of ATP, ADP and AMP on wild type fbp and fbp-A^R, respectively. If the inhibition of ATP and ADP were to be caused by AMP contamination, the IC₅₀_{ATP}, IC₅₀_{ADP} on the wild type and mutant of fbp may be different with IC₅₀_{AMP}, depending on the amount of contaminated AMP. However, the fold-change of IC₅₀_{ATP} or IC₅₀_{ADP} between the mutant and wild type should be the same as that of IC₅₀_{AMP}, since AMP is the intrinsic reason for inhibition, certainly in the present assumption. However, the fold change of IC₅₀_{AMP} is 95.6, while that of IC₅₀_{ADP} and IC₅₀_{ATP} is about 19.2 and 1.4, respectively (Table S5), suggesting that the contaminated AMP from these two possible conditions is not the determinant for ATP/ADP inhibition.

Furthermore, almost 100% activity of FBP was inhibited by 10 mM ATP or ADP, while more than 10% fbp activity is left at 10 mM AMP (Fig. S9C, D&E), suggesting that at high concentration, ATP/ADP is the determinant for ATP/ADP inhibition.

These results suggest at least that the ATP/ADP, rather than AMP, is the determinant for inhibition in our system. However, our data can't exclude the minor inhibitory effect of contaminated AMP in our system in a long-time range, due to the extremely low function concentration of AMP and instability of ATP/ADP.

fbp-A^R and fbp-AG^R improved G-6-P synthesis by diminishing ATP and ADP inhibition

We constructed mutant fbp-A^R and fbp-AG^R with more resistance to ATP and ADP, and applied them in the partial ensemble of the pathway, resulting in a significantly improvement of G-6-P production from DHA (Fig. 2D). Given that fbp-A^R and fbp-AG^R also displayed a ~4-fold higher activity than the wild type (Table S1), it is possible that the beneficial effect of the mutants was caused by their increased activity. To clear this, we also constructed fbp-G^R, which shows a similarly high activity as fbp-A^R and fbp-AG^R (Table S1), but was still inhibited by ADP and ATP (Fig. S9D&E). We found that fbp-G^R only produced increased G-6-P by 2-fold after 4 hours, while fbp-A^R and fbp-AG^R increased that by ~9-fold (Fig. S9F and Fig. 2D). This result indicates that fbp-A^R and fbp-AG^R improved the efficiency of G-6-P synthesis mainly by diminishing the inhibition of ATP and ADP, rather than by their increased activity.

Unfavorable equilibrium and released Pi of upper part of pathway repress starch synthesis via αGP

The failure of assembly C1e-C3a-C6b and Cna promoted us to analyze the interplays between them. We found that inorganic phosphate, the concomitant product of fbp, severely represses the starch synthesis from G-1-P via αGP, essentially depending on the ratio of Pi to G-1-P, rather than

on the absolute concentration of Pi (Fig. S10A). This suggests that Pi may function by reinforcing the reverse reaction catalyzed by α GP. In the assembly, fbp releases Pi with the same stoichiometry as F-6-P. However, the unfavorable equilibrium from F-6-P to G-1-P could make the concentration of Pi 28-fold higher than G-1-P (Fig. S10B) to form a high Pi/G-1-P ratio to inhibit starch synthesis via α GP. We noticed that α GP was used to synthesize amylose from sucrose and cellobiose (62, 68). In the former system, sucrose was phosphorylated to produce G-1-P with a very favorable equilibrium, while in the latter system, although cellobiose phosphorylation is unfavorable, a glucose consuming process was included to push the reaction toward G-1-P production. Furthermore, both systems recycled phosphate to avoid forming high Pi/G-1-P ratio. Our results are in line with the previous conclusion that α GP functions as a degradative enzyme, rather than a synthetic enzyme, under physiological conditions (67).

Screening of epPCR library and characterization of variants

fls (A28I-A394G-G419N-A480W-L90T-W89K-R188H) (21) was used as the parent for the first epPCR library generation. 2000 clones from each epPCR library were screened. After three rounds of epPCR library screening, M3 (fls+I28L/N283H/T90L) from the third round were identified. fls and M3 were characterized in detail for their kinetic parameters at 30 °C (Fig. S12A). Table S4 summarized the apparent k_{cat} and K_{half} values of parent fls and M3 by fitting the initial velocity of DHA generation to the Hill equation. The k_{cat} value of M3 is 1.6-fold higher than the starting enzyme fls. fls was known to product byproduct glycolaldehyde (GA) in addition to dihydroxyacetone (DHA) (29). We also characterized the product preference of wild type fls and fls-M3. As shown in Fig. S12B, fls produced about 25% and 55% GA at 2 mM and 10 mM formaldehyde, respectively. While, fls-M3 only produced about 9% and 24% GA at corresponding conditions. These results indicate that mutations I28L/N283H/T90L improved not only the kinetics, but also product preference of fls.

Insight of fls variants by molecular dynamic analysis

To figure out how the identified amino acid substitutions improved the enzyme activity of fls-M3, we predicted the structures of mutant fls and docked the product DHA into the active center of the parent fls and variant M3. The cofactor thiamine diphosphate (TPP) and the nearby residues from the chain-chain interface constituted the active center of the enzymes. The docking experiments show that the DHA molecules were stably binding to the active sites of the wild-type and mutant fls. The substitution I28L was found to be located at the active sites and was considered to be a key factor for the enzyme activity improvement. The conformation changes in mutation I28L and residue F484 had a joint contribution to the enzyme reaction efficiency improvement. On one hand, the substitution I28L enlarged the volume of substrate binding pocket about 2 Å³ by the side-chain conformation change (Fig. S12C&D), on the other hand, the obvious rotamer change at F484 induced by mutation I28L narrowed the substrate access gate which decreased the K_{half} value at a certain extent (Fig. S12E&F).

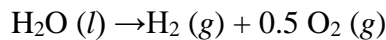
The substitution N283H and T90L were found far away from the active center and located in the chain-chain interface of M3. The substitution N283H not only introduced an extra hydrogen bond to the main-chain oxygen of H415, but also formed a strong π-N-π interaction with two vertical tyrosine residues, which improve the rigidity of the backbone conformation of the enzyme (Fig. S12G). In terms of substitution T90L, the hydrophobic interactions between threonine side chain with surrounding residues like I116, L418 and Y417 were significantly enhanced by

replacing the hydroxyethyl group with a big isobutyl group of leucine (Fig. S12H). Therefore, the substitution N283H and T90L mainly contributed to the stability improvement of the enzyme.

Energy efficiency calculation

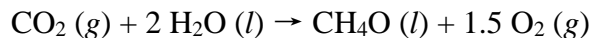
The theoretical hydrogen-to-methanol energy efficiency (η_{HME}) and methanol-to-starch energy efficiency (η_{MSE}) was calculated based on the Gibbs free energy gain ($\Delta_r G^\circ$) as previous work (PMID: 27257255). The Gibbs free energy gain ($\Delta_r G^\circ$) of chemicals, along with the corresponding chemical reactions, are listed in the following:

Hydrogen formation:



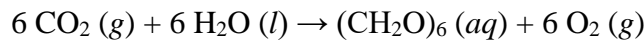
$$\Delta_r G^\circ_{\text{hydrogen}} \sim -\Delta_c H^\circ_{\text{hydrogen}} = 285.8 \text{ kJ mol}^{-1}$$

Methanol formation:



$$\Delta_r G^\circ_{\text{methanol}} \sim -\Delta_c H^\circ_{\text{methanol}} = 726.1 \text{ kJ mol}^{-1}$$

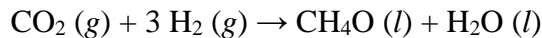
Starch (glucose) formation:



$$\Delta_r G^\circ_{\text{starch}} = 2882.2 \text{ kJ mol}^{-1}$$

Calculation of the theoretical hydrogen-to-methanol energy efficiency (η_{HME}):

The theoretical η_{HME} is calculated based on the following equations without considering the extra energy consumption for chemical catalyst production and for the high temperature and pressure in this chemical step. The energy input is $3 \times \Delta_r G^\circ_{\text{hydrogen}}$ and the energy output is $1 \times \Delta_r G^\circ_{\text{methanol}}$. Then, the theoretical η_{HME} is **85%**.



$$\text{Output energy} = 1 \times \Delta_r G^\circ_{\text{methanol}}$$

$$\text{Input energy} = 3 \times \Delta_r G^\circ_{\text{hydrogen}}$$

Estimation of the practical hydrogen-to-methanol energy efficiency ($\eta_{\text{HME}'}$):

The chemical step of CO_2 hydrogenation to produce methanol need the high temperature and pressure relative to typical biological processes. Thus, the energy for high temperature and pressure needed to be considered. The practical hydrogen-to-methanol energy efficiency ($\eta_{\text{HME}'}$,

considering the energy for high temperature and pressure) is estimated based on the previous work (37). The hydrogen for methanol production is calculated as $2274 \text{ m}^3 \text{ t}^{-1}$ methanol based on the electrolysis electricity of 39.3 GJ t^{-1} methanol and the electricity to hydrogen yield of $4.8 \text{ kWh m}^{-3} \text{ H}_2$. According to the Gibbs free energy gain of H_2 ($\Delta_f G^\circ_{\text{hydrogen}} = 285.8 \text{ kJ mol}^{-1}$) and density of H_2 (89.9 g m^{-3}), the input energy of H_2 is 29.2 GJ t^{-1} methanol. The energy input for high temperature and pressure and CO_2 capture is 4.3 GJ t^{-1} methanol. Then according to the Gibbs free energy gain of methanol ($\Delta_f G^\circ_{\text{methanol}} = 726.1 \text{ kJ mol}^{-1}$), the output energy is 22.7 GJ t^{-1} methanol. Thus, the practical η_{HME} is **68%**.

Calculation of the theoretical methanol-to-starch energy efficiency (η_{MSE}):

The theoretical η_{MSE} is calculated based on the following equations. The energy input of ATP was calculated by converting to H_2 in assuming a stoichiometry of 2.5 ATP per NADH and 1 NADH per H_2 . Then, the energy input is $6 \times \Delta_f G^\circ_{\text{methanol}}$ and $1.2 \times \Delta_f G^\circ_{\text{hydrogen}}$, and the energy output is $1 \times \Delta_f G^\circ_{\text{starch}}$. Thus, the theoretical η_{MSE} is **61%**.



$$\text{Output energy} = 1 \times \Delta_f G^\circ_{\text{starch}}$$

$$\text{Input energy} = 6 \times \Delta_f G^\circ_{\text{methanol}} + 1.2 \times \Delta_f G^\circ_{\text{hydrogen}}$$

Calculation of the theoretical solar-to-starch energy efficiency (η_{SSE}):

The theoretical solar-to-starch energy efficiency (η_{SSE}) via ASAP was calculated based on the assumption of coupling with photovoltaic and water-electrolysis devices. In this scenario, the solar energy was first transferred into electricity (η_{SEE}), then electricity was transferred into hydrogen (η_{EHE}), then the hydrogen was used to produce methanol (η_{HME}), and the methanol was converted into starch (η_{MSE}). Thus, the theoretical solar-to-starch energy efficiency (η_{SSE}) can be calculated by $\eta_{\text{SEE}} \times \eta_{\text{EHE}} \times \eta_{\text{HME}} \times \eta_{\text{MSE}}$. With an attainable solar-to-electricity efficiency (η_{SEE}) of **20%** for silicon crystalline solar cell (17), an attainable electricity-to-hydrogen efficiency (η_{EHE}) of **85%** for PEM electrolysis (18), a theoretical η_{HME} of **85%** and a theoretical η_{MSE} of **61%**, the theoretical maximal solar-to-starch efficiency ($\eta_{\text{SSE}} = \eta_{\text{SEE}} \times \eta_{\text{EHE}} \times \eta_{\text{HME}} \times \eta_{\text{MSE}}$) via ASAP will be **9%**.

Considering the extra energy consumption for high temperature and pressure in CO_2 hydrogenation step, the theoretical solar-to-starch efficiency ($\eta_{\text{SSE}} = \eta_{\text{SEE}} \times \eta_{\text{EHE}} \times \eta_{\text{HME}'} \times \eta_{\text{MSE}}$) via ASAP will be **7%**.

Fig. S1.

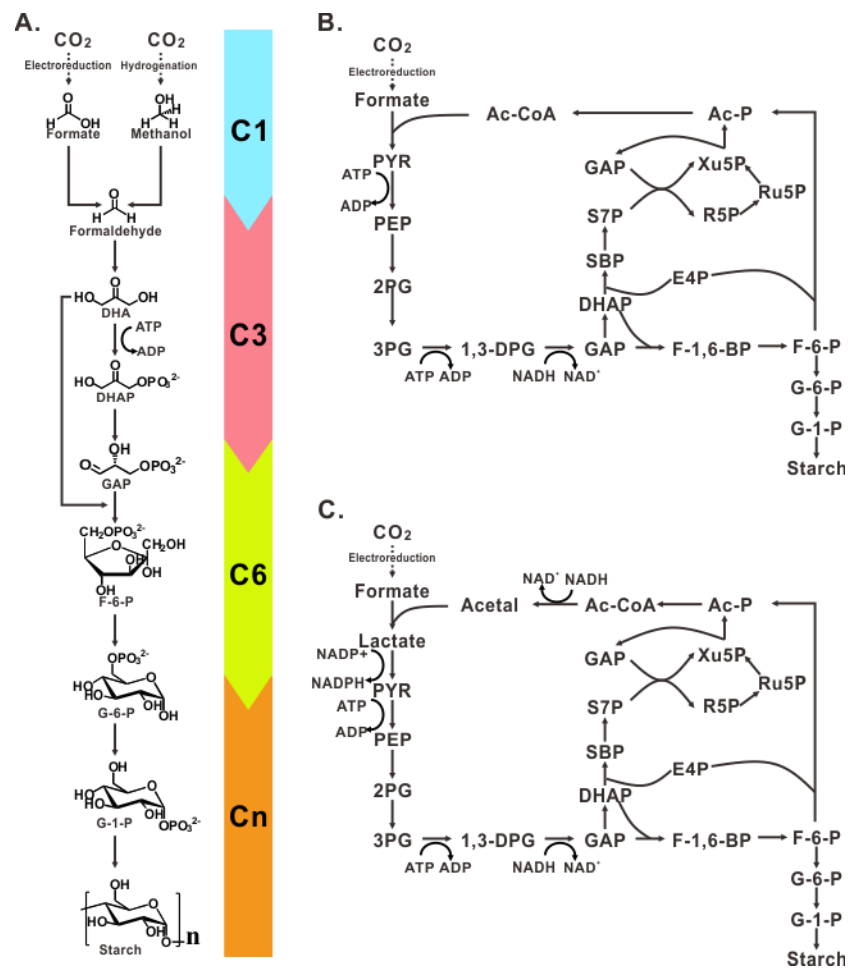


Figure S1. Artificial starch pathways drafted by computational pathway design.

(A) Two linear computationally-designed starch synthesis pathways with formic acid or methanol as intermediates. Two most concise pathways for starch synthesis involves only 9 reactions from CO_2 . The pathways were divided into four individual modules. The modules are denoted by different color blocks. (B-C) Two circular computationally-designed starch synthesis pathways with formic acid as intermediates. Acronyms: DHA, dihydroxyacetone; DHAP, dihydroxyacetone phosphate; GAP, D-glyceraldehyde 3-phosphate; F-6-P, D-fructose-6-phosphate; G-6-P, D-glucose-6-phosphate; G-1-P, α -D-Glucose-1-Phosphate; PYR, pyruvate; PEP, phosphoenolpyruvate; 2PG, 2-phospho-D-glycerate; 3PG, 3-phospho-D-glycerate; 1,3-DPG, 3-phospho-D-glyceroyl-phosphate; F-1,6-BP, D-fructose-1,6-bisphosphate; S7P, D-sedoheptulose 7-phosphate; SBP, D-sedoheptulose-1,7-bisphosphate; E4P, erythrose 4-phosphate; R5P, ribose 5-phosphate; Ru5P, ribulose 5-phosphate; Xu5P, xylulose 5-phosphate; Ac-P, acetyl phosphate; Ac-CoA, acetyl-CoA; Acetal, acetaldehyde.

Fig. S2.

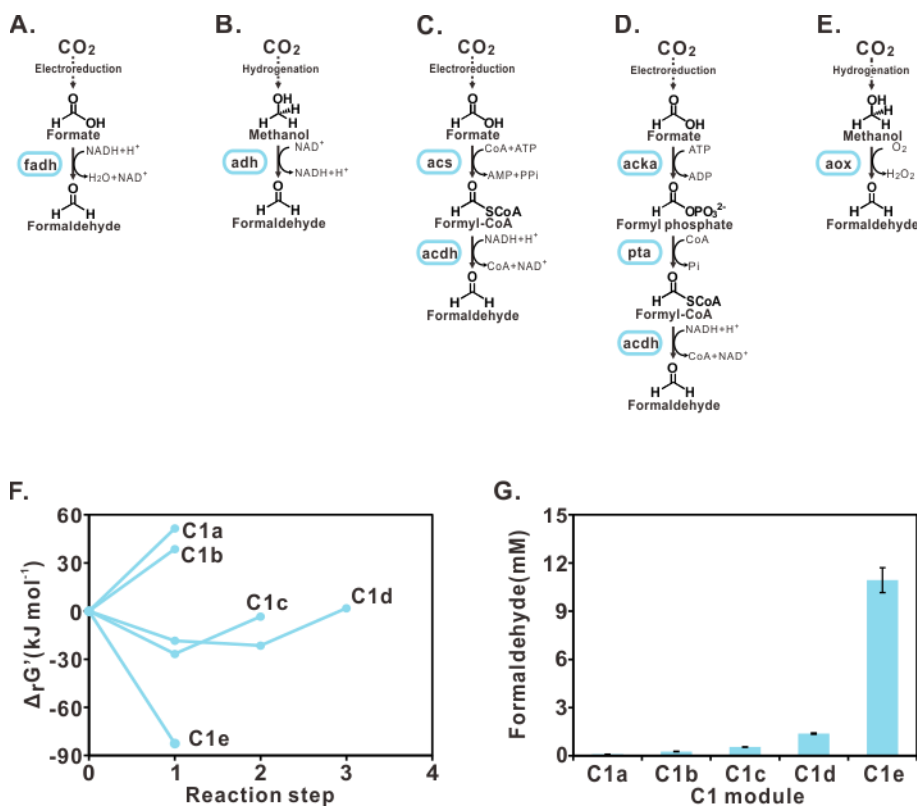


Figure S2. Construction and evaluation of C1 modules.

(A-E) Schematic representation of five C1 modules. (F) The Gibbs free energy profiles were calculated and estimated based on the data of reference (76). For C1 modules and following C3, C6 and Cn modules, the summerized Gibbs free energy profiles along with individual reactions for Δ_rG' were calculated at pH 7.5, ionic strength I = 0.20, and assuming the following metabolite concentrations: the substrates = 1 mM, intermediates = 1 mM, products = 1 mM, ATP = 2 mM, ADP = 2 mM, AMP = 2 mM, NADH = 2 mM, NAD⁺ = 2 mM, CoA = 0.5 mM, if necessary. The biological origins of enzymes in the C1 modules are indicated in Table S1. (G) Formaldehyde production of five C1 modules with formic acid and methanol as substrates, respectively (see supplementary material). The data was obtained for C1a and C1b after 3 hours, C1c and C1d after 1 hour, C1e after 0.5 hour. Values are means, and error bars indicate SD (n=3 replicates). Acronyms: fadh, formaldehyde dehydrogenase; adh, alcohol dehydrogenase; acs, acetate-CoA synthetase; acdh, acetaldehyde dehydrogenase; acka, acetate kinase; pta, phosphotransacetylase; aox, alcohol oxidase. The auxiliary pyrophosphatase (ppa) was introduced into C1c module for driving the reaction forward by hydrolyzing its byproduct pyrophosphate, formate dehydrogenases (fdh) into C1c and C1d modules for regeneration of reducing equivalents, and catalase (cat) into C1e module for detoxifying hydrogen peroxide.

Fig. S3.

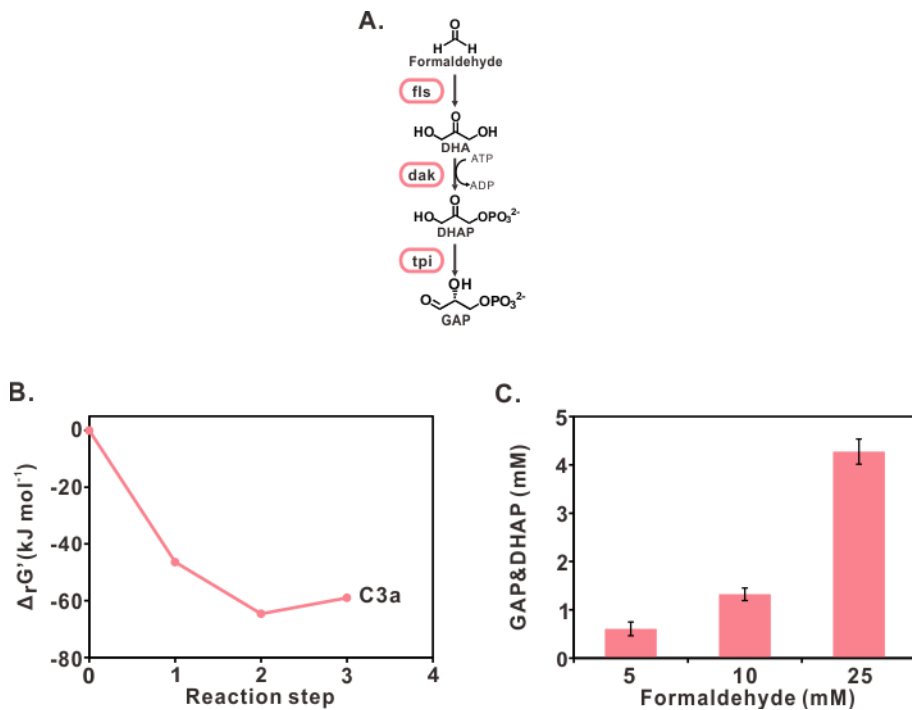


Figure S3. Construction and evaluation of C3 module.

(A) Schematic representation of C3a module. (B) Shown are the summerized Gibbs free energy profile of C3 module. The calculation is same with C1 modules. The biological origins of enzymes in C3 module are indicated in Table S1. (C) GAP & DHAP production of C3a modules with formaldehyde as substrate in corresponding reaction systems (see supplementary material). The data was obtained after 2 hours. Values are means, and error bars indicate SD (n=3 replicates). Acronyms: fls, formolase; dak, dihydroxyacetone kinase; tpi, triose-phosphate isomerase; DHA, dihydroxyacetone; DHAP, dihydroxyacetone phosphate; GAP, D-glyceraldehyde 3-phosphate.

Fig. S4.

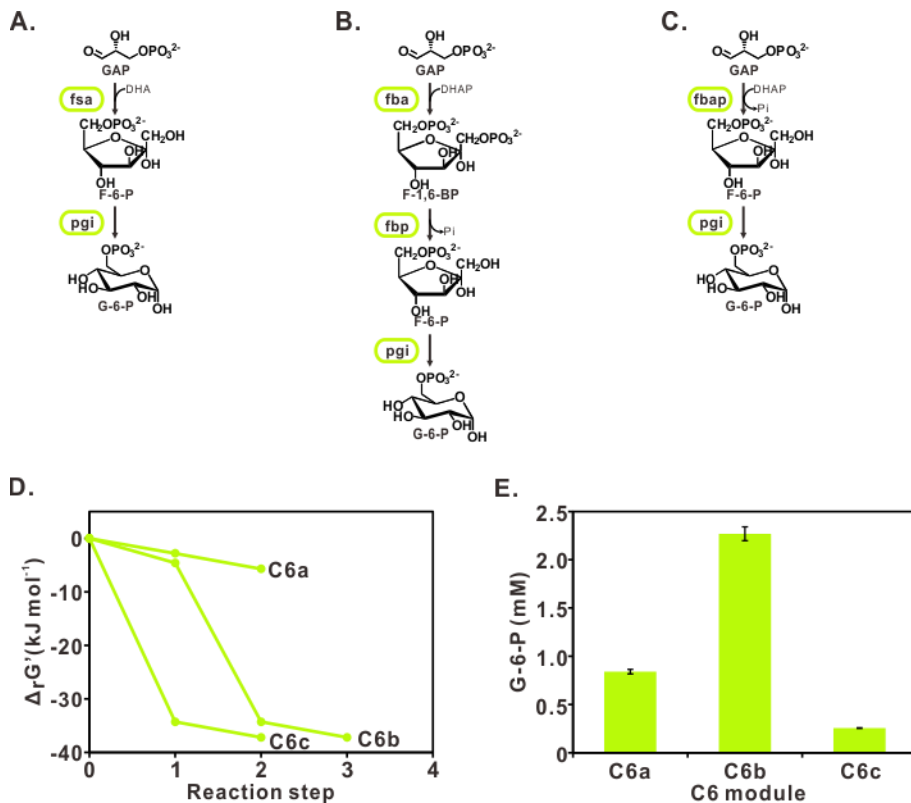


Figure S4. Construction and evaluation of C6 modules.

(A-C) Schematic representation of three C6 modules. (D) Shown are the summerized Gibbs free energy profile of C6 modules. The calculation is same with C1 modules. The biological origins of enzymes in C6 modules are indicated in Table S1. (E) G-6-P production of three C6 modules with C3 as substrates in corresponding reaction systems (see supplementary material). The data was obtained after 0.5 hour. Values are means, and error bars indicate SD (n=3 replicates). Acronyms: fsa, fructose-6-phosphate aldolase; pgi, phosphoglucose isomerase; fba, fructose-bisphosphate aldolase; fbp, fructose-bisphosphatase; F-1,6-BP, D-fructose-1,6-bisphosphate; F-6-P, D-fructose-6-phosphate; G-6-P, D-glucose-6-phosphate.

Fig. S5.

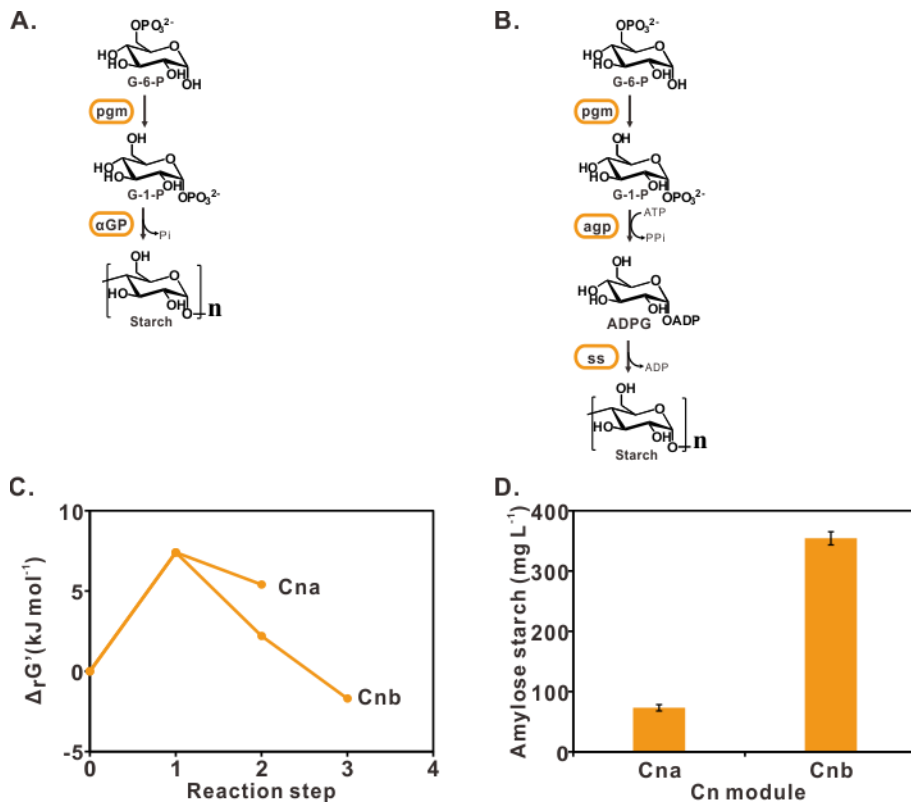


Figure S5. Construction and evaluation of Cn modules.

(A-B) Schematic representation of two Cn modules. **(C)** Shown are the summerized Gibbs free energy profile of C6 modules. The calculation is same with C1 modules. The biological origins of enzymes in C6 modules are indicated in Table S1. Δ_rG' for the reaction catalyzed by αGP was calculated based on the equation: G-1-P + glucose = maltose + Pi and Δ_rG' for the reaction catalyzed by ss was calculated based on the equation: ADPG + glucose = maltose + ADP. The biological origins of enzymes in Cn modules are indicated in Table S1. **(D)** Amylose starch production of two Cn modules with G-6-P as substrate in the corresponding reaction systems (see supplementary material). The data for Cna was obtained after 2 hours and Cnb after 1 hour. The auxiliary pyrophosphatase (ppa) was also included in Cnb module. Values are means, and error bars indicate SD (n=3 replicates). Acronyms: pgm, phosphoglucomutase; αGP, α-glucan phosphorylase; agp, ADP-Glc pyrophosphorylase; ss, starch synthase; G-1-P, α-D-glucose-1-phosphate; ADPG, adenosine diphosphate glucose.

Fig. S6.

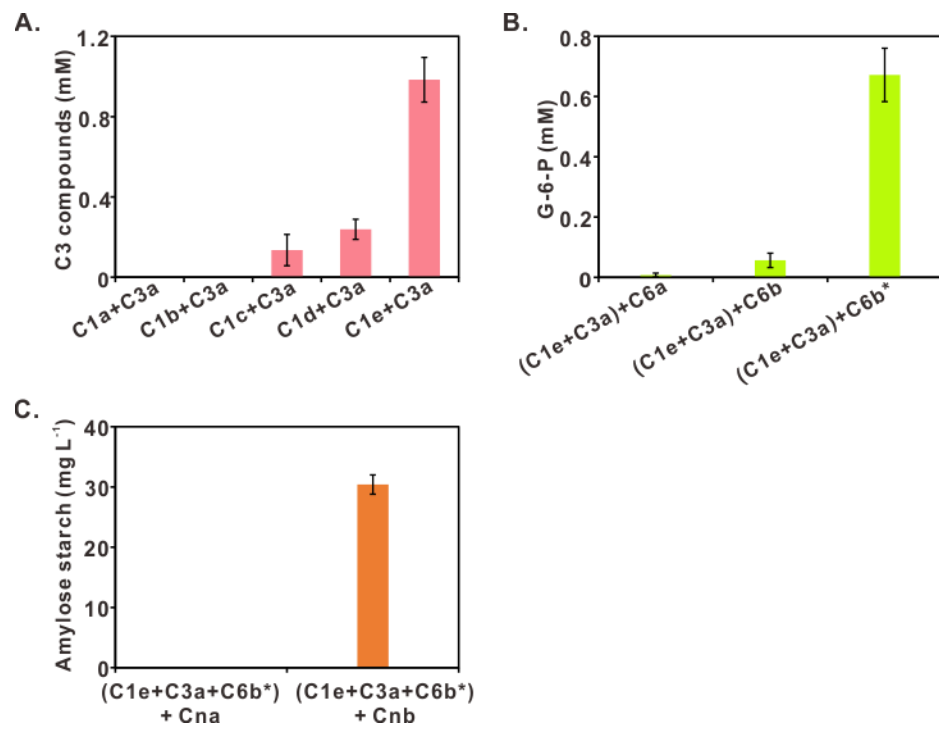


Figure S6. Stepwise assembling artificial starch pathway from C1 to Cn module.

(A) Assembling C1 modules with C3a module. The data for assembly of C1a to C1d was obtained after 6 hours and C1e after 2 hours. C3 compounds mean DHAP and GAP. (B) Assembling C1e+C3a with C6 modules. The C6c with poor performance was not applied for assembling. The data was obtained after 6 hours. *ATP regeneration system was applied. (C) Assembling C1e+C3a+C6b* with Cn modules. The data was obtained after 10 hours. See supplementary material for the reaction system of each assembly. Values are means, and error bars indicate SD (n=3 replicates).

Fig. S7.

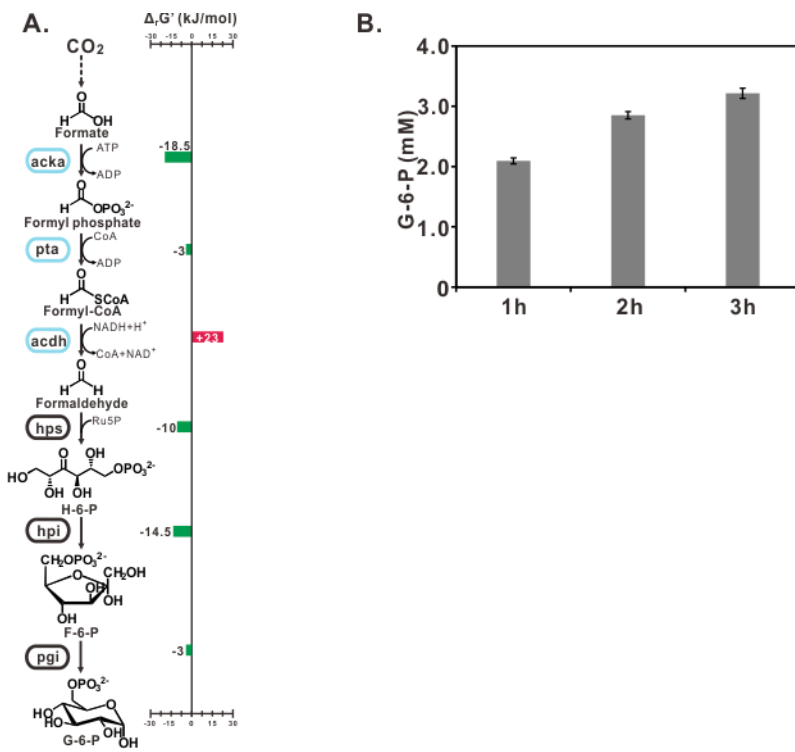


Figure S7. Assembling C1d module with part of RuMP cycle.

(A) The schematic representation and Gibbs free energy profile of C1d module with 3-hexulose-6-phosphate synthase (hps) and 3-hexulose-6-phosphate isomerase (hpi) of the RuMP cycle. The Gibbs free energy profile is calculated same as C1 modules. (B) G-6-P production from formic acid via C1d and hps-hpi. The reaction was performed in the C1d reaction system plus 0.09 mg ml⁻¹ hps from *Bacillus methanolicus*, 0.08 mg ml⁻¹ hpi from *Bacillus methanolicus*, 0.069 mg ml⁻¹ pgi and 5 mM ribulose 5-phosphate (Ru5P). At the indicated time, the reaction was terminated and applied for enzymatic quantification by G6PDH as described in methods. Values are means, and error bars indicate SD (n=3 replicates).

Fig. S8.

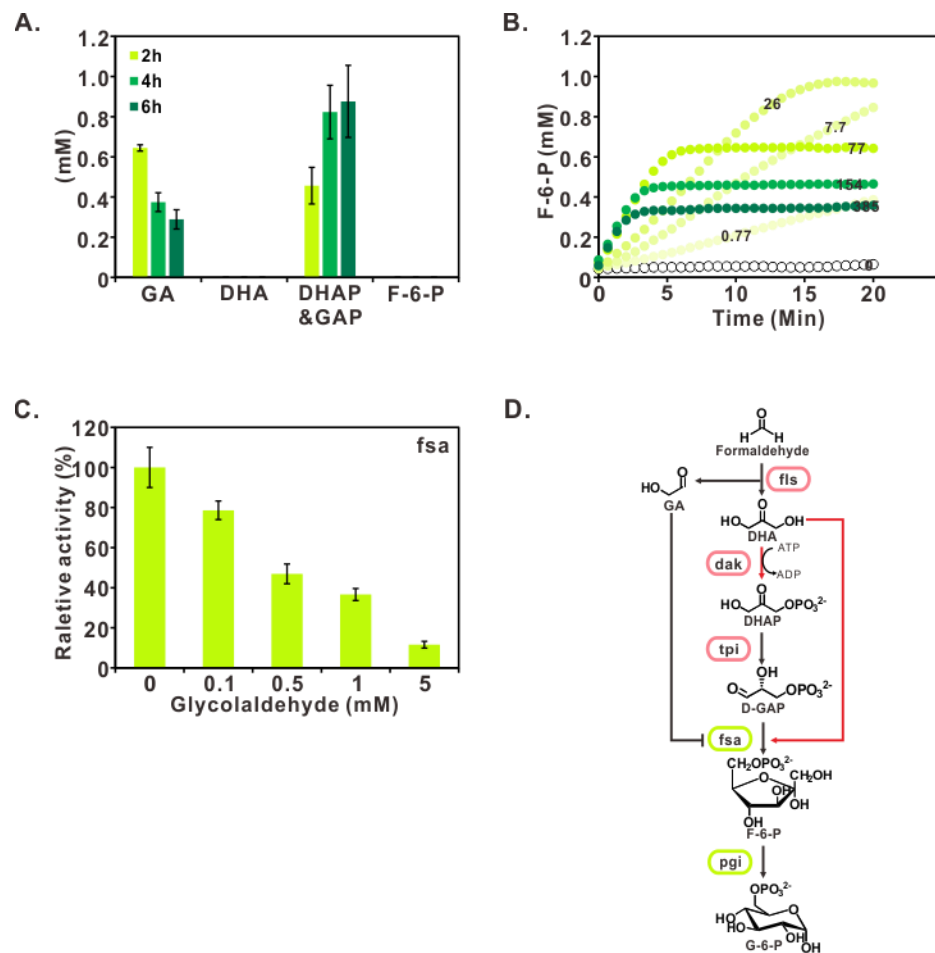


Figure S8. Incompatibility between C3a module and C6a module.

(A) Quantification of the main intermediates of the assembly of (C1e+C3a) + C6a at indicated time points. (B) Effect of dak level on F-6-P production from DHA. High level of dak may competitively consume DHA to accumulate triose phosphates and leave little DHA for fsa to synthesize F-6-P (as shown in Fig. S8D, red arrows). Analysis was performed in the reaction system including 2 mM DHA, 3 mM ATP, 3 mM NAD⁺, 0.33 mg ml⁻¹ tpi, 0.3 mg ml⁻¹ fsa, 0.023 mg ml⁻¹ pgi, 20 U ml⁻¹ G6PDH and indicated levels of dak (μ g ml⁻¹). (C) Inhibition of glycolaldehyde (GA) on fsa. The reaction system includes 2 mM DHA, 1 mM GAP, 2 mM NAD⁺, 0.3 mg ml⁻¹ fsa, 0.023 mg ml⁻¹ pgi and 20 U ml⁻¹ G6PDH. (D) The schematic representation of incompatibilities between C3a module and C6a module. Red arrows indicate two DHA-consuming reactions, catalyzed by dak and fsa, respectively. For A&C, values are means, and error bars indicate SD (n=3 replicates).

Fig. S9.

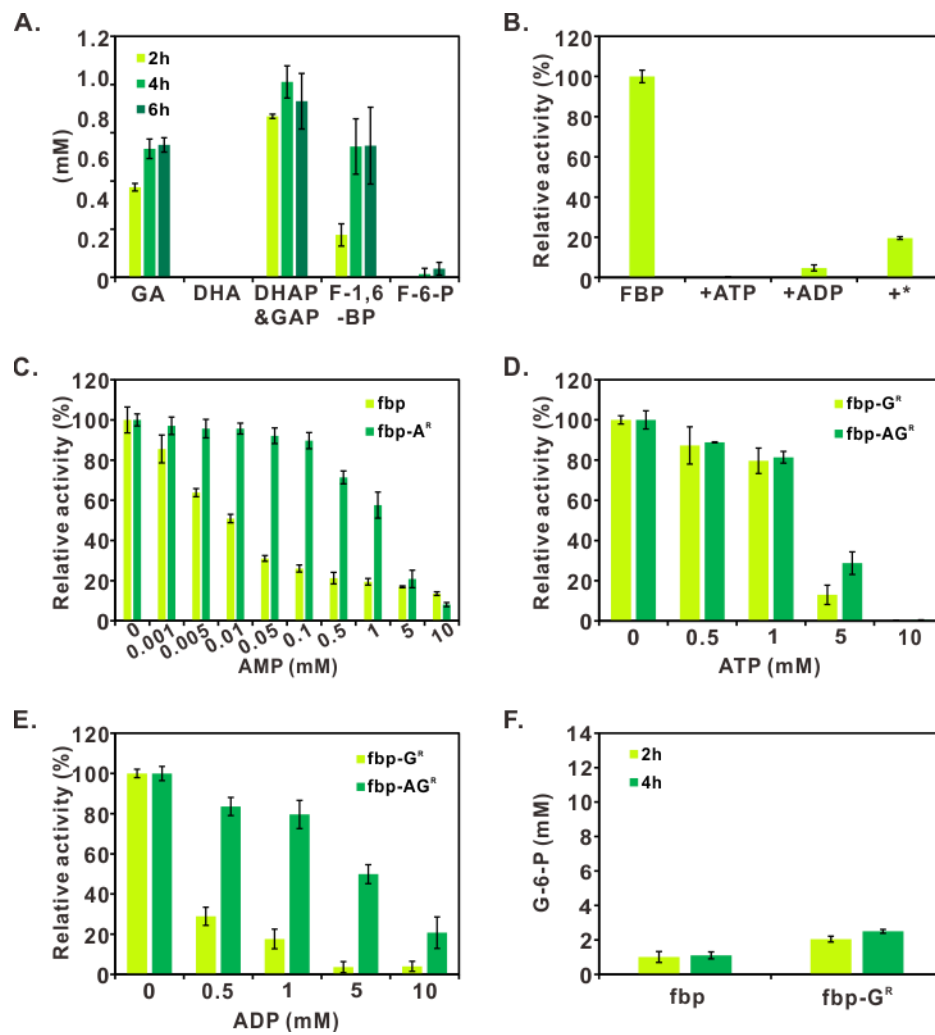


Figure S9. Incompatibility between cofactors and C6b module.

(A) Quantification of the main intermediates of the assembly of (C1e+C3a) + C6b at indicated time points. (B) Inhibitory effect of 10 mM ATP, 10 mM ADP and ATP regeneration system with 1 mM ATP and ADP (indicated as *) on *E. coli* fbp. ATP regeneration system contained 1 mM ADP, 0.2 mM polyphosphate and 0.22 mg ml⁻¹ ppk. The mutated residues in fbp-A^R are shown in blue. (C) Inhibition of AMP on fbp and fbp-A^R. (D-E) Inhibition of ATP and ADP on fbp-G^R and fbp-AG^R. (F) G-6-P production from 25 mM DHA via partial pathway in Fig. 2A with fbp and fbp-G^R, respectively. Values are means, and error bars indicate SD (n=3 replicates).

Fig. S10.

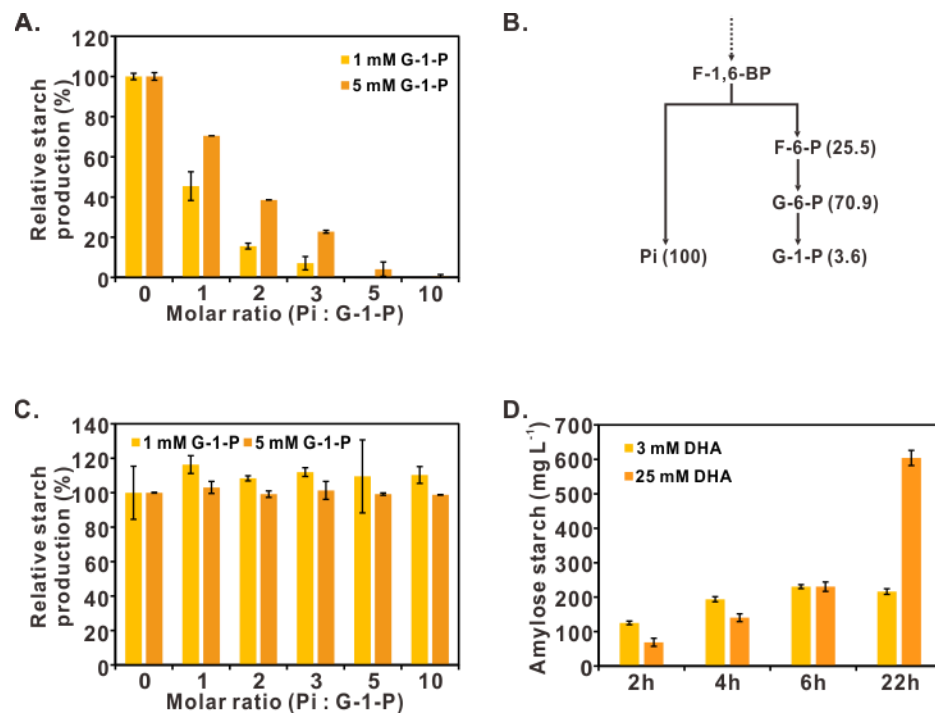


Figure S10. Incompatibility between C1e+C3a+C6b and Cn modules.

(A) Effect of molar ratio of phosphate (Pi) to G-1-P on starch synthesis via α GP in the reaction system including 10 mg L⁻¹ dextrin and 0.13 mg ml⁻¹ α GP, 1 mM or 5 mM G-1-P, and indicated levels of Pi. The data was obtained after 8 hours. (B) The theoretical Pi/G-1-P ratio in the assembly of (C1e+C3a+C6b) + Cna. The theoretical Pi/G-1-P was determined by assuming that the reactions from F-1, 6-BP to Pi and G-1-P had reached a chemical equilibrium and G-1-P had not been consumed. In this condition, the amount of (F-6-P + G-6-P + G-1-P) should equal to the amount of Pi, and the amount of F-6-P, G-6-P and G-1-P will satisfy with their equilibrium formulations. Assuming the amount of Pi is 100, then, the amount of F-6-P, G-6-P and G-1-P will be calculated as 25.5, 70.9 and 3.6. (C) Effect of molar ratio of phosphate (Pi) to G-1-P on starch synthesis via app and ss of Cnb module. The data was obtained after 2 hours. (D) Amylose starch production from 3 mM or 25 mM DHA via the pathway as depicted in Fig. 2A. For A, C and G, values are means, and error bars indicate SD (n=3 replicates).

Fig. S11.

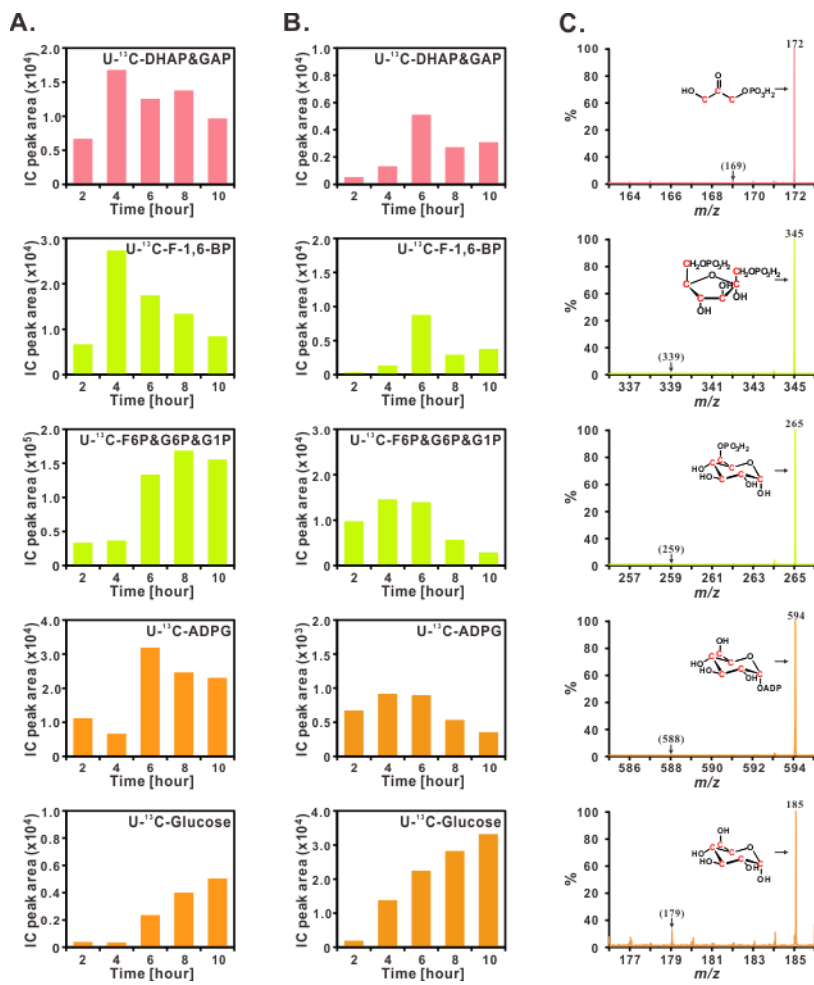


Figure S11. Dynamics analysis of ASAP 1.0 and 2.0.

Dynamics of key intermediates and product of ASAP 1.0 (**A**) and ASAP 2.0 (**B**) over 10 hours. Shown are the levels of uniformly ^{13}C -labeled intermediates. Isomers DHAP and GAP, and isomers F-6-P, G-6-P and G-1-P are indistinguishable via LC-MS. Starch was degraded into glucose before LC-MS analysis. (**C**)The mass spectra of ^{13}C -labeled intermediates. Mass of the ^{13}C -labeled intermediates is given as a lost a proton $[\text{M}-\text{H}]^-$, respectively. Mass of unlabeled intermediates and product is indicated in brackets.

Fig. S12.

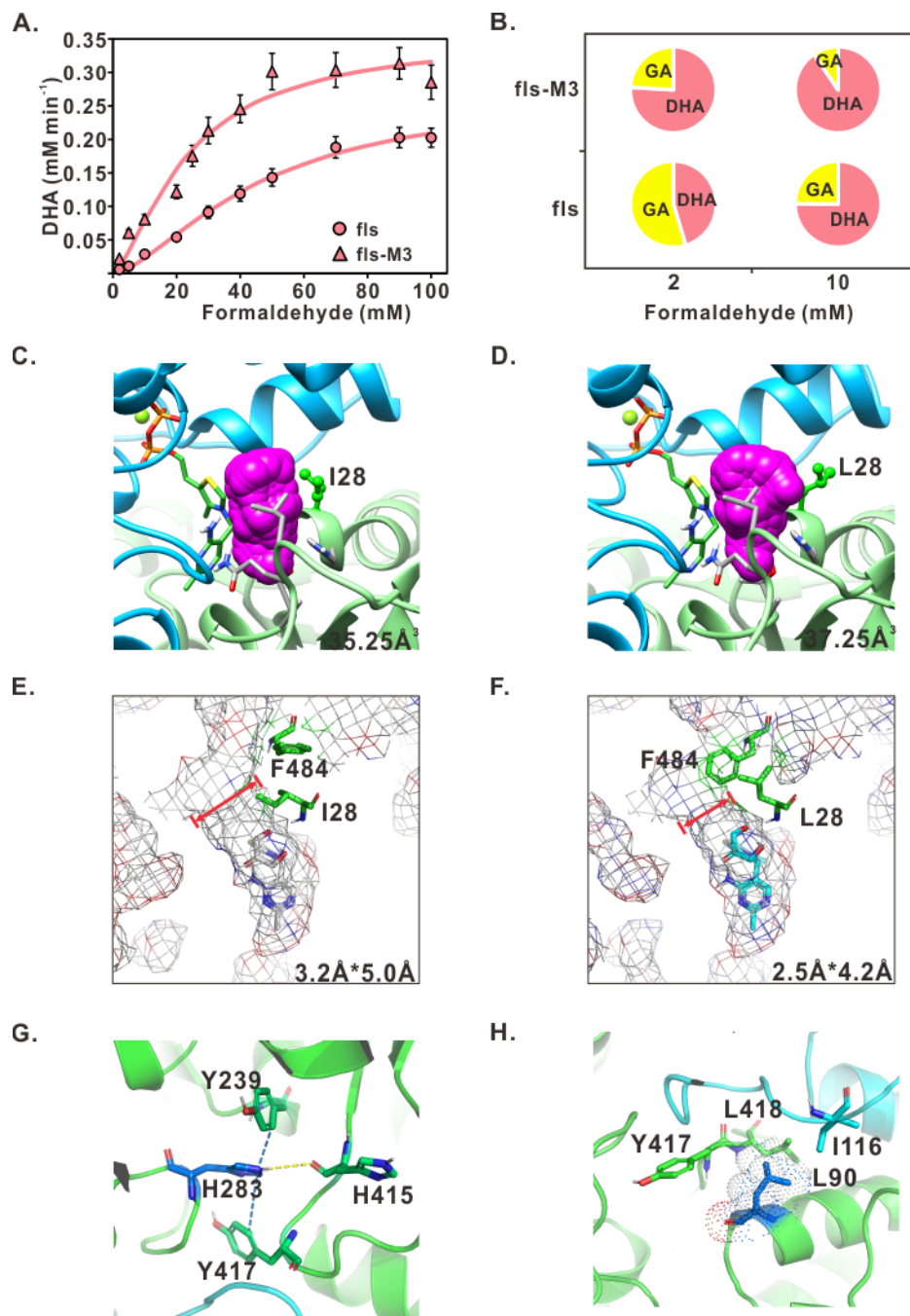


Figure S12. Characterization of fls and its variant.

(A) Michaelis-Menten graphs of fls parent and fls-M3. Values are means, and error bars indicate SD (n=3 replicates). (B) Percentage of DHA and the by-product glycolaldehyde (GA) of fls and fls-M3 at different concentrations of substrate formaldehyde. The pocket volume changes in the wild-type (C) and mutant fls (D). Pink spheres illustrated the volumes of the binding-pocket cavities. The radius changes of the substrate access gate in wild-type (E) and mutant (F) fls. The solvent access surface was shown as mesh and the gate radius of wild-type and mutant structures

were shown at the corner. The substrate DHA and cofactor TPP were shown as sticks. Key positions including 28 and 484 were shown as sticks and colored by green. (**G**) The structure changes nearby the residue 283 of mutant fls. The residues were shown as sticks. The residue 283 was colored in marine. (**H**) The local structural changes nearby the residue 90 of mutant fls. The T90L mutation introduced a hydrophobic group into the chain-chain interface of the enzymes. The residue 90 was colored by marine and shown as the dot representation.

Fig. S13.

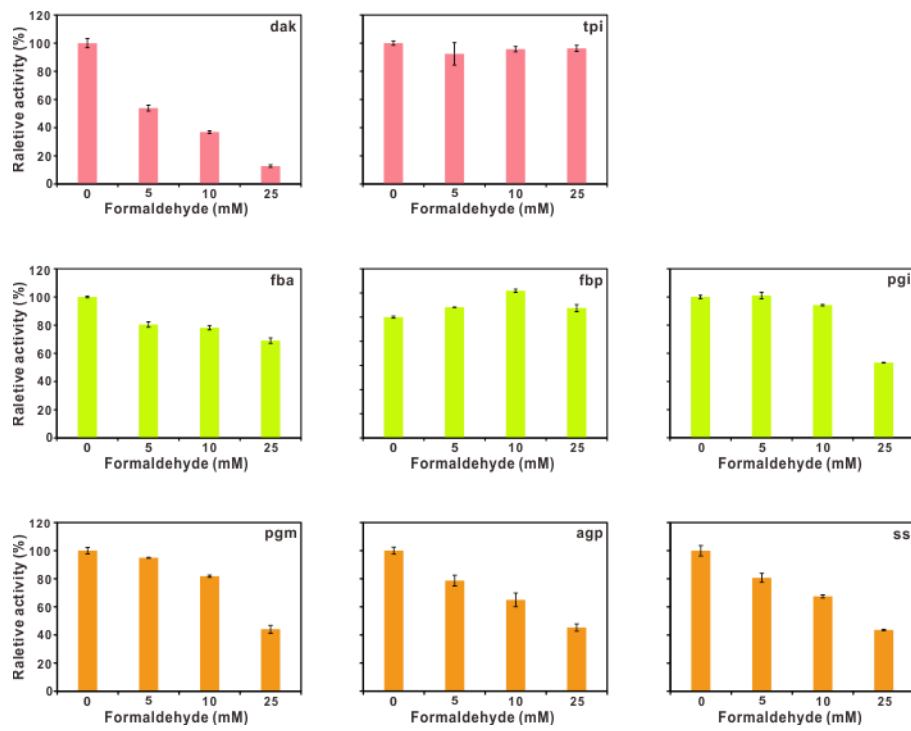


Figure S13. Toxic effect of formaldehyde on main enzymes of ASAP.

dak, tpi and pgi were performed similarly as kinetic assay in the presence of different concentration of formaldehyde. pgm was evaluated on the reversed reaction coupling with G6PDH. fba was performed on the reverse reaction coupling with GAPDH. fbp and agp were performed by detecting the release of phosphate group as the activity assay, and ss by detecting the formation of starch. Because 25 mM formaldehyde partially inhibited the activity of G6PDH, the inhibitory effect of formaldehyde on pgi and pgm was performed with extra G6PDH. Values are means, and error bars indicate SD (n=3 replicates).

Table S1.

Information list of enzymes for different modules.

Modules	ABB.	Enzyme full name	GenBank ID	Organism	k_{cat} (1 s ⁻¹)	K_m (mM)	Specific activity ($\mu\text{mol mg}^{-1} \text{min}^{-1}$)	Source of kinetic data
C1a	fadh	formaldehyde dehydrogenase	—	<i>Pseudomonas</i> sp.	—	—	1-6#	Sigma (F1879)
	fadh	formaldehyde dehydrogenase	BAG46824.1	<i>Burkholderia multivorans</i>	—	—	0.73#	This work
C1b	mdh	methanol dehydrogenase	AIE59127.1	<i>Bacillus methanolicus</i>	—	200	0.2	(77)
	adh	alcohol dehydrogenase	—	<i>Saccharomyces cerevisiae</i>	—	—	300#	Sigma (A7011)
C1c	acs	acetate-CoA synthetase	AAC77039.1	<i>Escherichia coli</i>	—	—	0.016	This work
	acdH	acetaldehyde dehydrogenase	CAC99712.1	<i>Listeria monocytogenes</i>	—	—	0.36†	This work
	acdH	acetaldehyde dehydrogenase	SDC77933.1	<i>Geotoga petraea</i>	—	—	0.034†	This work
	acdH	acetaldehyde dehydrogenase	APT75415.1	<i>Marinitoga</i> sp.1137	—	—	0.047†	This work
	acdH	acetaldehyde dehydrogenase	AAC74323.1	<i>Escherichia coli</i>	—	—	0.39†	This work
	acdH	acetaldehyde dehydrogenase	AAL20667.1	<i>Salmonella enterica</i>	—	—	0.2†	This work
C1d*	ackA	acetate kinase	AAC75356.1	<i>Escherichia coli</i>	1.11	41.55	—	This work
	ackA	acetate kinase	AAB18301.1	<i>Clostridium acetobutylicum</i>	0.79	44.96	—	This work
	ackA	acetate kinase	BAW30536.1	<i>Methanosarcina thermophila</i>	0.02	12.88	—	This work
	ackA	acetate kinase	AAN55929.1	<i>Shewanella oneidensis</i> MR-1	0.074	10.4	—	This work
	ackA	acetate kinase	AAD35363.1	<i>Thermotoga maritima</i>	0.0057	29.7	—	This work
	ackA	acetate kinase	AAL21238.1	<i>Salmonella enterica</i>	1.19	57.19	—	This work
	pta	phosphotransacetylase	AAC75511.1	<i>Escherichia coli</i>	—	—	0.063†	This work
	pta	phosphotransacetylase	AAK79708.1	<i>Clostridium acetobutylicum</i>	—	—	0.055†	This work
	pta	phosphotransacetylase	AAD36820.1	<i>Thermotoga maritima</i>	—	—	0.038†	This work
	pta	phosphotransacetylase	AAD36206.1	<i>Thermotoga maritima</i>	—	—	0.102†	This work
	pta	phosphotransacetylase	AKB12795.1	<i>Methanosarcina thermophila</i>	—	—	0.127†	This work
	pta	phosphotransacetylase	AAC75357.1	<i>Escherichia coli</i>	—	—	0.107†	This work
C1e	aox	alcohol oxidase	—	<i>Pichia pastoris</i>	—	—	10-40	Sigma (A2404)
C3a	fls	formolase	—	<i>Pseudomonas putida</i>	0.1457	34.14	—	This work
	gals	glycolaldehyde synthase	—	<i>Pseudomonas fluorescens</i>	0.43	59	—	(78)
	fls-M3	formolase	—	<i>Pseudomonas putida</i>	0.2375	23.59	—	This work
	dak	dihydroxyacetone kinase	AAC39490.1	<i>Pichia pastoris</i>	1.92	0.96	—	This work
	dak	dihydroxyacetone kinase	AEO55061.1	<i>Myceliophthora thermophila</i>	0.31	0.23	—	This work
	dak	dihydroxyacetone kinase	ODV85308.1	<i>Candida arabinofermentans</i>	1.44	0.39	—	This work
	dak	dihydroxyacetone kinase	EAQ87833.1	<i>Chaetomium globosum</i>	0.4	0.26	—	This work
	dak	dihydroxyacetone kinase	AHY10454.1	<i>Citrobacter freundii</i>	1.55	0.57	—	This work
	tpi	triose-phosphate isomerase	AAC76901.1	<i>Escherichia coli</i>	567	2.24	—	This work
	tpi	triose-phosphate isomerase	AAA88757.1	<i>Saccharomyces cerevisiae</i>	349	7.8	—	This work

	tpi	triose-phosphate isomerase	ABQ73190.1	<i>Mycobacterium tuberculosis</i>	188	3.37	—	This work
	tpi	triose-phosphate isomerase	BAW00817.1	<i>Thermus thermophilus</i>	135	1.25	—	This work
C6a	fsa	fructose-6-phosphate aldolase	AAC73912.2	<i>Escherichia coli</i>	0.26	1.33	—	This work
	fsa	fructose-6-phosphate aldolase	AAD35383.1	<i>Thermotoga maritima</i>	0.0065	0.064	—	This work
	pgi	phosphogluucose isomerase	AAC76995.1	<i>Escherichia coli</i>	244.98	0.36	—	This work
C6b*	fba	fructose-bisphosphate aldolase	AAC75158.2	<i>Escherichia coli</i>	0.75	0.52	—	This work
	fba	fructose-bisphosphate aldolase	CAA33111.1	<i>Saccharomyces cerevisiae</i>	0.57	0.755	—	This work
	fbp	fructose-bisphosphatase	AAC77189.1	<i>Escherichia coli</i>	—	—	1.58	This work
	fbp	fructose-bisphosphatase	ABB56537.1	<i>Synechococcus PCC 7942</i>	—	—	3.45	This work
	fbp	fructose-bisphosphatase	ABB58365.1	<i>Synechococcus PCC 7942</i>	—	—	0.43	This work
	fbp-A ^R	fructose-bisphosphatase	—	<i>Escherichia coli</i>	—	—	6.07	This work
	fbp-G ^R	fructose-bisphosphatase	—	<i>Escherichia coli</i>	—	—	6.13	This work
	fbp-AG ^R	fructose-bisphosphatase	—	<i>Escherichia coli</i>	—	—	5.4	This work
C6c*	fbap	fructose-1,6-bisphosphatase	ABK77197.1	<i>Cenarchaeum symbiosum</i>	0.01	0.45	—	This work
Cna	pgm	phosphoglucomutase	CAL97144.1	<i>Lactococcus lactis</i>	—	—	27.01	This work
	pgm	phosphoglucomutase	AAC73782.1	<i>Escherichia coli</i>	—	—	26.17	This work
	pgm	phosphoglucomutase	ABB56188.1	<i>Synechococcus PCC 7942</i>	—	—	0.13	This work
	pgm	phosphoglucomutase	ABB57298.1	<i>Synechococcus PCC 7942</i>	—	—	0.477	This work
	pgm	phosphoglucomutase	CAB12759.2	<i>Bacillus subtilis</i> 168	—	—	0.357	This work
	pgm	phosphoglucomutase	ABN52497.1	<i>Clostridium thermocellum</i>	—	—	2.607	This work
	pgm	phosphoglucomutase	AAM39942.1	<i>Xanthomonas campestris</i>	—	—	0.822	This work
	αGP	α-glucan phosphorylase	CAA36612.1	<i>Solanum tuberosum</i>	—	—	0.018	This work
	αGP	α-glucan phosphorylase	BAK00834.1	<i>Hordeum vulgare</i>	—	—	0.032	This work
	agp	ADP-glc pyrophosphorylase	AAC76455.1	<i>Escherichia coli</i>	—	—	0.378	This work
Cnb*	agp	ADP-glc pyrophosphorylase	ABB56635.1	<i>Synechococcus PCC 7942</i>	—	—	0.02	This work
	agp-M1	ADP-glc pyrophosphorylase	—	<i>Escherichia coli</i>	—	—	10.32	This work
	agp-M2	ADP-glc pyrophosphorylase	—	<i>Escherichia coli</i>	—	—	13.43	This work
	agp-M3	ADP-glc pyrophosphorylase	—	<i>Escherichia coli</i>	—	—	19.22	This work
	ss	starch synthase	AAC76454.1	<i>Escherichia coli</i>	—	—	0.27	This work
	ss	starch synthase	CAB15073.1	<i>Bacillus subtilis</i> 168	—	—	0.027	This work
	ssIII※	starch synthase	BAF49176.1	<i>Phaseolus vulgaris L.</i>	333	0.32	—	(79)
NADH re-generation	sbe	glycogen branching enzyme	ADV88080.1	<i>Vibrio vulnificus</i>	—	—	3.17	(35)
	fdh	formate dehydrogenases	BAC92737.1	<i>Thiobacillus</i> sp. KNK65MA	—	—	10	(80)
H ₂ O ₂ elimination	cat	catalase	CAB12710.2	<i>Bacillus subtilis</i> 168	—	—	37000	(81)
ATP re-generation	ppk	polyphosphate kinase	ABQ58103.1	<i>Mycobacterium tuberculosis</i>	50	0.001	—	(82)

PPi Hydrolyzation	ppa	pyrophosphatase	AAC77183.1	<i>Escherichia coli</i>	389	0.13	-	(83)
--------------------------	-----	-----------------	------------	-------------------------	-----	------	---	------

fls-M3: fls contains mutations of I28L, N283H and T90L; fbp-A^R: fbp contains mutations of K104Q and R132I; fbp-G^R: fbp contains mutations of Y210F and K218Q; fbp-AG^R: fbp contains mutations of K104Q, R132I, Y210F and K218Q; agp-M1: agp contains mutations of G336D; agp-M2: agp contains mutations of P295D; agp-M3: agp contains mutations of G336D and P295D. #: Kinetic parameters were determined on the reverse reaction; †: Their natural substrates were used to determine kinetic parameters; ≈: ssIII without TP domain; *: shared enzymes are not presented. Colored enzymes are used for modules construction.

Table S2.

The list of combinatorial reaction set used in comb-FBA for pathways design.

MetaCyc ID	Reaction	KEGG ID	EC number
FORMALDEHYDE-DEHYDROGENASE-RXN	FORMATE_c + NADH_c + 2.0 PROTON_c -> FORMALDEHYDE_c + NAD_c + WATER_c	R00604	1.2.1.46
GARTRANSFORMYL2-RXN	_5_45_PHOSPHO_45_RIBOSYL_45_GLYCINEA MIDE_c + FORMATE_c + ATP_c -> PROTON_c + _5_45_P_45_RIBOSYL_45_N_45_FORMYLGLY CINEAMIDE_c + ADP_c + Pi_c	R06974	2.1.2.-
RXN-10066	AICAR_c + FORMATE_c + ATP_c -> PHOSPHORIBOSYL_45_FORMAMIDO_45_CARBO XAMIDE_c + ADP_c + Pi_c	R06975	6.3.4.23
RXN0-1382	FORMATE_c + OXALYL_45_COA_c -> FORMYL_45_COA_c + OXALATE_c	R07290	2.8.3.16
RXN-17561	CPD_45_612_c + FORMATE_c + PROTON_c -> CPD_45_18974_c + WATER_c	--	3.7.1.M3
PYRUVFORMLY-RXN	FORMATE_c + ACETYL_45_COA_c -> PYRUVATE_c + CO_45_A_c	R00212	2.3.1.54
FORMATETHFLIG-RXN-THF/ATP/FORMATE//10-FORMYL-THF/ADP/Pi.38.	THF_c + ATP_c + FORMATE_c -> _10_45_FORMYL_45_THF_c + ADP_c + Pi_c	--	--
LACTATE-ALDOLASE-RXN	ACETALD_c + FORMATE_c -> L_45_LACTATE_c	R00753	4.1.2.36
FORMATE--DIHYDROFOLATE-LIGASE-RXN-DIHYDROFOLATE/FORMATE/ATP//CPD-14932/ADP/Pi.44.	DIHYDROFOLATE_c + FORMATE_c + ATP_c -> CPD_45_14932_c + ADP_c + Pi_c	--	--
FORMATETHFLIG-RXN-CPD-1301/ATP/FORMATE//CPD-17116/ADP/Pi.39.	CPD_45_1301_c + ATP_c + FORMATE_c -> CPD_45_17116_c + ADP_c + Pi_c	--	--
FORMATE-DEHYDROGENASE-NADP+-RXN	FORMATE_c + NADP_c -> CARBON_45_DIOXIDE_c + NADPH_c	R00134	1.17.1.10
RXN0-3281	FORMATE_c + Acceptor_c + PROTON_c -> CARBON_45_DIOXIDE_c + Donor_45_H2_c	--	1.17.98.e
RXN-12274	FORMATE_c + Oxidized_45_hydrogenase_45_3_c -> CARBON_45_DIOXIDE_c + Reduced_45_hydrogenase_45_3_c	--	--
1.2.1.2-RXN	FORMATE_c + NAD_c -> CARBON_45_DIOXIDE_c + NADH_c	R00519	1.17.1.9
FHLMULTI-RXN	PROTON_c + FORMATE_c -> CARBON_45_DIOXIDE_c + HYDROGEN_45_MOLECULE_c	--	--

RXN-8095	METOH_c + MTAC_c + PROTON_c -> METHYL_45_MTAC_c + WATER_c	--	2.1.1.90
METHTRANSBARK-RXN	METOH_c + CPD_45_8_c -> CPD_45_9_c + WATER_c	--	--
MTAMBARKMULTI-RXN	METOH_c + CoM_c -> Me_45_CoM_c + WATER_c	R09098	--
RXN-11451	METOH_c + Acceptor_c -> FORMALDEHYDE_c + Donor_45_H2_c	--	1.1.99.37
METHANOL-OXIDASE-RXN	OXYGEN_45_MOLECULE_c + METOH_c -> HYDROGEN_45_PEROXIDE_c + FORMALDEHYDE_c	R00608	1.1.3.13
METHANOL-DEHYDROGENASE-RXN	METOH_c + NAD_c -> PROTON_c + FORMALDEHYDE_c + NADH_c	R00605	1.1.1.244
RXN-14189	METOH_c + HYDROGEN_45_PEROXIDE_c -> FORMALDEHYDE_c + 2.0 WATER_c	R00602	1.11.1.6
RXN-2861	METOH_c + 2.0 Cytochromes_45_CL_45_Ox_c -> FORMALDEHYDE_c + 2.0 Cytochromes_45_CL_45_Red_c + 2.0 PROTON_c	--	1.1.2.7

Table S3.

Components for different versions of ASAP.

ABB.	ASAP 1.0	ASAP 2.0	ASAP 3.0	ASAP 3.1
Core enzymes (mg ml⁻¹)				
aox	0.15	0.15	0.75	0.75
fls	10			
fls-M3		5	5	5
dak	0.035	0.035	0.77	0.77
tpi	0.3315	0.3315	0.3315	0.3315
fba	0.1	0.1	0.15	0.15
fbp	0.2			
fbp-AG ^R		0.2	0.6	0.6
pgi	0.023	0.023	0.069	0.069
pgm	0.113	0.113	0.113	0.113
agp	0.2			
agp-M3		0.2	1	1
ss	0.2	0.2	0.5	0.5
sbe				0.019
Auxiliary enzymes (mg ml⁻¹)				
cat	0.021	0.021	0.42	0.42
ppk	0.22	0.22	0.44	0.44
ppa	0.05	0.05	0.2	0.2
Substrates				
Methanol	20 mM	20 mM		
Dextrin	10 mg L ⁻¹	10 mg L ⁻¹	50 mg L ⁻¹	50 mg L ⁻¹ L
ADP	1 mM	1 mM	1 mM	1 mM
Polyphosphate*	0.2 mM	0.2 mM	0.4 mM	0.4 mM

*: for ASAP 3.0 and 3.1, additional 0.2 mM polyphosphate was added at 140 min, 160 min, 180 min and 210 min, respectively.

Table S4.

Apparent kinetic constants of parent fls and its variants.

Variants	k_{cat} (s ⁻¹)	K_{half} (mM)	n
fls (Parent)	0.15 ± 0.01	34 ± 3	2.0 ± 0.3
M3 (fls+I28L/N283H/T90L)	0.24 ± 0.02	24 ± 4	1.5 ± 0.2

Values are means, and error bars indicate SD (n=3 replicates).

Table S5.IC₅₀ of adenosine phosphate on fbp and its variant.

	fbp		fbp-A ^R		Folds
	IC ₅₀ (μM)	R ²	IC ₅₀ (μM)	R ²	
AMP	14.2	0.93	1361	0.99	95.6
ADP	234.5	0.99	4510	0.96	19.2
ATP	1817	0.98	2590	0.91	1.4

IC₅₀ was calculated from the data of Fig. 2B&C and Fig. S9C by fitting to Dose-response - inhibition curve with variable slope.

Table S6.

List of plasmids.

Plasmids	Short description	Primer-F	Primer-R	Source
pET28a-fadh	pET28a based vector, carrying <i>fadh</i> gene from <i>Burkholderia multivorans</i> ; Kan ^r	CCCAAGCTTGCATGAGCA GCAATCGTGGC	CCGCTCGAGGGCTGC CAGCAGGCCGTG	This study
pET21b-acs	pET21b based vector, carrying <i>acs</i> gene from <i>Escherichia coli</i> MG1655; Amp ^r	CGCGGATCCGATGAGCCA AATTACAAACACAC	AAGGAAAAAAAGCGGC CGCCGATGGCATCGC GATAGC	This study
pET21b-acdh-Lm	pET21b based vector, carrying <i>acdh</i> gene from <i>Listeria monocytogenes</i> EGD-e; Amp ^r	CGCGGATCCGATGGCAAT TAAAGAAAATGCGGCC	AAGGAAAAAAAGCGGC CGCAACACCTTTGTAA GCTTCAAGGTAG	This study
pET21b-acdh-Gp	pET21b based vector, carrying <i>acdh</i> gene from <i>Geotoga petraea</i> ; Amp ^r	/	/	This study
pET21b-acdh-Mar	pET21b based vector, carrying <i>acdh</i> gene from <i>Marinibacteria</i> sp. 1137; Amp ^r	/	/	This study
pET21b-acdh-Ec	pET21b based vector, carrying <i>acdh</i> gene from <i>Escherichia coli</i> MG1655; Amp ^r	CGCGGATCCGATGGCTGT TACTAATGTCGCT	ATAAGAACGCGCCG CAGCGGATTTTCGC TTTTTC	This study
pET21b-acdh-Se	pET21b based vector, carrying <i>acdh</i> gene from <i>Salmonella enterica</i> ; Amp ^r	CGCGGATCCGATGGCTGT TACTAATGTCGCT	AAGGAAAAAAAGCGGC CGCAGCGGATTTTC GCTTTT	This study
pET28a-acka-Ec	pET28a based vector, carrying <i>acka</i> gene from <i>Escherichia coli</i> MG1655; Kan ^r	GGGAATTCCATATGTCGA GTAAGTTAGTACTGGTCT GAAC	CCGCTCGAGTCAGGC AGTCAGGCGGCT	This study
pET21b-acka-Ca	pET21b based vector, carrying <i>acka</i> gene from <i>Clostridium acetobutylicum</i> ; Amp ^r	CGCGGATCCGATGAAAAA CTTAGTTATTAACTGCG	AAGGAAAAAAAGCGGC CGCTTTAACTTGCGCT ACTATATCTTG	This study
pET28a-acka-Mt	pET28a based vector, carrying <i>acka</i> gene from <i>Methanosaericina thermophila</i> ; Kan ^r	/	/	This study
pET28a-acka-So	pET28a based vector, carrying <i>acka</i> gene from <i>Shewanella oneidensis</i> MR-1; Kan ^r	CGCGGATCCATGTCTAAT AAACTGGTTTACTGAC	CCCAAGCTTTATTTA GTAATGAGTTAACG AA	This study
pET28a-acka-Tm	pET28a based vector, carrying <i>acka</i> gene from <i>Thermotoga maritima</i> ; Kan ^r	GGGAATTCCATATGAGAG TACTGGTGATAAACTCGG	CCGCTCGAGTTACCTG CCAATCTCTCGACTA TT	This study
pET21b-acka-Se	pET21b based vector, carrying <i>acka</i> gene from <i>Salmonella enterica</i> ; Amp ^r	CGCGGATCCGATGTCGAG TAAGTTAGTACTGGTTC	AAGGAAAAAAAGCGGC CGCGGAGTCAGACG GCTCGCGT	This study
pET28a-ptt-Ec	pET28a based vector, carrying <i>pta</i> gene from <i>Escherichia coli</i> MG1655; Kan ^r	CCGGAATTCATGATTATT GAACGTTGCGTG	CCGCTCGAGTCATTCA ACCAGTGTGAAAC	This study
pET21b-ptt-Ca	pET21b based vector, carrying <i>pta</i> gene from <i>Clostridium acetobutylicum</i> ; Amp ^r	/	/	This study
pET21b-ptt-Tm-1755	pET21b based vector, carrying <i>pta</i> gene from <i>Thermotoga maritime</i> ; Amp ^r	ACCGCTCGACATGCGCTG TCCTTGGAGAAAAAC	AAGGAAAAAAAGCGGC CGCCCCCTTTCTGT GCGACCAGTACG	This study
pET21b-ptt-Tm-1130	pET21b based vector, carrying <i>pta</i> gene from <i>Thermotoga maritime</i> ; Amp ^r	ACCGCTCGACATGTTCT GGAAAAACTGGTTGAG	AAGGAAAAAAAGCGGC CGCAGCGAAGACCGC CGAGAGGGCTA	This study
pET21b-ptt-Mt	pET21b based vector, carrying <i>pta</i> gene from <i>Methanosaericina thermophila</i> ; Amp ^r	/	/	This study
pET21b-ptt2-Ec	pET21b based vector, carrying <i>pta</i> gene from <i>Escherichia coli</i> MG1655; Amp ^r	ACCGCTCGACATGTCGG TATTATTATGCTGATC	AAGGAAAAAAAGCGGC CGCCTGCTGCTGTGCA GACTGAA	This study

pET21a-fls	pET21a based vector, carrying <i>fls</i> gene; Amp ^r	/	/	(21)
pET28a-gals	pET28a based vector, carrying <i>gals</i> gene; Kan ^r	/	/	(78)
pET28a-dak-Pp	pET28a based vector, carrying <i>dak</i> gene from <i>Pichia pastoris</i> ; Kan ^r	/	/	This study
pET28a-dak-Mt	pET28a based vector, carrying <i>dak</i> gene from <i>Myceliophthora thermophila</i> ; Kan ^r	/	/	This study
pET28a-dak-Ca	pET28a based vector, carrying <i>dak</i> gene from <i>Candida arabinofermentans</i> ; Kan ^r	/	/	This study
pET28a-dak-Cg	pET28a based vector, carrying <i>dak</i> gene from <i>Chaetomium globosum</i> ; Kan ^r	/	/	This study
pET28a-dak-Cf	pET28a based vector, carrying <i>dak</i> gene from <i>Citrobacter freundii</i> CFNIH1; Kan ^r	/	/	This study
pET21b-tpi-Ec	pET21b based vector, carrying <i>tpi</i> gene from <i>Escherichia coli</i> MG1655; Amp ^r	CGCGGATCCGATGCGACA TCCTTAGTGATGG	ATAAGAATGCAGGCCG CAGCCTTTAGCCGC TTCTG	This study
pET21b-tpi-Sc	pET21b based vector, carrying <i>tpi</i> gene from <i>Saccharomyces cerevisiae</i> ; Amp ^r	GGAATTCCATATGGCTAG AACTTCTTGTGGTG	CAACTCGAGGTTCTA GAGTTGATGATATCA ACAAATTIC	This study
pET21b-tpi-Mt	pET21b based vector, carrying <i>tpi</i> gene from <i>Mycobacterium tuberculosis</i> ; Amp ^r	/	/	This study
pET20b-tpi-Tt	pET20b based vector, carrying <i>tpi</i> gene from <i>Thermus thermophilus</i> ; Amp ^r	/	/	You C's Lab
pET21b-fba-Ec	pET21b based vector, carrying <i>fba</i> gene from <i>Escherichia coli</i> MG1655; Amp ^r	CGCGGATCCGATGTCTAA GATTTTGATTCGTA	ATAAGAATGCAGGCCG CCAGAACGTCGATCG CGTT	This study
pET21b-fba-Sc	pET21b based vector, carrying <i>fba</i> gene from <i>Saccharomyces cerevisiae</i> ; Amp ^r	GGAATTCCATATGGGTGT TGAACAAATCTAAAG	CAACTCGAGTAAAGT GTTAGTGGTACGGAA AGT	This study
pET21b-fbp-Ec	pET21b based vector, carrying <i>fbp</i> gene from <i>Escherichia coli</i> MG1655; Amp ^r	CGCGGATCCGATGAAAAC GTTAGGTGAATTATTG	ATAAGAATGCAGGCCG CCGCCTCCGGAAACT CACG	This study
pET21b-fbp-Syn0505	pET21b based vector, carrying <i>fbp</i> gene from <i>Synechococcus</i> PCC 7942; Amp ^r	CGCGGATCCGATGGAGAA GACGATCGGTCTC	ATAAGAATGCAGGCCG CACGGAGGCTAACCG TTTGAC	This study
pET21b-fbp-Syn2335	pET21b based vector, carrying <i>fbp</i> gene from <i>Synechococcus</i> PCC 7942; Amp ^r	CGCGGATCCGATGGCTCA ATCCACCACCTTC	ACGCGTCGACGGGCA CCGACTCAGCCAAGC	This study
pET21b-fbp-Sc	pET21b based vector, carrying <i>fbp</i> gene from <i>Saccharomyces cerevisiae</i> ; Amp ^r	GGAATTCCATATGCCAAC TCTAGTAAATGGACC	CAACTCGAGCTGTGA CTTGCCAATATGGTC	This study
pET21b-pgi-Ec	pET21b based vector, carrying <i>pgi</i> gene from <i>Escherichia coli</i> MG1655; Amp ^r	CGCGGATCCGATGAAAAA CATCAATCCAACGC	ATAAGAATGCAGGCCG CACCGGCCACGCTTT ATA	This study
pET21b-fsa-Ec	pET21b based vector, carrying <i>fsa</i> gene from <i>Escherichia coli</i> MG1655; Amp ^r	CGCGGATCCGATGGAACT GTATCTGGATACCTCAGA C	ATAAGAATGCAGGCCG CAATCGACGTTCTGCC AAACG	This study
pET21b-fsa-Tm	pET21b based vector, carrying <i>fsa</i> gene from <i>Thermotoga maritime</i> ; Amp ^r	CGCGGATCCGATGAAGAT CTTCTGGACACAGCA	ATAAGAATGCAGGCCG CTTCTTCAGGTTCTC CAAATACTTT	This study
pET21b-fbap-Cs	pET21b based vector, carrying <i>fbap</i> gene from <i>Cenarchaeum symbiosum</i> Amp ^r	/	/	This study

pET21b-pgm-Ll	pET21b based vector, carrying <i>pgm</i> gene from <i>Lactococcus lactis</i> subsp. <i>lactis</i> ; Amp ^r	CGCGGATCCGATGAAAAA AATATTAAGTTCGACA	ATAAGAATGCGGCCG CAGCTTCTTCATCGC AATAA	This study
pET21b-pgm-Ec	pET21b based vector, carrying <i>pgm</i> gene from <i>Escherichia coli</i> MG1655; Amp ^r	CGCGGATCCGATGGCAAT CCACAATCGTGC	ATAAGAATGCGGCCG CCCGGTTCAGAAC TTCGC	This study
pET21b-pgm-Syn0156	pET21b based vector, carrying <i>pgm</i> gene from <i>Synechococcus</i> PCC 7942; Amp ^r	CGCGGATCCGATGAAAT CCACACTGTCGCGAC	ATAAGAATGCGGCCG CCGTGATCACTGTCG GTTGATCG	This study
pET21b-pgm-Syn1268	pET21b based vector, carrying <i>pgm</i> gene from <i>Synechococcus</i> PCC 7942; Amp ^r	CGCGGATCCGATGTCTGC TGTGCATCTCACTGTT	ATAAGAATGCGGCCG CGCAGCGCTGCGCCC AATCCTTA	This study
pET21b-pgm-Bs	pET21b based vector, carrying <i>pgm</i> gene from <i>Bacillus subtilis</i> 168; Amp ^r	CGCGGATCCGATGACTTG GAGAAAGAGCTATGAAC	ATAAGAATGCGGCCG CTTTGCTGTTGACTC AACAAATTTC	This study
pET21b-agp-Ec	pET21b based vector, carrying <i>agp</i> gene from <i>Escherichia coli</i> MG1655; Amp ^r	ACCGCTCGACATGGTTAG TTTAGAGAAGAACGATC	ACCGCTCGACATGGT TAGTTTAGAGAAGAA CGATC	This study
pET21b-agp-Syn	pET21b based vector, carrying <i>agp</i> gene from <i>Synechococcus</i> UTEX2973; Amp ^r	CGCGGATCCGATGAAAAA CGTGCTGGCGATC	ATAAGAATGCGGCCG CGATCACCGTGTGTC GGGAATAA	This study
pET21b-ss-Bs	pET21b based vector, carrying <i>ss</i> gene from <i>Bacillus subtilis</i> ; Amp ^r	/	/	This study
pET21b-ss-Ec	pET21b based vector, carrying <i>ss</i> gene from <i>Escherichia coli</i> MG1655; Amp ^r	CGCGGATCCGATGCAGGT TTTACATGTATGTCAG	ATAAGAATGCGGCCG CTTTCAAGCGATAGTA AAGCTCACG	This study
pET21b-ssIII-Pv	pET21b based vector, carrying <i>ssIII</i> gene from <i>Phaseolus vulgaris</i> ; Amp ^r	/	/	This study
pET21b-sbe-Vv	pET28a based vector, carrying <i>sbe</i> gene from <i>Vibrio vulnificus</i> ; Kan ^r	/	/	This study
pET21b- α GP-St	pET21b based vector, carrying α GP gene from <i>Solanum tuberosum</i> ; Amp ^r	CGCGGATCCGATGGGAGC ACACTTGTCAACCATTAC	ATAAGAATGCGGCCG CTGCTATTCACAGC TTCAATGT	This study
pET20b- α GP-Hv	pET20b based vector, carrying α GP gene from <i>Hordeum vulgare</i> ; Amp ^r	/	/	This study
pET20b-fdh-Ts	pET20b based vector, carrying <i>fdh</i> gene from <i>Thiobacillus</i> sp. KNK65MA; Amp ^r	/	/	This study
pET26b-cat-Bs	pET21b based vector, carrying <i>KatA</i> gene from <i>Bacillus subtilis</i> 168; Kan ^r	/	/	(8I)
pET28a-ppk-Mt	pET28a based vector, carrying <i>ppk</i> gene from <i>Mycobacterium tuberculosis</i> ; Kan ^r	/	/	This study
pET21b-ppa	pET21b based vector, carrying <i>ppa</i> gene from <i>Escherichia coli</i> MG1655; Amp ^r	CGCGGATCCGATGAGCTT ACTCAACGTCCC	ATAAGAATGCGGCCG CTTTATTCTTGCGCG CTCGAA	This study

Table S7.

List of synthesized genes and their optimized sequences.

TTACCGCAGGCATTGGAGAAAACAGTCAAGCATCGAAAGAGAACATCTTCGGGCTTGAGAACATTGGAATAAAGATT
GACGAGAAGAAAAGATAAAGGGGACAGGAAATCGACATCTCACCCCAGATTCAAAAGTCGGGCTTTGTATCCCG
ACCATTAAGGAGCTTACCATTTGCAAGGGACACAAAGGAAATTGTGAGACCGAAGCTAAACTGCGCAGCTATACCTGTC
TGACTGCGCAGCTCTATAACCTGTCGA

ATGGATTAAAGAAAAGCATATGGAGTGTGCTAACGCAAGACAAAAAAAGGATAATTAGCTGAAGGTTGAAGAAAAAAAG
AAATCTAATTGCCAGATAAAATTATCAGGAGGGATTAGCGAGAGCTTGTCTTGAGGTGATGAAAAAATAAAATTAAGA
AAAAGCAAGTGGATTGAACTTGTGACATTGTCAGGAGCTGAAATAATGATCCAGACAGACTCACTAAAACAGAACATATGC
TAGAGATTTTATGAACTTAGAAAACACAAAGGAATGACTATTGAAAATCTGAAAATGTTGAAGAGATCTCTTATT
GCAACATGGCTTAAAGATGGCTATGGTGTGGAATGGTTCAGGAGCTTCACACAATGGAGATTATAAGGACAG
GACTCTAACATTAAAACACTGCACCGAGGTAAAGTATCAGGATTCTTGTGATGATAACTCTGACTGCAGATTAG
TGAAGAGGGTCTTTATTATTCAGATTGTGCTGTAATCCTAACCCAAACATCAGATGAACTAGCTGATATTGCTATAACTA
CAGCTGAAACAGCTAGAAAATTATGTAACAGTGGCTAACAGTGGCTTCACCTCTCAACTATGGGAAGTGGAAACAG
GCGAAATGGTAGATAAGGGTAAAAAAATGCTGTTGAAATCACAAGAAAGATTCAGACCGGGATCTGCTATTGTTGAGCTC
AGCTTGATGTCGAATAGATAGTGAAGTAGCGGCTTAAAGCACCTCTAGTAATGTTGCAAGGAAATGCAATGTTCTGT
ATTCGGAGATCTTCAACACGGAAACATTGGTACAAGCTTGTCAAAGATTGCAAAAGCAAAAGCAATAGGACCTATATG
TCAAGGATTGTCAAAACCTTAAATGATTATCAAGGGCTGTAGCTCAGAGGATATAGTAAATGTTGCTATAACTGTT
GTTCAAGGCTCAAGAGGTATAAA

pta-Mt TTGGTAAACATTTTAGAAAAAAATCAGTGAAGAGGCAAGAAAACCTAACAGACAATCGTTAACCTGAAACTGAAGATA
 AGAACCTCTCCAAGCAGCTGCCAACGGTCCTTGAAGAGGAGTATTGCAATGTGTCCTTATCGTAAGGAGAACATCAA
 GAACCTCTCAGGAGATCTTGACCTCTCAAAGCAAGGATGTAGATCCCGAGACTTATGAGAGAAAAGACGAATATGTAAG
 ACCCTTTATGAGCTGAGAAAGCACAAGGGTGTACCCCTGACAGCGCAGCTGAATTATGAGGACTACGTTAACCTCGTGC
 TTATGATGCGAAAACCTCGGAGAAGTTCAGGTTGTCGTTGAGCTTCACCTCTCTTGACACTCTAACCTGAGCTGTCGTC
 CAGATCGTTAAACCGCCCCAGATTGCTCGCATCTGCGTCTTATTTCGCGTACCTGACTGTGAATGGAATCTGAGCTCAA
 TGGAACGTTCTCTCGTACTCGGGCATGGTAGAGATGCCAACTGTAGAACAGGCTGCCACACATTGCCGAACTCTGCA
 AAAGACCTCTCGAGCTTCTGGTCAAGGACACCCCCTATCTGCAAGTGTCTTCTACCTCAACTAAGGGAAAGGCTCACAGCAG
 TGACTGGAGCAACAGTCGTCGAACAAAAGCTGCACAGGAACTTGCCTCCAGATATAGCAATCTGATGGTAACTTCAGGTAG
 ATGCAGCAATTGTTCCAAGITGTCAGCTCAAAGCACCAGGAAGCCCTGTCGAGGTAAAGGCAATGTTCTTATTTCCT
 TGAGCTTAACCGGGAAACATCGCATATAAGATGCCATAGGCTTGCACAGGCTGAGGCTTATGCCCTATAACCCAGGG
 CTGGCAACGGCTTAAATGACCTCTCCAGAGGTTGCGACGGCAGAAGACATTTGCGCTGTTGCAATTACCTGTGTTCAAGG
 CCAGCTCAGCAAAATAAGCAGCTCAGCAAAATAA

ATGGCGCAGCACCCATCATCATCATCACAGCAGGCCGCTGGTGCAGGCCGACCATATGTCACCGCTACCTGTCC
CGACCCCTGGATGGTCCTGGCGAACGCTCTGGCTGCACTGGCAGCACCAACGCCGCTGAACCTGGACGAGAACACC
GCGTTATCTACGACCCGCTCTCTCTCGTCAACGTTAGCATCATCAGCGGTGCGGCTCCGGCACAGAGCCGGATGGTC
TGGTTACGTGGCGCCAACATGCTGTCAGCCGTGGCGGTACGTTTGCTCTCCAAAGCACCAAGAACATCTGGCA
GCCGTTGACCGGGTGGCGCTGATAAGGGCACCTGCTGGTATCACAACATACCCGGGACTCTGCTGCACTTGGCTGG
CGGCTGAGAAAACCAAGGGCAAGGGTGCCTCTGCTGATCTGGGAGACGAGCTGGGACGAGTAAGCTGGGAGAAGGGT
GGTCTCTGGTGGCGCTCGGGCTGGCTGGTCAAGATCGGCGTGTAGAATCTGGGTGCGCCGCCAGAGGGTGGT
CTCTGGACGAGCTGTAACGACCTGGCCACCGCGTTAACAGCGCATCTGGATCATCTGGTGCACCTGGGACTACTGCCACGT
TCCGGTCTGCTACCGAGACGGTGGCTCGAGGGAGACGAAGTGGAGATTGGTACCGGTCACACAAACGAGCGGGTTACGG
TAAGCTGACCCCCAGGCCAACGGCTGAGGGTCTGGTAAAGAGATCTCTGAAGTAGCTCTGGACGAGACGCCAGGAAACG
TGGCTACGTTAACCTCAAGGCCGTGACCGAGACCGCGCTGTTAGTAGCAACTTCGGCGCATGAGCAACCTGGAGCTGGG
CGGTCTGGTGAACGAGCTGTCGAACACAACACTGTAAGGACTGGAAACATCCAGCGGTTCTGTGTAACGGCGTGTGGCTGGAA
ACCTCCCTCAAGCGCCGGCTTCTCTGGTGAACCTTCACCTCTGGCATGACATCTTCAACCTTCTGGTGTGGCTGAC
GATCAAGGGCTCTCTGGACCTGAAGACCGACACCGCGTGGGAAGCTGTTGCGGTGCCCAGAGCTATCGCAGCGCTGCTCC
GCGTGCAGAGCAGCTGGTCAAGGCCTGCTGGAGTCAAGAAGGCCGTGGACACGCCGCGCTGATGTTAAAGGGTACCC
GGCGTCTGGTGAAGCGATCTGCTGGCTGGTCTGGAGGGCTTATCGCGGCCAGCGGCCACTGACCCGTTGGGATACCGT
ATGGGGCAGCGCTGACTCGGGCTGACCTCTGAAGACGGCGCCAGCGCTGCTGGACATCGCAGCAAGAAGATCGCG
GCCGTTGGTCTGGTGAAGGTGCTGGCGAGCTGGAGGGAGATCTGAGGGCAAGATGGCGGCCACCTGGGGCGCATC
CTGGGACATCTCTCTGGTCTCTGCTGCTGGCGCCGCTGCAAGGAACACGCCGCTGGCCAGGGCGGAAGGGCTGTTGCGCTG
GGTCTGGTCTGGAGGGCTGCAACCTGGCCACTACACCCGGCAAGGGCGGCCATGCGCCACTGTTAGGACA
CCCTGATTGGCTTGGAGGGCATGGTGTGCAAGCAGAGCTTGTAGGAAGGGCTTGGCGGCCGCGTGAAGCGTGGCGAG
CGACAAAGACCATGCTGGCTGGCTGGTGTGCAACTACAGTGGTGTGGCTGAAGGTAAGGAGCTGCGGCCGATCC
GGTCTGGTCTGGGGCCCATGGTGGCATCTGGTGTGCAAGGAGACTGCCATTAAGCAACTTAA
ATGGGGCAGCGCCATCATCATCATCATCACAGCAGGCCGCTGGCAGCACCAACGCCGCTGAACCTGGTACGATCTGGTGA

dak-Ca ATGGCCAACTGCCCATACATCACTCATCACAGCGGAGGCCTGTGCCCGCGGACCATATGCCATACAGCTGCTGTT
CAGCAAATGGGTGCGGGATCTCATGTCCTACTGGAAAGGCAATTGGAATTAACAAAGGATGATTAGTTCACTCACATTAAAGGGTT
TATGTCGAAATCAACCTGTGATTAAGGATAATTGACTCGGAGAGGTTGTTATGGCCAATCTCCTCTTCTCAAAGTCG
ATCTTATCAGGGAGTGATCTGGGATCGAACCTTACATGCTGATTGTTGGAGAAGGTTGTTAGATGTCGGTGTGCAAG
GTTACATTTGATCTCCTCAACTAAACAGATTACGCTGGTTGAAAAGTAAGCCAAGTGATAAAGGTACATTGATCGTT
GTCAAGAACATACTGGGTGATATCTTACATTGACTGAGCTGAAAGGCTAAAGCTGAGGTTTAAAGGTGTTAGGTGTT
TGATGTTCAAGATGACTTGTGTTGGAAAGACTAAAAATGGTAGTGGCTGAGAAGGTTTACGAGGTACATCTGGT
TCATAAAATGTTGGTGCTAAATCTGCCAAAGATAGCAATAAAAGCTTCTGAAAGAAGTTTCAAGTGGTGAAGCTGTT
GTGCTGAAATCTAGTACTGGTGTCTCATAGGACCTATGTCCTTCAAGGCTAACAGACATAGGAAAGAAGAAGCTGACG
ATGAGAAGAAGGTTGAAACAAGCATTTAAAGGAAGATGAAATCGAAGITGGTATGGTTATTCACATAGTGTGTTAGGTA

TTAACCGTGTTCCTCCAATCTACAGTTGACGATTATGTGCTGAGTTAGAATACTTAAAGCTAAAGACGATAAGGA
AAGAAAGACTACGTTGATTGTAAGAACAGATGATGCTCTTAAATCAATAATTGGGTTGCTTCTGTTTGAGATTG
TTGCTATCCAGAACACTGGTTGGACTATTGGAACAGGAATATAGTTAAAGCCTGCTCAGAATTATTCTGCTCATTC
ACATCTTAGATGGTCAGGTTCTCATCTACTTTGAACGCTACCAAAGCTGGTGGTGTGAAATCTTGAAGATGCTTAGA
TTATCACACACTGTCAGGTTGGACTTCAACACAACACAACTTGGCTCTTCAACAGCTGACTATTATGGA
GCCCGAGAACTGAGGTTAAACACATCTCTTGGTAACTGTGATGCTACTATTTCAGGCTATTAAGCTTAAAG
TTGTAAGAAATTATGACAAAAGAACAAAAATTACCTTATGATACCGTGGCTGATGGTATTGCTGAAACGTTG
GCTAATGGTGCCTCATGCAACTTGGACTTAATTCAAAAGATAACCTGATTGGATGATGGTGTGAGAGCCCTAACTCAAA
TTACAGATGGTGTGAAACTGCTATGGGTTGACATCTGGTGGATTACTCTTCTGCTCTGAGCTAAAGGTT
AAAGAAAAGAACACTCAAAAGTGGTAAATCAAGAAGTGACAACTTCAACATTATCAATGCTGATGAGCTTGA
TTATATAAGTATACAAGAGCTAGTGGTGCAGAGAACTTGTGATGCTGCGTTAGCTCATTGCGAAACCTTITAGCTAC
AAAAGGTGATTGACAAAGCTAATGCTGCTGATGAGCTGGTGAATCAACCGAAAAGTTAAAGGCTAAATTGGTAG
AGCTTCTATGTTGGTGAAGAAGATTCAGCAACTTGAAGCTGGAGGAGGATTGCTGATCTGGTGTATTGGATTGCT
GCCTTAAATTGACGGTTTGGCAGCTTATAGTAAAATTGGATCTAATCTATAA

ATGGGCAGCAGCCATCATCATCATCACAGCAGGCCCTGGTGCCTCGCGCAGCCATGTCACCGACATCTCT
CCACGCTCAGCAGGGCTCTGCCTCCAAGGGCTCTCCGGCAGTCGTCAGCAACCCGGCTCAACTCGACGAGGACAACC
GGCTGCTCTTCGACCCGGCTCCGGCCCTCCAGGTCACTGACATCATCAGCGGCCGGCTCCGGCATGAGCCAGATGTC
GGGCTACGTGGCACAACATGTCGCGGCTGCGTGGCGGGGAGCTGTCGCTGCCGAGCACAAAGCAGATCTGGC
CGCGGTCGAGGGCGTTCCCGAACAGGGCAGCTGCTCATACCAACTACAGGGGAGCTGTCGATTGGGCTC
GGGGCGAGGGAGAACAGGCAAGGCCAACAGGGCTCGCGCATGACTCGGGGAGCTGAGCTCTATCGGAAAAGGGC
GGGTCTATGGTCGGCGCCGGCTACCGGGCAGATTGGTGTCTCAAGGTTCTGGGGCAGGGCTTCCAGGGCGGT
CGCTTGACGAGCTACGACCTCGGGACGGCCATCAACGGCCAGATGTCGACATCGTGCAGGACCTGGATATTGCCATG
CCCGGGCGGAGCAGGAGCACGGTAGCTGGAGGCTAACAGGGTTGGAGATCGGGACAGGGCGCACAAAGGCGGGTACA
GGAGACTCTCCCCGGCGCCACCGCAGAGGGCTGTAACAGGATTCTCAAGTACTGCTGGACGAGCGATGCCGAG
GAGGCTACGTCACCTCAAGCCGGGGAGAGACAGGCTGTCGTCAGCAACTCGCGGAGCTGCAACCTGGAGCTCG
GGGGCTGCTGCAAGGACTCTCCAACAACTCTCAAGGACTGGAACTGAGCAGCTGCTGGCTGCCAG
AACCTGCTCAACGGCGGGCTCTCCGGTCTCCGGTCACTCAACCTCTCCGGTCACTGGCTCCAAACACCCCCTACTCGCTGA
AAATCAAGGGCTTCTTCGACCTCAAAACCGACAGCGCTGGGAAGCGCTGCCGGAGCGAGACGACCCGCGCAGCGC

dak-Cg

AAATCAAGGGCTTCTCGACCTCAAAACGACACCGCTGGGAAGCCGCTGCCGGAGCCAGAACGACCCGCCGCAGCC
CGCGCGCCGAGCACCTCTGCCGCCACCCCGGAGAAGAAAAGAACATCAGCAGCACCCGCCGACCTGAAGTCGACCCCG
CGCTGTGGAGCGCATGCTCGAGGCGCGGCCAGGGCCTCATCGCCGGAGCCGGACCTCAACAGTGGACACCGTCA
TGGGCGACGGCAGCTGCGGCTGACGCTCGAGACGGCGCCAAGGCCCTCTCGACCCCTCAACACCCGGCACATCGCC
CGCGCGGGTCTCGCTGAGGTGCTCACCGAGCTCGAGGACATCTCGAGGGCAAGATGGCGCACCCGGCATCC
TGGGACATCTTCTCGCTGCTGCCGACCCGGCGAGGACATCGCACAGCAACAAACAACAAACAACAAACACC
AAACAAACAAACAGAAGCGGCCATGGTGGCGTGGCTGGCCAGGGCAAGGGCTGAGCTGGCCGAGGGCCTGGGGCACCTGGC
CACTACACGCCGCCAGGTGGCGACCGGACGGTGATGGACACCATCATCCGCTGCCGAGGCCATGAGGGCAGCGAG
AGCTTGGCGAGGGCTGGCGCCGCGGTGAGGGGCCGAGGGCAGGACAGCTGAAGCCGAGACTGGGGCCGGCAG
CTACGTGGCGCGGGCGGCCAGGGCAAGGGAGTTGCCCGATCCCCGGCTGGGGGCCATGGTGGTATTGGGGCT
GCATGCGTCATGTAA

ATGGGCAGCAGCCATCATCATCATCACAGCAGCGGCCGTGGTGCCTGCCGCGGCAAGCCATATGTCATAATTCTTTAAC
AACCGACCCAGCTTGTGAGCGCAGTGTACGCCGTTGAAATTACCAAGCCGGTGGATAAACCTGGCCGCTGGAGAGCGC
ATCCGGCCTTCTCGCGCTGGTCCGCCGACCTTAAACAAAATACCGTGGCGGTATGTCCTCCGGCGCTGGTCAAGGGCAGA
ACCCGCGCAGTGGGTTATCGGCAAAGGTATGTCGACTGCCGCGCTGCCGACGTGTCGCCCTCCCCGAGCGTGGAT
GCCGGTACTGACCCTATTAGCGCAGTGACCGGTTAGGCCGCTGGTCTGGTATGTCGAAGAAACTAACCCGGTACGCCGTT
ATCTTCGGCTCTCGCCGGAGAAAAGCGCAGGCCGCTGGCTAACAGCTTAAATGCTGATAGCTGTGAGCACATCTCCCTGCC
GGATAACAAACACCCACCGCGCATGCCGAAACCATCTGGTCATAAAATGCCGCTATTCGCTGAACGCCCTACAA
CTCTGCCAACCGCTCTCGCTGGTAAGCGCAGTACGCCGACCAAAACACCCCTGGCTGCCGCTCCAGTGTCTCG
CGCGAACAGAACCGGCCGCCGCCATCATCGGCCGCTATGCCGGCTATGTCGACTGCCGCTGGCGCTGCCCTCCAGTGTCTCG
TCGGTTATTGATACCCAAAACAGTGGCAGGTGTAACCTGATGGTGGATAACTGCTGACAGTCTTACCTGGAACCGGC
AGAGTGGCGTGTGATTAACAACTTCTGGCGGCCGTATCGCTGGAAATGCCATTACCCGGCAACTGGCCAGCTT
CACTATCCCACCGCATCACTGGCTGATGGTCCGCCCTGGCTGACCGCTGGATATGAAGGATTCTCACTAACGGC
CATCATGTCGAAAGAGACATGCCGAAAGAGCTGCTGACCGAAGTGGAAACCCAGCACTGGCCGACTCCCGTCCACCGGC
TGAAGATCTGACCGGCCACCATCCGGCTGGTAAGTCCGACGCCCTGCCAACCGGCCGGGTTGCCGAAATT
CTGGCGACCTGCAAGCGGCAAGCTGGTACGCCGCTGGTAAGTCCGACGCCCTGCCAACCGGCCGGGTTGCCGAAATT

dak-Cf

CATCATGCTCGAAGAGAGACATCGAAAAGCCTGCTGACCGAACTGGAAACCAGCACTGGCCACTCCGTCCACCGCG
TGAATACCTGACCTGGCCACATCCCGCTGAGCCGCCGGCTGGAACTTCGACGCCCTGCACCGCCGGTCCGGCAAAATT
TGCGGAGCAGGGTACCGGGAAACGCTTCTCAATCTGGAAGCACATCTCACCGCTGAGCTGGATGCAACAGTCGGCGATGGGATAAC
GGTTCAACCTTTGCGCCGGCGCCTGAAATTCGCACTGCTGCAAGCCTGAGCTTCCGCTGAGCTTCCACGC
TGTGCGGCTTATGGCAACGCTGACCGCTGTTGAGCTGGGGGTTCCAGCGGGCTGCTGATGCTGTCTTATTTCTTACCGCCGCC
GGCGAACAACTGGAACAGGGAGCTAACGCTTCCAGGCGAACGCTGAAATGGGGTCTGGAGCAGATGAATGCTTACGGCGGCC
AGACGAAGGGATCGCACCATGATAGATGCACTGCAACCCGGCTGACCTCACTGCTGGCGCAGCGGACAACCTGATGC
TGTCTTGCAGCCCGCAAGCCGGGGCGAACGAACTGTTGTCAGCAAAGCGAATGCGGGTCCGGCATCGTATCTGAG
CAGCGAACAGTTGCTGGGTAATATGGATCCC GGCGCATGCCGTGCAATGGTATTAAAGCGCTGGGGAGAGTGAATT
GGGTTAA

tni-Mt

ACGTCCGGAGGGGGAAATCTGGGCCCCAACATCGAACAGTCGCTGGATCTGGCCGGGATATTGGCCAGCAGA
TCGGCAGCTCGTCATCGGCCATACGGGCTTGGCGATCGGCCAGGGCGGCTGGCGACGCCAGGAGG
TGTGTGGCGCATCGAAAAGAGTTGGCCTGTTGGCTCGCCGAGATTGCGCATACGGTGCCTGGTCTACGGCGGCTC
GGTGAACGCCAAAAGCTGGCGACATCGTGGCCAGATGACGTCATGGTGGCTGGTCTGGTGCCTGGCGCTGGACGG
GGAGCATTCGGCAGCTGGCGGCAATTGGCGGGCTGGTCTGGTCCGGTAG

ATCGTGTATCACCCTGAGCGCATTAAGCCGATGTGGGGGAATTGGAGGTACACACTGCTAGTAGCGGACTGCTGGATG
CTGTTCTGCTGAAAGTTCTGTCGAAGCTCTCTGATGTTGACTTATGGCTATTGTTGGGATGATGTTCACTATGTCATG
ACTCATACACTGGCACCGATAATAGCGATATCTCATAAACTCTGGCGTGGGACGCCCTCATGAAAGGAACCTGTTGCAA
GAAGAGGGCTGTATGGTCTGGTCAGACCTGCTGCAGGATTCATTTCGGGAACGTTAAAGGGATGGTCTGGAGTG
GCAGAGCTGAAGAATTCGAAGAACCTGCTAATAGGGCCTTACCGCTGTTGCTGGATAAACCGAACCTGGACCTTCACAT
ATCTCTTCTATCGTATGTTGCTGACTCTGAGCATACTGCTGATCGTGAATAAAAAGCTTGGCGGAAGGGTTGTTATT
AACATTATGGACGTGCTCAAAGCTGTCAGCTGCTGTTACTGTTGGAGGATAAAACCAACCATCGAAGCAGCACTGATG
TATCTGGCCCTTTGTTGAGCAGCTGGAAACCCGTGATGGAGAACCTGATGCTCTGCTGACTAGCATGCTGCTGATA
ACATTTGGCCGACCTATGTTGGGAAAGATGACCGGATTGTTCTGGTCTGACACAGAAACGTTTCTGGCGACGGAAAGC
TGGTCTGCTCAATAACCCACACTATGTTGGGGGTAAATACTGTTGCTGACACCCATGCGCTGATGCTGTCCTG
ATTCTCCGGCTCTACACTCTGATCCGGATCTGGGAAGCTGTTTACGATGCGACAGGGGCCCTGACTGGACCT
TTTGATGGCTCTACGCTGATGGGAGCTGTCGGCTACTGCTACTGCCGCTGATGCGATGCGCTGCAAGGATT
CGTTCATCCGGCTACCTGGCTGATGAGCTGGAGTATGCCGAAGGTTATGTTCTGCTATGGACGTGCTGGATAGCAAA
ATGGTCTGGCTGAAAGATTCAGGCTGTCGGTACAGGACGTCTTATGAAGATCCGGATCTGGAGCATCACCACATCATC
ACTGTTACCTTCTG

ATGTTGAAGATAATTTCCTGTGTCAGAATGCCACCCATTGTAAGAACAGGGAGCTTCCGGATAGCAGGTCTCG
CAAAGGCCTGCGATTAGGAATGGCTAGGAGTCTGATGCTGCCAAAGTACAGGAAATACCTGAAACCGTGGAAAAAGC
TGATGAAAAAACAGGGTAGGTACCTGACTGTCGCGTGGCAGCAATATTGCCAAATGACATATTGCCAGAGAATG
ATGTAATTATTACTCATGACAATGAGTACTATTCAACAGGGATTGTAACGGGTGACGGTGTGAGCGGGTT
TGCCTTTTCTCAAGAGCTGTCGGAGGCTGCAAAGTGTCAAGCCGATATTGTCATACTCACGATGGCATA
CAGCGATGTCATTATTGCTGAAAGAGGAGTACAGAAAATCCTTTATGACGGATGAAAAGCGTGTCAAGATCC
ACAACTGCAAGGATATTCCCTCTGATGTCACACATGACTTCTGGGCTCTGAGATGGATCATTTCTCATATGAA
AGGTTAGAATGCAAGGGATTGTTAATTATGAAAGCGGGCATCTGCGCTGATCATGTAACACTGTGAGGCCCAACT
ACAGAAAATGAAATCATGACGCCGTATTGAGCAGCTGGAAACAGGTTGCAATATAGGGAAAGATGTAACGGGCA
TATTAAATGGCATGATGACCTCTATCACGGCAGAACGGCCATTATAGAGGGCCAATACCGATTAGGGGATCTTGC
ATGCAAGCTGAAAACAAAAGCTAGCAGCGATGGGGCTTCCAGAGAAAACGATATTCCGCTGATCACTGGT
GACAAGGCTACTAACAAAAGGGGCTTGTACTTGTGCGCAAGATTATGCGAAGACCTCTGAGGGAGCAAGACATACAG
GGTTGCTAGGCACAGGAGAACGTGAAATTGAGAATTATTCCGGTATGCGAAGAATTGCTTTCATGAGAAAGTGGGGCT
TATATCGGGTTGATGAGGGCTGACCCATCAAAATTATGCGGCTCTGATGTTTGTGAGCGCTGAAATTGAGCGGTG
CGGTTGGGCAGCTTGTCTCAATATGGGCCATTCCGATTGTCAGGGAAACGGGCGGTCTTACGACACTGCGT
GCCATGAGGAAAGGGCAAGGGGCAATGGCTTACGGTTTCCGCCATTGCGCATGTCGAATATTACGATAGAAA
GGGGCTGCTTATTGCAACAGGATGATGAGGACATGTCAGGACCGTATGAATGCGAGATTACAGCTGGGGA
ATCGGGCTAAAGAGTATCGCGTATTTCGAGCAGGTGCAAGGGAGTGGACGGGATTTCTCGAGTAA
ATGGTGAGCGAAGTTAGGGTGTGATAAAAAACAGACCGTGGATGTAATCTGGATGATGATAAGAAGGCGCGTGG
ATTAGCGGAAGATGTCGCTTGAAGTGTGATTGTCGACCGCTTAAATTGCGGCAACTGGGCGTCTGCTGCTGGAT
GAAACCTGTAATGTTGAAATAGCCGCGCAATATTAGCGATTATGCGGCTCTGATGAGCGGACAGTGGAACTG
GATATTCCGATAATGGGCCGTGGGATTGGAAGATGCGAAGAAGGCCCTGCTGGATCGCGGAAATTGATGAAAT
GATGAAATGCGGCTTGTGAGGGGATTTCTGGGATTTGCGGCTTGTGAGCGGCTCTGCTGGATCGCGGAAATTGATGAAAT

ATTTAGCGGAAGATGTCGGCTTGTGAAAGTAGTGTATCGCAGCGATGGAAATTAGTCGACGGGCTATGTGGCAACTGCTGTTGGAT
GAAACCGTGAAATGTGATTGAAAATAGCCAGCGGAATTAGCATTATCGACGAGGGCTGGAAAGTGTGAACTGAAAGGAA
GATATTCCGATAATGGCGCGTGGCATGTGGAAGATAGCGAAGAAGGCCCTGCTGGATCGCCGGAATTGTGAAAT
GTGAAAGATACCAAAACCGACACCCTGGATGAAATTACCGAAGAAGCGGTGGAAAGGCGCACCGCAATGTATCGC
CATTAAGAACAGGACGGCCGCTGCTGAAACTGGAAAGAAATCGCCAGCAGGAAATTGAAGCATTGCGCTTGC
AAGAAAAACTGAGCCAGGGACCACAAACTGTTGTATCCCGGGTGGTAAACCGGATCAGGATATTGAAGTGTCTGA
ATAAAAAGCTGAGGCCGCTGAGCGATGAACCCGAGATTCTGTATTATGGCCGCTTGTAAATGTTGAAATGAAAAGCTTGA
CGCTGAAGCTGATAAACCGCCCTGCTGAAAGGGCATGGTGGAGCTGCGCAATTGTGATGTGCGCCGCAAGCGTATCAGGTGG
ATTITGTGTTTTAACGGCCAGAATGTGATGACAATAACGACCAGAAAGACTTTCGATCGCAGTCAGGGCGCATGG
TCCGAGGCCATTGAAAATTTCGCTGATGAAAGGCGCAAGGAGCTGGAAAGAACCTGGCCGCCGTGCAAGCGAACCTG
ACGTCAGGAGAACACCGCCATTGAAAGCGGAGCTGGTAAAGGCGAACAGGCGAACCTG
CTCAACCGCATGCAAGAACCCCTGGCGCATGGTCTGAAAGCATGTTAATGTGTTGATATTGAGCGCA
GCGATTTTAACGGCAAGACCTGATTCCCTGTATTATAACCGCAGCAGCGGCCCTGTTAGTGCATCGGAATGAAATTGGAT
TCATGGGCCATAATACTGGAAATATGGCCCTGAGCATTATCGACGCCCTGGTAAAGGCGTGTGAAAGGCCGCGGATTG
TTGGTATGCCGATGTGATTGTGCCGATCAGGCCCTGTTCTGGATTGGGTTTGTGGATGCCGCGGCCAAAAGCGGGT
ATTATGATAATAATCGCAAGCAGGATTCCACCGCAGTCGCGATGGTACCCCCGGATGAAACATATTGGGTGGAAGA
GAACAGCTGTAATCGCAAATTTCAGGAAAGAACCGCCCTGCGCAGTGAAGCGATGCGTATAAACGCGAAAAAATTGCG
CATGAAAGCGGAAACCAAAAGAAAAACCCCTGAAAGACCTGTTCTGTGAGCGAGAACATATTGTGTTACCGATCCGCTG
GATGTCAGGGGGCAAGCAGCTGTTACCGTTTTAATACCGAGCAATACCGAAGCGAACCGGAAAGTGTGGTTTC

**ssIII-
Pv**
GATGTGCAGGGGGCAGCACTGTTACCGTTTATAATCCGAGCAATACCAACCTGAACGGCAACCGGAAGTGTGGTTTC
GCTGCGACTTAACTATTGGGCCCATAGAACATGGCAGCGGCCACCGCATGTCGCCAGCAGAAATGGCACCATGTA
TAAGCGAGCGCTGAAAGTGGCGCTGGATGCGTATAAATGGATTGTTGTTAGCGAGAGCGAGCATGGCGCTGTTGTA
TAATAAACTGGCATGATTACACATCCGGTGGCGCATTTGAAAGAACCGGCCGTGATATTGTCATATTGCG
GTGAAATGGGCCATTGGCGAAAGTGGGCCATTAGGGCATGTTGGTGGACCAAGCTTAAGCCGCCGGTTCAGGATTGGAAT
CATATAATGTTGATTATTCCTGGCAAGTACCGATTGCGTGAACCTGAGCAATTAAAGACTTGGACTGCCAGAAAATACCC
TGTTGGCGGCCAGCATTAAGATGTTGCGCATGGCAAGTGGGCCAGCTGAGCCTGTTGCTTTTGCATGCCGCTGGAATTCTG
TTTTCAGGTGGCTGCGTGTATGGCGCGCAATGATGAGAACACGCTTTGGCTTTTGCATGCCGCTGGAATTCTG
CTGCGAATGGCTTCTGGCATATTATTCTGGCACGATTGGAGCAGGCCGCCGGTGGCTGGATTTTAAAGATAATT
ATGCCGCACTACGGCCTGAGCAAAAGCGGCCGTTTACCATTAATCTGGAAATTGGCGGCCATTATGCCGAAG
GATGCACTATGCCGATAAAGCGACCACCGTAGCCGACACTAGCCGAAATTGCCGCAATCCGGTATTGCCGCGCA
TCTGCATAAATTCTGGCATTAAACGGCATGCCGGATAATTGGGCCGCTATAATGATAAAATTATCCGGTGAGCT
ATAGCGCGAAATGTGGTGAGAGGAAAAAGCGGCCAGAGGACTGGCTGAGCAGAACACTGGCCGTAAGCGCGGAT
CTGGCGTAGTTGTTATTACCGCCCTGACCCATCGAAAGGACTCATCTGATAAAACCGCGATTGGCGCACCTCTG
AACCGCCGCGCTCAAGTGTGTTATTGGCAGCGGCCAGATCCGCGCATTCAGAATGATTGTAACTGAAAACCGAGCT
GCATAGCGACCCATAATGATGCCGCCGCGCTGCTGGCGATGATGAACTTAAAGGCCATCTGATTGTTGCGGCCGAT
TTTACTCTGGTCCGAGCATTTGTAACCGTGGCGCTGACCCAGCTGACCGTAGCTGGTATTGGTAGCATTCGGTTGTC
CAAACCGCCGCTGTTGATAGCGTGTGTTGATGTCATGACAAGGATCGCGCAGCGCAAGGTTGAAACCAA
TGGTTTGGCTTGACGCCAGTGGGCCGCGTGTATTGCTTAATGCCGCGATTACCCACTGTTGATAGCGC
GATTGGTTAATGCCGTGCAACAGCGTAGTGGAACAGGATTGGAGCTGGAATGCCGCCGTTGAGATTCTGGAACTGT
ATCATGCCGCCGCTGCAACTGCA

ATCAGGCGCCGTCAACAACTGAG
ATAGAGAATTGTGTTTACCAACCTGGCAGTGTGGAGAGGCCAAAAGGCCGAAAAAAACTGGTGAAGAAGCAAGTGAATCA
GATGTTGAAAAACTGAGGCAGCAGCTGCACTGACCATTTGCCCCATTATAGATCCCACCAAGGTGCC
CTGAGACTGGAGTGCTGGCCTGGTGCAGTGTGGCTTCTGGCAGAGTCAGCCAGAAGATTGCCCTGGAAAGGAAAAAA
GAAAGTCGCTTATTCGAAAGCAGATCTGACACTGACCATTCAGCTGGCATTGATTGGAATGGTGTGGAC
AGCTGATTGATGATCCATACAGTATCATGGCATTTATCAGAATATGATGATCTGCATACCCAAAACCAGTATCAGCA
CATGGGCACTGGATTGACCTGGAAAGAGATGCGAAAAGCATTAGTCGATTGACCTTATGCTGATGCCACATGCC
ACTGCGATGAGCTGGCTGGCTGCTTATTAATGATGGGATGCGAACAGACATCCATGCGAGACTGGATTATGCCATTGG
GGCCTGTTATTCCTGGCTGACTGAAGGTGAGCTATAATTGAAATGAAAGGCCAAAAGGTGAAGGCCACATCA
AAGCAGACATCATGGGGCTTTATGCAAGACAGTATCCAAAGCTTGCAGTGTGACCTATGATCATGCAAGATATCAGTGGCA
AAGTGCACAGTGGCAGACTGACCTGTGACTGAAAAAAAAGAAGGCCCTGACCTTATGAACTGCGATCTGGCAGCTG
GAAAAGAAAATGAAACAAGGTGAATTCTGAACTATAGAGAACTGGCAGCAGAACTGGTGCATATCTGGTGGATATGGGCTA
TACCCATGTGAAGTGCCTGTTGAGTGAACATCCATTATGGCAGCTGGGCTATGCCCTGTGGCTTGTGCCCCA
ACTAGCAGATATGGCAGCCCTGATGATTTTAAATTGCTGGATGCCATCACAGTGGCATTGGTGTGGTGTGGATTG
GGTGCCTGCCATTCTCAAGTGTGATCATGGCTGCCAACCTTGTGATGCCACCCACTGTCTCATGATCTGATCCAAGAA
GAGGCTGCCATCAAGATTGGAACAGCTTATGATCTGGCAGAGAACACAAGTGAAGAGATTCTGGTGTGAGCAATGCC
TGTATGGGTTGAACAGCTTATGATCTGGCAGTGGATGCACTGGCAGAGTGAAGATCTGGTGTGAGCAATGCC
CCATGGTCACTGGATCTTCAACATGGTGGCAGTGGATGCACTGGCAGAGTGAAGATCTGGTGTGAGCAATGCC
ATGGTGAATGCACTGGCAGTGGCTATGCCACCCCTGAATGATGGTGTGAGCAATGCC

sbe-Vv GGTGCTGCCATTTCAGTGTATGATCATGGCTGCCAACTTTGATGGCAGCCCACTGTGTTCATGATCTGATCCAAGGA
GAGGGCTGGCATCAAGATGGAACAGCTTATTATGATCTGGGCAGAGAACAAAGTGAGAAGAGATTCTTGTGAGCAATGCCC
TGTTATTGTTGACAGCTTCAATTGATGCCATTAGTGGATGCGAAGCTGAGCATGTCGATCTGAGTACTAGCAGAACAG
CCATGGTCAGTGGATTCACAACTGGATGGCAATGAAAACATGATGCCATTGCCACCTGTGAAATTGGATGAATGAAAG
AGTGTATAAATATTTCATTAATGCCATTGCGACATGGCAGAAAGAACAGTGCCTTCTCTGTGAGTGGCCCAACCTTATG
GGTGGCTCTGGCTTGGCTTAAATGGCACATGGGTGATGCGATAGCTGAGTATTAAGAAGAACCTGTGCTATA
GAAAATATCATATAACACCTGACCTTCACTGGTGTATGCCATAGTAAAACATGTCGAGCTGAGCCATGATGA
AGTGTGTATGGCAAAAGGCAGCTTCAACAAAATGCTGGTGTATGGCAAGCAGACTGCCAACCTGAGGCTATT
TGGCTATATGATGGTCAGCTGGCAAAAACATGAACTTATGGGTGCAAGAAATTGGTCAAGCTGAGAATGGAACCATG
TGATCAGCTGCACTGGTTCTGTGGATTTCAGACATCAAGGTGTGCAAGGCCCTGACTAGAGATCTGAAACCATCTGTAT
AGAAAATGAGAACGGCCCTGCACTGATCAAGATGGCAGTCTCTGCTGGATTGAGAGACTGCAAGATGGCAGAACAGAGC
ATTATTGGCCATGAAGAAATTGTAGAAGCTGGTGAAGAATGCTGGTGTGAGCAACTTACCCCTGTGCAAGAGATGAAT
TITAGACTGGGTGTGCCAACAAAGGCAGATATCAGCTGCTGTAACACTGATGATGCAAATATGCTGGCAGTGGCTATG
AAGTGGTGTGGTGTGGATGCAAAAGTGAAGCAGCTGGTGTGAGTGAAGATCTGGCACAGAGCATGTGCTGAGACTGCCACCACTGA
GCCACCTGTTTATAAACTGCTGTA A

ATGGCAACTGCGTACCTCCTTACGCCGCGTTTCGCTTATGAGCGGGCGGGTGGTAGCGGTGGTTAGTGTGGGTG
 CAGGTGCAGGTGGCACCTCGCGTGGTGTGGTTAGTGTGTCGAGCGCATGATAGCAGCGCATGCGAGCAACATCAGCATATGC
 TCGGAGCACCGAAGAAGAACTGAGCGGGTGTGACCAGCATGATAGCAGCGCATGCGAGCAACATCAGCATATGC
 GGATTITACCCCGCTGTTAGCCCGAACATAGCAGCCCGTGAAGCGTATCATGCGACCGCGAAAAGCGTGTGTTGATAGC
 CTGATTATGAACTGGAACAGCGAACCTATGACTATTACAACAGGTGAACCGCGAACAGCGTATTATCTGAGCATGGAGTTT
 TACAGGGCCCGCGTTAACCAATCGCATTGGCAACCTGAACTGACCGCCAATATGCGGAACCGCTGAACACAGTGGGCC
 ATAACCTGGAAGATGTGGCGAGCGAACCTGATCCGGCGTAGGTAAACGGTGTCTGGGTCTGTGGCGAGCTGCTTTT
 AGATAGCCTGGCAGCCCTGAATTATCCGGCTGGGCTATGGTCTGTTATCGCTATGGCTTCTCAAAACAGATTATCACC
 AAGGATGGCCAGGAAGAAGTGGCGAAAAGCTGGTGGAAAGGTACCGATGGCCGAAACATTGGATTGGCGGAAAACATTAAAGCGGT
 GCGCGATGTTCCGATTCCGGCTATAACCAACACCTGGCTCTGTGGGCAACTGTCGAGCCAGTACTGTCCGAGCCAG
 AACCTGATCTGGCGCTTAACCGAGCGAACAGCGAACAAATTCTGCCCTGAACAGCAGTATACCTGTAGCGAGCGCTG
 CAGGATATTAGCCTGTTGAAGCGTGTGGCGATTCACTGACTGAACTGGGAAGATTTCGAGCAGGAAAGTGGCGGTGAG
 ATGAACGATACCCATCGCAGCTGTGGCATTCTGACTGCGCATTCTGATGGGATATTAAAGGCGTGGAGCTGGAAACAGGATG
 CGTGGAGCATTACCGAACGCGACCTGGCGTAGGACCAACCATACCGCTTACCGGAAGCGCTGGAAAATGGAGCTGGAGCAG
 TTATGCGAGAAACTGCTGCCGCATGTGGAAATTATTGAGACTATCGATGAGGAACGATGAGAACACATCGTGGAGCAG
 ATGCGACCGGAGATAGCACCATTAGCAAATGGATCGCGAGCGATGATTGATTCTGAACACCGATAAATGGCGG
 CCTGGGAAACCTGTTTACAGCGAACAGAACACCGCGAACACTGCTGGTGGAAAGCATTGGGAAGCGGAT
 GAAAAAACCGAACAGCGAACAGTGGAAACATCTGAGCGAACACCAGGAAAAGCGGAAAGCGGATAGCGAACAG
 CGCGGATCGGAAAAGAAGATCCGGAGTATGAACTGGATCGCTTCGCGAAATATGATCCGAGTTCCGCGCGTTGTC
 GCATGGCGAATCTGTGTGGTGGCATAGCGTTAATGGCGGAAATTCTAGCGAAATCTGAGCGAACAGGATG
 TGTCGAGCATTACCGAACCTGAGCGAACAGCGAACACCGCTGGGAGCCTGGGATTCACCGTGTAGCGAACAGGATG
 TTGCAACCCGAACTGAGCACCATTAGCAAATGGATCGCGAGCGATGATTGATTCTGAACACCGATAAATGGCGG
 CCTGGGAAACCTTACCTCTGGAGCGAACACTGAGCGCATTTAGCGAACAGCTGGGAATTCGCGAACAGTGGCGAAGA
 GCGCTGATTGCGTGAACATTCTGGCATTTGTGATCGCTACAAGAAGATGAAAGAGATGAGCGGAAAGGATCGCG
 CAAACAGCGCTGAGCAGTGGGGCCGGATTGGCGGAAACGGCTTGCGACTATGCGAGGGAAACCCGATTG
 GAAATTTCGAGTGAACCGCTGTTACTGATTGGCACCTTAGATGGCGAACCTGGGAATTCGCGAACAGTGGCGAAGA
 AAACCTTTCTGTTGCGCATGCGCTGAAATTGGCGGCTGGCGAACAGTGGCGGAAAGGCAAAATTGCGCGGAT
 CTGCGCTTGAAGAGGTGAAGAAATATGCGCAGCGCGTCTTGGCACCAGCAACTATGATGAACTGATGGCAGCGT
 GAAGGCAATGAAGGTTATGGCGCGCGGATTATTTCTGTTGGCACCAGGAAAGATTTCGAGCTACATTGAATGCCAGGAGAAA
 GTGGATGAAGCTATCGCAGAACACTGCGACCGCATGAGCATTAAACACCGCGGGCAGCCCCAAATTAGCAG
 GATCGCACCATCATGAATATCGGAAGGACATCTGGGATATTAGCCCGTGTAGCTCGAGCACCCACCAAC
 ACTGA

ppk-
 Mt

ATGGGCAGCAGCCATCATCATCATCACAGCAGCGGCCCTGGTGCCTGGCGCGCAGCCATATGGCTAGCATGACTGGTGG
 CAGCAAATGGTGCCTGGATCATGATACCTCGCTGGTGTGAGCGACCGCCGACCAACCGGGCGCTCGAGAGCG
 AAGGGACACAGATCGCGCCGGCGCGAACAGATCTCGATGCGCTTACCAAGCGAACATTGTTCGGCTGCAAACA
 GAATTCTGTAAGCTGCAAGAGTGGGGCCGGATTCCGGTGCCTGGTGTCTGGTGTCTGGTGTCTGGTGTCTGGT
 AAGGGTGGCGCCATCAACGGATCACCGAGTACCCCAACCCGGAGTGGCTGCGGGCATGGCGGGAGGGAT
 CGCGAGGGGGCATGGTACTACCAGCTGTTATATGCCCCTCTCCGGCAAAGGTGAGATAGTGTCTCTCGATCGGT
 GGTACAACCCGCCGGTGGAGAAGGTATGGGTTCTGACTGCCAGGGAGTATGTTGTTTGGCGCACGCCCCGAT
 TTTCGAGCAGATGCTGATGACGGGATTCTGCTTCCGAAATACTGGTCTCAGCGCCAACAGTGGCG
 TTCAAGGCTGACGGAAATGGCGGCTGGCGCATAGGAACATGGGAGCTCGGATATGGTGTATCGGTGGAGGAGAC
 TATTGCGCGCAAGAGCAGAGATGATGGTGTACCGACACCCCGTCAAGGCGCTGGTGTACTGGTGGAGTCTGATATA
 AAGCACCGCGGCTGAAACATGATGCCACTTGTGTGTCACGATTGACTACCGAGATGTGGAAAGCGAACAGCTG
 CCCACCGGGCTTGTGAGTGGCAACTACAGGCCCGCGAGTGTGCGACATACGTCGAGACTATGTGGCCACGT
 TGATCGCGGGTGA

fdh-Ts

ATGGCGAAGATTCTGTTCTGACGATGCCGCGTTGACGGTTATCGAACAGACCTATGCCGCGATGACCTGCCGAGA
 TTGACCACTATGCCGCGTCAAGACCGTCCGACGCCAACCGTACGTTTACCCCGGCCAACCTGCTGGTAGTGTGTC
 CGCGAACACTGGGCTCGTAAATACCTGAAAGCGAACCGCATACCTTGTGTTACCGACGATAAAAGACGGTCCGGATCT
 GTGTTGCGAAAGGAACTGGTGTGATGCTGACGCTGTTGATTTCTACCGCTTCTGGGGCATATGACCCGGAAACGATCG
 CAAAAGCTAAGAACCTGAAACTGGACTGACGGCTGGATTGGTAGTGTACGCTGGACCTGCACTCCGCGCATGATCGCG
 GCATCACCGTGCAGGAAGTGGCTGAAATCTGCGAACATGGGAGCTGGTGTACGCTGGAGTCTGATGATTCTGGTGTGG
 AACTACATCCGAGCCAGTGGGCTGCGAACAGGGTTGGAAATATCGGGATGTTGTTGACATAGCTGATGATCTGGAA
 GGCATGACCGTTGGTCTGGTGTGCGACAGCGTGTATTGGTCTGGCAGTCTCGCTGGCACCGTTGATGTAAGCTG
 ATTATACCGACCGTCACTGGTGTGCGAACAGCGTGGAAAGAACACTGGGCTGTTGGCATGATACCCGCGAACAGCATGT
 ACCCGCACTGCGATGTTGTTACGCTGAACGCTCCCGCTGCATCGGAAACACATGATGAAACCGCTGAAAC
 TGTGTTAAGCGTGGCCCTTATATTGTAACACCCGCCCGTAAACTGGCAGATGCTGACGCTATGTTGCGTCAATCGAAAG
 CGGTCACTGGCAGGGTACGCAAGGTGATGTTGGTCCCGAACCGGACCGAACAGGACCATCGTGGCGTACCATGAGT
 GGAAGGCATGACCCCGACATACCGGGTACGAGCTGACGGCTGTCACAGGCACTGGTGTACCGCGAACATTCTGGA
 ATGCTTTCGAAAGTCGTCGATTGCGATGAAATATCTGATCGTGCAGGGTGTGACTGGTGTGACCGGGTACCGGT
 TACTCCAAAGGCAACCGAACGGCGGTAGCGAAGAAGCGGCCAAATTCAAAAGGCAGGTGA

References and Notes

1. P. L. Keeling, A. M. Myers, Biochemistry and genetics of starch synthesis. *Annu. Rev. Food Sci. Technol.* **1**, 271–303 (2010). [Medline](#)
2. R. Höfer, “Sugar- and starch-based biorefineries” in *Industrial Biorefineries and White Biotechnology*, A. Pandey, R. Höfer, M. Taherzadeh, M. Nampoothiri, C. Larroche, P. L. Keeling, A. M. Myers, Eds. (Elsevier, 2015), chap. 4A, pp. 157–235.
3. R. L. Whistler, J. R. Daniel, “Molecular structure of starch” in *Starch: Chemistry and Technology*, R. L. Whistler, J. N. Bemiller, E. F. Paschall, Eds. (Academic Press, ed. 2, 1984), pp. 153–182.
4. T. Saithong, A. Meechai, S. Cheevadhanarak, S. Bhumiratana, A formal path inference of starch biosynthesis via mathematical modelling of metabolic changes in excess CO₂. *J. Comput. Sci. Syst. Biol.* **5**, 24–37 (2012). [doi:10.4172/jcsb.1000087](#)
5. M. R. Abt, S. C. Zeeman, Evolutionary innovations in starch metabolism. *Curr. Opin. Plant Biol.* **55**, 109–117 (2020). [doi:10.1016/j.pbi.2020.03.001](#) [Medline](#)
6. J. Li, E. Baroja-Fernández, A. Bahaji, F. J. Muñoz, M. Ovecka, M. Montero, M. T. Sesma, N. Alonso-Casajús, G. Almagro, A. M. Sánchez-López, M. Hidalgo, M. Zamarbide, J. Pozueta-Romero, Enhancing sucrose synthase activity results in increased levels of starch and ADP-glucose in maize (*Zea mays* L.) seed endosperms. *Plant Cell Physiol.* **54**, 282–294 (2013). [doi:10.1093/pcp/pcs180](#) [Medline](#)
7. N. Li, S. Zhang, Y. Zhao, B. Li, J. Zhang, Over-expression of AGPase genes enhances seed weight and starch content in transgenic maize. *Planta* **233**, 241–250 (2011). [doi:10.1007/s00425-010-1296-5](#) [Medline](#)
8. M. Hakata, M. Kuroda, T. Miyashita, T. Yamaguchi, M. Kojima, H. Sakakibara, T. Mitsui, H. Yamakawa, Suppression of α-amylase genes improves quality of rice grain ripened under high temperature. *Plant Biotechnol. J.* **10**, 1110–1117 (2012). [doi:10.1111/j.1467-7652.2012.00741.x](#) [Medline](#)
9. A. Bahaji, J. Li, A. M. Sánchez-López, E. Baroja-Fernández, F. J. Muñoz, M. Ovecka, G. Almagro, M. Montero, I. Ezquer, E. Etxeberria, J. Pozueta-Romero, Starch biosynthesis, its regulation and biotechnological approaches to improve crop yields. *Biotechnol. Adv.* **32**, 87–106 (2014). [doi:10.1016/j.biotechadv.2013.06.006](#) [Medline](#)
10. A. Bar-Even, E. Noor, N. E. Lewis, R. Milo, Design and analysis of synthetic carbon fixation pathways. *Proc. Natl. Acad. Sci. U.S.A.* **107**, 8889–8894 (2010). [doi:10.1073/pnas.0907176107](#) [Medline](#)
11. A. Satanowski, B. Dronsell, E. Noor, B. Vögeli, H. He, P. Wichmann, T. J. Erb, S. N. Lindner, A. Bar-Even, Awakening a latent carbon fixation cycle in *Escherichia coli*. *Nat. Commun.* **11**, 5812 (2020). [doi:10.1038/s41467-020-19564-5](#) [Medline](#)
12. M. Scheffen, D. G. Marchal, T. Beneyton, S. K. Schuller, M. Klose, C. Diehl, J. Lehmann, P. Pfister, M. Carrillo, H. He, S. Aslan, N. S. Cortina, P. Claus, D. Bollschweiler, J.-C. Baret, J. M. Schuller, J. Zarzycki, A. Bar-Even, T. J. Erb, A new-to-nature carboxylation module to improve natural and synthetic CO₂ fixation. *Nat. Catal.* **4**, 105–115 (2021). [doi:10.1038/s41929-020-00557-y](#)

13. T. Schwander, L. Schada von Borzyskowski, S. Burgener, N. S. Cortina, T. J. Erb, A synthetic pathway for the fixation of carbon dioxide *in vitro*. *Science* **354**, 900–904 (2016). [doi:10.1126/science.aah5237](https://doi.org/10.1126/science.aah5237) [Medline](#)
14. T. E. Miller, T. Beneyton, T. Schwander, C. Diehl, M. Girault, R. McLean, T. Chotel, P. Claus, N. S. Cortina, J.-C. Baret, T. J. Erb, Light-powered CO₂ fixation in a chloroplast mimic with natural and synthetic parts. *Science* **368**, 649–654 (2020). [doi:10.1126/science.aaz6802](https://doi.org/10.1126/science.aaz6802) [Medline](#)
15. T. P. Korman, P. H. Opgenorth, J. U. Bowie, A synthetic biochemistry platform for cell free production of monoterpenes from glucose. *Nat. Commun.* **8**, 15526 (2017). [doi:10.1038/ncomms15526](https://doi.org/10.1038/ncomms15526) [Medline](#)
16. S. Sher Khanov, T. P. Korman, S. Chan, S. Faham, H. Liu, M. R. Sawaya, W. T. Hsu, E. Vikram, T. Cheng, J. U. Bowie, Isobutanol production freed from biological limits using synthetic biochemistry. *Nat. Commun.* **11**, 4292 (2020). [doi:10.1038/s41467-020-18124-1](https://doi.org/10.1038/s41467-020-18124-1) [Medline](#)
17. M. Green, E. Dunlop, J. Hohl-Ebinger, M. Yoshita, N. Kopidakis, X. J. Hao, Solar cell efficiency tables (version 57). *Prog. Photovolt. Res. Appl.* **29**, 3–15 (2021). [doi:10.1002/pip.3371](https://doi.org/10.1002/pip.3371)
18. S. Shiva Kumar, V. Himabindu, Hydrogen production by PEM water electrolysis – A review. *Mater. Sci. Energy Technol.* **2**, 442–454 (2019). [doi:10.1016/j.mset.2019.03.002](https://doi.org/10.1016/j.mset.2019.03.002)
19. Y. Y. Birdja, E. Pérez-Gallent, M. C. Figueiredo, A. J. Göttle, F. Calle-Vallejo, M. T. M. Koper, Advances and challenges in understanding the electrocatalytic conversion of carbon dioxide to fuels. *Nat. Energy* **4**, 732–745 (2019). [doi:10.1038/s41560-019-0450-y](https://doi.org/10.1038/s41560-019-0450-y)
20. R.-P. Ye, J. Ding, W. Gong, M. D. Argyle, Q. Zhong, Y. Wang, C. K. Russell, Z. Xu, A. G. Russell, Q. Li, M. Fan, Y.-G. Yao, CO₂ hydrogenation to high-value products via heterogeneous catalysis. *Nat. Commun.* **10**, 5698 (2019). [doi:10.1038/s41467-019-13638-9](https://doi.org/10.1038/s41467-019-13638-9) [Medline](#)
21. J. B. Siegel, A. L. Smith, S. Poust, A. J. Wargacki, A. Bar-Even, C. Louw, B. W. Shen, C. B. Eiben, H. M. Tran, E. Noor, J. L. Gallaher, J. Bale, Y. Yoshikuni, M. H. Gelb, J. D. Keasling, B. L. Stoddard, M. E. Lidstrom, D. Baker, Computational protein design enables a novel one-carbon assimilation pathway. *Proc. Natl. Acad. Sci. U.S.A.* **112**, 3704–3709 (2015). [doi:10.1073/pnas.1500545112](https://doi.org/10.1073/pnas.1500545112) [Medline](#)
22. R. Caspi, R. Billington, L. Ferrer, H. Foerster, C. A. Fulcher, I. M. Keseler, A. Kothari, M. Krumannacker, M. Latendresse, L. A. Mueller, Q. Ong, S. Paley, P. Subhraveti, D. S. Weaver, P. D. Karp, The MetaCyc database of metabolic pathways and enzymes and the BioCyc collection of pathway/genome databases. *Nucleic Acids Res.* **44**, D471–D480 (2016). [doi:10.1093/nar/gkv1164](https://doi.org/10.1093/nar/gkv1164) [Medline](#)
23. N. Hadadi, J. Hafner, A. Shajkofci, A. Zisaki, V. Hatzimanikatis, ATLAS of biochemistry: A repository of all possible biochemical reactions for synthetic biology and metabolic engineering studies. *ACS Synth. Biol.* **5**, 1155–1166 (2016). [doi:10.1021/acssynbio.6b00054](https://doi.org/10.1021/acssynbio.6b00054) [Medline](#)
24. X. Yang, Q. Yuan, H. Luo, F. Li, Y. Mao, X. Zhao, J. Du, P. Li, X. Ju, Y. Zheng, Y. Chen, Y. Liu, H. Jiang, Y. Yao, H. Ma, Y. Ma, Systematic design and *in vitro* validation of novel one-carbon assimilation pathways. *Metab. Eng.* **56**, 142–153 (2019).

[doi:10.1016/j.ymben.2019.09.001](https://doi.org/10.1016/j.ymben.2019.09.001) [Medline](#)

25. A. Ebrahim, J. A. Lerman, B. O. Palsson, D. R. Hyduke, COBRApy: Constraints-based reconstruction and analysis for Python. *BMC Syst. Biol.* **7**, 74 (2013). [doi:10.1186/1752-0509-7-74](https://doi.org/10.1186/1752-0509-7-74) [Medline](#)
26. T. J. Erb, P. R. Jones, A. Bar-Even, Synthetic metabolism: Metabolic engineering meets enzyme design. *Curr. Opin. Chem. Biol.* **37**, 56–62 (2017).
[doi:10.1016/j.cbpa.2016.12.023](https://doi.org/10.1016/j.cbpa.2016.12.023) [Medline](#)
27. A. Chou, J. M. Clomburg, S. Qian, R. Gonzalez, 2-Hydroxyacyl-CoA lyase catalyzes acyloin condensation for one-carbon bioconversion. *Nat. Chem. Biol.* **15**, 900–906 (2019).
[doi:10.1038/s41589-019-0328-0](https://doi.org/10.1038/s41589-019-0328-0) [Medline](#)
28. Y. S. Tai, K. Zhang, C1 metabolism redesigned. *Nat. Chem. Biol.* **11**, 384–386 (2015).
[doi:10.1038/nchembio.1819](https://doi.org/10.1038/nchembio.1819) [Medline](#)
29. S. Poust, J. Piety, A. Bar-Even, C. Louw, D. Baker, J. D. Keasling, J. B. Siegel, Mechanistic analysis of an engineered enzyme that catalyzes the formose reaction. *ChemBioChem* **16**, 1950–1954 (2015). [doi:10.1002/cbic.201500228](https://doi.org/10.1002/cbic.201500228) [Medline](#)
30. J. K. Hines, C. E. Kruesel, H. J. Fromm, R. B. Honzatko, Structure of inhibited fructose-1,6-bisphosphatase from *Escherichia coli*: Distinct allosteric inhibition sites for AMP and glucose 6-phosphate and the characterization of a gluconeogenic switch. *J. Biol. Chem.* **282**, 24697–24706 (2007). [doi:10.1074/jbc.M703580200](https://doi.org/10.1074/jbc.M703580200) [Medline](#)
31. J. S. Yang, S. W. Seo, S. Jang, G. Y. Jung, S. Kim, Rational engineering of enzyme allosteric regulation through sequence evolution analysis. *PLOS Comput. Biol.* **8**, e1002612 (2012).
[doi:10.1371/journal.pcbi.1002612](https://doi.org/10.1371/journal.pcbi.1002612) [Medline](#)
32. C. R. Meyer, J. A. Bork, S. Nadler, J. Yirsa, J. Preiss, Site-directed mutagenesis of a regulatory site of *Escherichia coli* ADP-glucose pyrophosphorylase: The role of residue 336 in allosteric behavior. *Arch. Biochem. Biophys.* **353**, 152–159 (1998).
[doi:10.1006/abbi.1998.0648](https://doi.org/10.1006/abbi.1998.0648) [Medline](#)
33. C. R. Meyer, J. Yirsa, B. Gott, J. Preiss, A kinetic study of site-directed mutants of *Escherichia coli* ADP-glucose pyrophosphorylase: The role of residue 295 in allosteric regulation. *Arch. Biochem. Biophys.* **352**, 247–254 (1998). [doi:10.1006/abbi.1998.0593](https://doi.org/10.1006/abbi.1998.0593) [Medline](#)
34. J. Wang, G. Li, Z. Li, C. Tang, Z. Feng, H. An, H. Liu, T. Liu, C. Li, A highly selective and stable ZnO-ZrO₂ solid solution catalyst for CO₂ hydrogenation to methanol. *Sci. Adv.* **3**, e1701290 (2017). [doi:10.1126/sciadv.1701290](https://doi.org/10.1126/sciadv.1701290) [Medline](#)
35. H. J. Jo, S. Park, H. G. Jeong, J. W. Kim, J. T. Park, *Vibrio vulnificus* glycogen branching enzyme preferentially transfers very short chains: N1 domain determines the chain length transferred. *FEBS Lett.* **589**, 1089–1094 (2015). [doi:10.1016/j.febslet.2015.03.011](https://doi.org/10.1016/j.febslet.2015.03.011) [Medline](#)
36. S. Sundaram, C. Diehl, N. S. Cortina, J. Bamberger, N. Paczia, T. J. Erb, A modular *in vitro* platform for the production of terpenes and polyketides from CO₂. *Angew. Chem. Int. Ed.* **60**, 16420–16425 (2021). [doi:10.1002/anie.202102333](https://doi.org/10.1002/anie.202102333) [Medline](#)
37. E. S. Van-Dal, C. Bouallou, Design and simulation of a methanol production plant from CO₂ hydrogenation. *J. Clean. Prod.* **57**, 38–45 (2013). [doi:10.1016/j.jclepro.2013.06.008](https://doi.org/10.1016/j.jclepro.2013.06.008)

38. X. G. Zhu, S. P. Long, D. R. Ort, What is the maximum efficiency with which photosynthesis can convert solar energy into biomass? *Curr. Opin. Biotechnol.* **19**, 153–159 (2008). [doi:10.1016/j.copbio.2008.02.004](https://doi.org/10.1016/j.copbio.2008.02.004) Medline
39. Y. H. P. Zhang, C. You, H. Chen, R. Feng, “Surpassing photosynthesis: high-efficiency and scalable CO₂ utilization through artificial photosynthesis” in *Recent Advances in Post-Combustion CO₂ Capture Chemistry*. M. Attalla, Ed. (American Chemical Society, 2012), pp. 275–292.
40. C. S. Kuehn, J. G. Linn, D. G. Johnson, H. G. Jung, M. I. Endres, Effect of feeding silages from corn hybrids selected for leafiness or grain to lactating dairy cattle. *J. Dairy Sci.* **82**, 2746–2755 (1999). [doi:10.3168/jds.S0022-0302\(99\)75531-1](https://doi.org/10.3168/jds.S0022-0302(99)75531-1) Medline
41. M. M. Bradford, A rapid and sensitive method for the quantitation of microgram quantities of protein utilizing the principle of protein-dye binding. *Anal. Biochem.* **72**, 248–254 (1976). [doi:10.1016/0003-2697\(76\)90527-3](https://doi.org/10.1016/0003-2697(76)90527-3) Medline
42. P. A. Lanzetta, L. J. Alvarez, P. S. Reinach, O. A. Candia, An improved assay for nanomole amounts of inorganic phosphate. *Anal. Biochem.* **100**, 95–97 (1979). [doi:10.1016/0003-2697\(79\)90115-5](https://doi.org/10.1016/0003-2697(79)90115-5) Medline
43. M. A. Tang, H. Motoshima, K. Watanabe, Cold adaptation: Structural and functional characterizations of psychrophilic and mesophilic acetate kinase. *Protein J.* **33**, 313–322 (2014). [doi:10.1007/s10930-014-9562-1](https://doi.org/10.1007/s10930-014-9562-1) Medline
44. H. Bi, Y. Bai, T. Cai, Y. Zhuang, X. Liang, X. Zhang, T. Liu, Y. Ma, Engineered short branched-chain acyl-CoA synthesis in *E. coli* and acylation of chloramphenicol to branched-chain derivatives. *Appl. Microbiol. Biotechnol.* **97**, 10339–10348 (2013). [doi:10.1007/s00253-013-5262-6](https://doi.org/10.1007/s00253-013-5262-6) Medline
45. M. Molin, J. Norbeck, A. Blomberg, Dihydroxyacetone kinases in *Saccharomyces cerevisiae* are involved in detoxification of dihydroxyacetone. *J. Biol. Chem.* **278**, 1415–1423 (2003). [doi:10.1074/jbc.M203030200](https://doi.org/10.1074/jbc.M203030200) Medline
46. E. González-Mondragón, R. A. Zubillaga, E. Saavedra, M. E. Chávez-Cárdenas, R. Pérez-Montfort, A. Hernández-Arana, Conserved cysteine 126 in triosephosphate isomerase is required not for enzymatic activity but for proper folding and stability. *Biochemistry* **43**, 3255–3263 (2004). [doi:10.1021/bi036077s](https://doi.org/10.1021/bi036077s) Medline
47. O. N. Rozova, V. N. Khmelenina, I. I. Mustakhimov, A. S. Reshetnikov, Y. A. Trotsenko, Characterization of recombinant fructose-1,6-bisphosphate aldolase from *Methylococcus capsulatus* Bath. *Biochemistry (Mosc.)* **75**, 892–898 (2010). [doi:10.1134/S0006297910070114](https://doi.org/10.1134/S0006297910070114) Medline
48. C. V. Iancu, S. Mukund, H. J. Fromm, R. B. Honzatko, R-state AMP complex reveals initial steps of the quaternary transition of fructose-1,6-bisphosphatase. *J. Biol. Chem.* **280**, 19737–19745 (2005). [doi:10.1074/jbc.M501011200](https://doi.org/10.1074/jbc.M501011200) Medline
49. S. Schneider, T. Sandalova, G. Schneider, G. A. Sprenger, A. K. Samland, Replacement of a phenylalanine by a tyrosine in the active site confers fructose-6-phosphate aldolase activity to the transaldolase of *Escherichia coli* and human origin. *J. Biol. Chem.* **283**, 30064–30072 (2008). [doi:10.1074/jbc.M803184200](https://doi.org/10.1074/jbc.M803184200) Medline
50. D. Mathur, L. C. Garg, Functional phosphoglucose isomerase from *Mycobacterium*

- tuberculosis* H37Rv: Rapid purification with high yield and purity. *Protein Expr. Purif.* **52**, 373–378 (2007). [doi:10.1016/j.pep.2006.10.006](https://doi.org/10.1016/j.pep.2006.10.006) [Medline](#)
51. C. You, S. Myung, Y. H. Zhang, Facilitated substrate channeling in a self-assembled trifunctional enzyme complex. *Angew. Chem. Int. Ed.* **51**, 8787–8790 (2012). [doi:10.1002/anie.201202441](https://doi.org/10.1002/anie.201202441) [Medline](#)
52. X. Ji, Z. Su, P. Wang, G. Ma, S. Zhang, Tethering of nicotinamide adenine dinucleotide inside hollow nanofibers for high-yield synthesis of methanol from carbon dioxide catalyzed by coencapsulated multienzymes. *ACS Nano* **9**, 4600–4610 (2015). [doi:10.1021/acsnano.5b01278](https://doi.org/10.1021/acsnano.5b01278) [Medline](#)
53. S. Freger, I. Dahlquist, B. Gruvberger, A simple method for the detection of formaldehyde. *Contact Dermatitis* **10**, 132–134 (1984). [doi:10.1111/j.1600-0536.1984.tb00017.x](https://doi.org/10.1111/j.1600-0536.1984.tb00017.x) [Medline](#)
54. G. Hernández-Alcántara, G. Garza-Ramos, G. M. Hernández, A. Gómez-Puyou, R. Pérez-Montfort, Catalysis and stability of triosephosphate isomerase from *Trypanosoma brucei* with different residues at position 14 of the dimer interface. Characterization of a catalytically competent monomeric enzyme. *Biochemistry* **41**, 4230–4238 (2002). [doi:10.1021/bi011950f](https://doi.org/10.1021/bi011950f) [Medline](#)
55. C. A. Smith, T. Kortemme, Backrub-like backbone simulation recapitulates natural protein conformational variability and improves mutant side-chain prediction. *J. Mol. Biol.* **380**, 742–756 (2008). [doi:10.1016/j.jmb.2008.05.023](https://doi.org/10.1016/j.jmb.2008.05.023) [Medline](#)
56. J. D. Durrant, L. Votapka, J. Sørensen, R. E. Amaro, POVME 2.0: An enhanced tool for determining pocket shape and volume characteristics. *J. Chem. Theory Comput.* **10**, 5047–5056 (2014). [doi:10.1021/ct500381c](https://doi.org/10.1021/ct500381c) [Medline](#)
57. I. W. Davis, D. Baker, RosettaLigand docking with full ligand and receptor flexibility. *J. Mol. Biol.* **385**, 381–392 (2009). [doi:10.1016/j.jmb.2008.11.010](https://doi.org/10.1016/j.jmb.2008.11.010) [Medline](#)
58. S. Kim, P. A. Thiessen, E. E. Bolton, J. Chen, G. Fu, A. Gindulyte, L. Han, J. He, S. He, B. A. Shoemaker, J. Wang, B. Yu, J. Zhang, S. H. Bryant, PubChem Substance and Compound databases. *Nucleic Acids Res.* **44**, D1202–D1213 (2016). [doi:10.1093/nar/gkv951](https://doi.org/10.1093/nar/gkv951) [Medline](#)
59. N. M. O’Boyle, M. Banck, C. A. James, C. Morley, T. Vandermeersch, G. R. Hutchison, Open Babel: An open chemical toolbox. *J. Cheminform.* **3**, 33 (2011). [doi:10.1186/1758-2946-3-33](https://doi.org/10.1186/1758-2946-3-33) [Medline](#)
60. S. C. Li, Y. K. Ng, Calibur: A tool for clustering large numbers of protein decoys. *BMC Bioinformatics* **11**, 25 (2010). [doi:10.1186/1471-2105-11-25](https://doi.org/10.1186/1471-2105-11-25) [Medline](#)
61. E. Lilkova, P. Petkov, N. Ilieva, L. Litov, The PyMOL Molecular Graphics System Version 2.0. (Software, Schrödinger LLC., 2015).
62. C. You, H. Chen, S. Myung, N. Sathitsuksanoh, H. Ma, X. Z. Zhang, J. Li, Y. H. Zhang, Enzymatic transformation of nonfood biomass to starch. *Proc. Natl. Acad. Sci. U.S.A.* **110**, 7182–7187 (2013). [doi:10.1073/pnas.1302420110](https://doi.org/10.1073/pnas.1302420110) [Medline](#)
63. P. Kang, S. Zhang, T. J. Meyer, M. Brookhart, Rapid selective electrocatalytic reduction of carbon dioxide to formate by an iridium pincer catalyst immobilized on carbon nanotube electrodes. *Angew. Chem. Int. Ed.* **53**, 8709–8713 (2014). [doi:10.1002/anie.201310722](https://doi.org/10.1002/anie.201310722)

[Medline](#)

64. R. K. Singh, R. Singh, D. Sivakumar, S. Kondaveeti, T. Kim, J. Li, B. H. Sung, B.-K. Cho, D. R. Kim, S. C. Kim, V. C. Kalia, Y.-H. P. J. Zhang, H. Zhao, Y. C. Kang, J.-K. Lee, Insights into cell-free conversion of CO₂ to chemicals by a multienzyme cascade reaction. *ACS Catal.* **8**, 11085–11093 (2018). [doi:10.1021/acscatal.8b02646](https://doi.org/10.1021/acscatal.8b02646) [Medline](#)
65. R. F. Say, G. Fuchs, Fructose 1,6-bisphosphate aldolase/phosphatase may be an ancestral gluconeogenic enzyme. *Nature* **464**, 1077–1081 (2010). [doi:10.1038/nature08884](https://doi.org/10.1038/nature08884) [Medline](#)
66. S. Fushinobu, H. Nishimasu, D. Hattori, H. J. Song, T. Wakagi, Structural basis for the bifunctionality of fructose-1,6-bisphosphate aldolase/phosphatase. *Nature* **478**, 538–541 (2011). [doi:10.1038/nature10457](https://doi.org/10.1038/nature10457) [Medline](#)
67. A. M. Smith, S. C. Zeeman, S. M. Smith, Starch degradation. *Annu. Rev. Plant Biol.* **56**, 73–98 (2005). [doi:10.1146/annurev.arplant.56.032604.144257](https://doi.org/10.1146/annurev.arplant.56.032604.144257) [Medline](#)
68. K. Ohdan, K. Fujii, M. Yanase, T. Takaha, T. Kuriki, Enzymatic synthesis of amylose. *Biocatal. Biotransform.* **24**, 77–81 (2006). [doi:10.1080/10242420600598152](https://doi.org/10.1080/10242420600598152)
69. J. I. Kadokawa, Enzymatic synthesis of functional amylosic materials and amylose analog polysaccharides. *Methods Enzymol.* **627**, 189–213 (2019). [doi:10.1016/bs.mie.2019.06.009](https://doi.org/10.1016/bs.mie.2019.06.009) [Medline](#)
70. F. Y. H. Chen, H. W. Jung, C. Y. Tsuei, J. C. Liao, Converting *Escherichia coli* to a synthetic methylotroph growing solely on methanol. *Cell* **182**, 933–946.e14 (2020). [doi:10.1016/j.cell.2020.07.010](https://doi.org/10.1016/j.cell.2020.07.010) [Medline](#)
71. J. Ren, P. Yao, S. Yu, W. Dong, Q. Chen, J. Feng, Q. Wu, D. Zhu, An unprecedented effective enzymatic carboxylation of phenols. *ACS Catal.* **6**, 564–567 (2016). [doi:10.1021/acscatal.5b02529](https://doi.org/10.1021/acscatal.5b02529)
72. A. Chang, I. Schomburg, S. Placzek, L. Jeske, M. Ulbrich, M. Xiao, C. W. Sensen, D. Schomburg, BRENDa in 2015: Exciting developments in its 25th year of existence. *Nucleic Acids Res.* **43**, D439–D446 (2015). [doi:10.1093/nar/gku1068](https://doi.org/10.1093/nar/gku1068) [Medline](#)
73. X. Garrabou, J. A. Castillo, C. Guérard-Hélaine, T. Parella, J. Joglar, M. Lemaire, P. Clapés, Asymmetric self- and cross-aldol reactions of glycolaldehyde catalyzed by D-fructose-6-phosphate aldolase. *Angew. Chem. Int. Ed.* **48**, 5521–5525 (2009). [doi:10.1002/anie.200902065](https://doi.org/10.1002/anie.200902065) [Medline](#)
74. V. Helaine, R. Mahdi, G. V. Sudhir Babu, V. de Berardinis, R. Wohlgemuth, M. Lemaire, C. Guerard-Helaine, Straightforward synthesis of terminally phosphorylated l-sugars via multienzymatic cascade reactions. *Adv. Synth. Catal.* **357**, 1703–1708 (2015). [doi:10.1002/adsc.201500190](https://doi.org/10.1002/adsc.201500190)
75. A. Szekrenyi, X. Garrabou, T. Parella, J. Joglar, J. Bujons, P. Clapés, Asymmetric assembly of aldose carbohydrates from formaldehyde and glycolaldehyde by tandem biocatalytic aldol reactions. *Nat. Chem.* **7**, 724–729 (2015). [doi:10.1038/nchem.2321](https://doi.org/10.1038/nchem.2321) [Medline](#)
76. A. Flamholz, E. Noor, A. Bar-Even, R. Milo, eQuilibrator—The biochemical thermodynamics calculator. *Nucleic Acids Res.* **40**, D770–D775 (2012). [doi:10.1093/nar/gkr874](https://doi.org/10.1093/nar/gkr874) [Medline](#)

77. A. Krog, T. M. B. Heggeset, J. E. N. Müller, C. E. Kupper, O. Schneider, J. A. Vorholt, T. E. Ellingsen, T. Brautaset, Methylotrophic *Bacillus methanolicus* encodes two chromosomal and one plasmid born NAD⁺ dependent methanol dehydrogenase paralogs with different catalytic and biochemical properties. *PLOS ONE* **8**, e59188 (2013). [doi:10.1371/journal.pone.0059188](https://doi.org/10.1371/journal.pone.0059188) [Medline](#)
78. X. Lu, Y. Liu, Y. Yang, S. Wang, Q. Wang, X. Wang, Z. Yan, J. Cheng, C. Liu, X. Yang, H. Luo, S. Yang, J. Gou, L. Ye, L. Lu, Z. Zhang, Y. Guo, Y. Nie, J. Lin, S. Li, C. Tian, T. Cai, B. Zhuo, H. Ma, W. Wang, Y. Ma, Y. Liu, Y. Li, H. Jiang, Constructing a synthetic pathway for acetyl-coenzyme A from one-carbon through enzyme design. *Nat. Commun.* **10**, 1378 (2019). [doi:10.1038/s41467-019-10905-z](https://doi.org/10.1038/s41467-019-10905-z) [Medline](#)
79. T. Senoura, A. Asao, Y. Takashima, N. Isono, S. Hamada, H. Ito, H. Matsui, Enzymatic characterization of starch synthase III from kidney bean (*Phaseolus vulgaris* L.). *FEBS J.* **274**, 4550–4560 (2007). [doi:10.1111/j.1742-4658.2007.05984.x](https://doi.org/10.1111/j.1742-4658.2007.05984.x) [Medline](#)
80. H. Choe, J. C. Joo, D. H. Cho, M. H. Kim, S. H. Lee, K. D. Jung, Y. H. Kim, Efficient CO₂-reducing activity of NAD-dependent formate dehydrogenase from *Thiobacillus* sp. KNK65MA for formate production from CO₂ gas. *PLOS ONE* **9**, e103111 (2014). [doi:10.1371/journal.pone.0103111](https://doi.org/10.1371/journal.pone.0103111) [Medline](#)
81. H. Zheng, Z. Yu, W. Shu, X. Fu, X. Zhao, S. Yang, M. Tan, J. Xu, Y. Liu, H. Song, Ethanol effects on the overexpression of heterologous catalase in *Escherichia coli* BL21 (DE3). *Appl. Microbiol. Biotechnol.* **103**, 1441–1453 (2019). [doi:10.1007/s00253-018-9509-0](https://doi.org/10.1007/s00253-018-9509-0) [Medline](#)
82. K. T. Shum, E. L. H. Lui, S. C. K. Wong, P. Yeung, L. Sam, Y. Wang, R. M. Watt, J. A. Tanner, Aptamer-mediated inhibition of *Mycobacterium tuberculosis* polyphosphate kinase 2. *Biochemistry* **50**, 3261–3271 (2011). [doi:10.1021/bi2001455](https://doi.org/10.1021/bi2001455) [Medline](#)
83. S. Avaeva, P. Ignatov, S. Kurilova, T. Nazarova, E. Rodina, N. Vorobyeva, V. Oganessyan, E. Harutyunyan, *Escherichia coli* inorganic pyrophosphatase: Site-directed mutagenesis of the metal binding sites. *FEBS Lett.* **399**, 99–102 (1996). [doi:10.1016/S0014-5793\(96\)01296-3](https://doi.org/10.1016/S0014-5793(96)01296-3) [Medline](#)